

1-1-2010

# Stabilization Of Polystannanes Via Alkyne Insertion

Aman U. Khan  
*Ryerson University*

Follow this and additional works at: <http://digitalcommons.ryerson.ca/dissertations>

 Part of the [Molecular Biology Commons](#)

---

## Recommended Citation

Khan, Aman U., "Stabilization Of Polystannanes Via Alkyne Insertion" (2010). *Theses and dissertations*. Paper 1507.

This Thesis is brought to you for free and open access by Digital Commons @ Ryerson. It has been accepted for inclusion in Theses and dissertations by an authorized administrator of Digital Commons @ Ryerson. For more information, please contact [bcameron@ryerson.ca](mailto:bcameron@ryerson.ca).

# STABILIZATION OF POLYSTANNANES VIA ALKYNE INSERTION

by

Aman Ullah Khan

A thesis

presented to Ryerson University

in partial fulfillment of the

requirements for the degree of

Master of Science

in the Program of

Molecular Science

Toronto, Ontario, Canada, 2010

©(Aman Ullah Khan) 2010



## **Author's Declaration**

I hereby declare that I am the sole author of this thesis.

I authorize Ryerson University to lend this thesis to other institutions or individuals for the purpose of scholarly research.

Name: \_\_\_\_\_ Signature: \_\_\_\_\_

I further authorize Ryerson University to reproduce this thesis by photocopying or by other means, in total or in part, at the request of other institutions or individuals for the purpose of scholarly research.

Name: \_\_\_\_\_ Signature: \_\_\_\_\_



# **Title: STABILIZATION OF POLYSTANNANES VIA ALKYNE INSERTION**

Master of Science, 2010

Aman Ullah Khan

Molecular Science

Ryerson university

## **Abstract:**

Di-*n*-butylstannane, polydi-*n*-butylstannane and the acetylene inserted carbodistannanes were prepared using the methods described in literature. Their structures were confirmed by NMR analysis. Finally acetylene inserted polydibutylstannane, was prepared in a similar fashion and was evident from its unique  $^{119}\text{Sn}$  NMR chemical shift values that were similar to that for  $(n\text{-Bu})_3\text{SnCH=CHSn}(n\text{-Bu})_3$ . A highly unusual head to head dimer (hexamethyl-1,4-diphenyldistannyl-1,3-butadiene) was obtained and characterized by X-ray crystallography. The quantitative conversion of  $(n\text{-Bu})_3\text{SnH}$  into  $(n\text{-Bu})_6\text{Sn}_2$  was achieved by heating the neat  $(n\text{-Bu})_3\text{SnH}$  under different conditions. This route was extended to a secondary stannane,  $(n\text{-Bu})_2\text{SnH}_2$  which yielded evidence (NMR) for  $\text{H}(n\text{-Bu})_2\text{SnSn}(n\text{-Bu})_2\text{H}$ , polystannane  $[(n\text{-Bu})_2\text{Sn}]_n$  and various cyclic stannanes  $[(n\text{-Bu})_2\text{Sn}]_n = 5,6$ . Further evidence for  $[(n\text{-Bu})_2\text{Sn}]_n$  was afforded by GPC where a broad, moderate molecular weight, but highly dispersed polymer was obtained ( $M_w = 1.8 \times 10^4$  Da, PDI = 6.9) and a characteristic UV-Vis absorbance ( $\lambda_{\text{max}}$ ) of  $\approx 370$  nm observed.

## Acknowledgements

It is a pleasure to thank all who made this thesis possible. Firstly, I gratefully acknowledge Dr. Daniel Foucher for his supervision, advice and guidance throughout the work. I am grateful to him in every possible way and hope that he will provide me the opportunity to work under his supervision in the future.

Secondly, I would like to convey my gratitude to Dr. Robert Gossage for his advice, and supervision which made it possible to complete my thesis work on time.

I also deeply indebted to Dr. Stephen Wylie for his valuable discussions and supervision in molecular modeling portion of this work. I gratefully thank Dr. Russ Viirre for his advice and guidance.

I am thankful to the people at the University of Toronto who are instrumental in support of this thesis, Dr. Alex Young for MS and Dr. Alan Lough for crystallography. I would like to extend my thanks to Damion Miles for his advice and willingness to share his bright thoughts with me and Sossina Gezahegn whose presence was always helpful and memorable. Thanks must also be extended to Jon Ward for using his physical power when it is required to complete some heavy lifting assignments in lab and to Shawn Mcfadden for helping to solve the technical issues in RUAC.

Special thanks to my parents for their eternal support and prayers. My special thanks go to my wife Gulshan Ara whose dedication and confidence in me which enabled me to take this load on my shoulders.

Finally I would like to thank Ryerson University and the Molecular Science Graduate Program who give me the opportunity to complete this research.

# **Dedication**

Dedicated to my parents and wife Gulshan Ara  
and  
Sons Rizwan, Shahryar and Shehroze

## Table of contents

### **1.0 Introduction**

|        |   |    |
|--------|---|----|
| 1.1    | Group 14 and Group 14 Polymers                        | 1  |
| 1.2    | Polystannanes   |    |
| 1.2.1  | History of Tin Compounds/Polystannanes                | 3  |
| 1.2.2  | Synthesis of Polystannanes                            | 7  |
| 1.2.3  | Characterization of Polystannanes                     | 14 |
| 1.2.3a | Nuclear Magnetic Resonance                            | 14 |
| 1.2.3b | Gel Permeation Chromatography                         | 18 |
| 1.2.3c | Thermal Analysis                                      | 19 |
| 1.2.4  | Structural and Electronic Properties of Polystannanes | 23 |
| 1.3    | Insertion of Alkyne into a Sn-Sn bond                 | 27 |
| 1.4    | Distannanes and Oligostannanes                        | 31 |
| 1.5    | Molecular Modeling of Oligostannanes                  | 33 |
| 1.6    | Molecular Modeling Approaches                         | 34 |
| 1.6.1  | Density Functional Model                              | 35 |
| 1.6.2. | Semi-Empirical Models                                 | 35 |
| 1.6.3. | Molecular Mechanic model                              | 35 |
| 1.6.4  | Calculated (gas phase) Vs Crystallographic Data       | 36 |
| 1.7    | Objectives  | 38 |

### **2.0 Experimental**

|     |           |    |
|-----|-----------|----|
| 2.1 | General   | 39 |
| 2.2 | Materials | 40 |

|        |   |    |
|--------|---|----|
| 2.3    | Polystannanes   |    |
| 2.3.1  | Synthesis of <i>n</i> -Bu <sub>2</sub> SnH <sub>2</sub> <b>13</b>   | 40 |
| 2.3.2  | Polymerization of <b>13</b>   | 41 |
| 2.3.3  | Polymerization of <b>13</b> using Pd(PPh <sub>3</sub> ) <sub>4</sub> <b>27</b>  | 42 |
| 2.4    | Insertion of alkynes into Sn-Sn bond  |    |
| 2.4.1  | Synthesis of ( <i>n</i> -Bu) <sub>3</sub> SnCH=CHSn( <i>n</i> -Bu) <sub>3</sub> <b>50</b>   | 43 |
| 2.4.1a | Reaction of ( <i>n</i> -Bu) <sub>3</sub> SnSn( <i>n</i> -Bu) <sub>3</sub> <b>45</b> with C <sub>2</sub> H <sub>2</sub> <b>25</b> in toluene | 43 |
| 2.4.1b | Reaction of <b>45</b> with <b>25</b> in dioxane   | 43 |
| 2.4.2  | Synthesis of Me <sub>3</sub> SnCH=CHSnMe <sub>3</sub> <b>30</b>   | 44 |
| 2.4.3  | Reaction of (nBu <sub>2</sub> Sn) <sub>6</sub> <b>7</b> with <b>25</b>  | 45 |
| 2.4.4  | Reaction of <b>5</b> with <b>25</b>   | 46 |
| 2.4.5  | Reaction of Me <sub>3</sub> SnSnMe <sub>3</sub> <b>29</b> with PhC≡CH <b>26</b>   | 47 |
| 2.5    | Distannanes and Oligostannanes  |    |
| 2.5.1  | Large scale thermal dehydrocoupling of <b>43</b> under reduced pressure<br>(open system)  | 49 |
| 2.5.2  | Small scale thermal dehydrocoupling of <b>43</b> under reduced pressure<br>(open system)  | 49 |
| 2.5.3  | Small scale thermal dehydrocoupling of <b>43</b> under reduced pressure<br>(closed system)  | 49 |
| 2.5.4  | Small scale thermal dehydrocoupling of <b>43</b> under inert atmosphere<br>(open system)  | 50 |
| 2.5.5  | Small scale thermal dehydrocoupling of <b>44</b> under reduced pressure<br>(open system)  | 50 |

|       |  |    |
|-------|--|----|
| 2.5.6 | Small scale thermal dehydrocoupling of <b>44</b> under reduced pressure<br>(closed system)               | 51 |
| 2.5.7 | Small scale thermal dehydrocoupling of <b>43</b> and <b>44</b> under reduced pressure<br>(closed system) | 51 |
| 2.5.8 | Small scale thermal dehydrocoupling of <b>13</b> under nitrogen<br>(open system)                         | 52 |
| 2.5.9 | Small scale thermal dehydrocoupling of <b>13</b> under reduced pressure<br>(Open system)                 | 52 |
| 3.0   | <b>Results and Discussion</b>  |    |
| 3.1   | Polystannanes  |    |
| 3.1.1 | Di- <i>n</i> -butylstannane <b>13</b>  | 54 |
| 3.1.2 | Poly di- <i>n</i> -butylstannane <b>5</b>  | 55 |
| 3.2   | Inserted distannanes and oligostannanes  | 57 |
| 3.2.1 | Hexa- <i>n</i> -butyldistannyl ethylene <b>50</b>  | 57 |
| 3.2.2 | Insertion of acetylene in ( <i>n</i> Bu <sub>3</sub> Sn) <sub>n</sub> <b>5</b>                           | 62 |
| 3.2.3 | Hexamethyldistannyl ethylene <b>30</b>   | 64 |
| 3.2.4 | Hexamethyl-1-phenyldistannyl ethylene <b>32</b>  | 66 |
| 3.3   | Distannanes and oligostannanes   | 71 |
| 3.4   | Modelling of oligostannanes and alkyne inserted stannanes  | 78 |
| 4.0   | Conclusion   | 83 |
| 5.0   | Future work  | 85 |
| 6.0   | References   | 86 |

## List of Tables

|     |   |    |
|-----|---|----|
| 1.1 | Electronegativities, Covalent Radii, and some mean Bond Energies<br>(kJ/mol) for Group 14 elements                  | 2  |
| 1.2 | Historical timeline of polystannanes  | 4  |
| 1.3 | $^{119}\text{Sn}$ NMR spectroscopic data for poly(dialkylstannane)s   | 15 |
| 1.1 | $^1\text{H}$ NMR spectroscopic data for poly(dialkylstannane)s  | 16 |
| 1.5 | $^{119}\text{Sn}$ NMR spectroscopic data for poly(diarylstannane)s  | 17 |
| 1.6 | Molecular weight data of polystannanes  | 18 |
| 1.7 | TGA data of poly(dialkylstannane)s and poly(diarylstannane)s  | 19 |
| 1.8 | Transition temperatures of poly(dialkylstannane)s   | 20 |
| 1.9 | UV Spectroscopic data for polystannanes   | 25 |
| 3.1 | Fragmentation of <b>42</b>  | 61 |
| 3.2 | $^{119}\text{Sn}$ NMR data of <b>30</b>   | 64 |
| 3.3 | $^{119}\text{Sn}$ NMR data of <b>32</b>   | 66 |
| 3.4 | Catalyst and solvent free coupling of tin hydrides  | 73 |
| 3.5 | Bond angles $\alpha(\text{Sn}-\text{Sn}^x-\text{Sn})$ and bond lengths $d(\text{Sn}^x-\text{Sn}^y)$ of tin skeleton | 78 |
| 3.6 | Calculated and experimental values of $\lambda_{\text{max}}$ of polytin species                                     | 80 |
| 3.7 | Calculated values $\lambda_{\text{max}}$ of alkyne inserted distannanes and oligostannanes                          | 81 |
| 3.8 | Calculated values $\lambda_{\text{max}}$ of distannanes and oligostannanes  | 82 |

## List of Figures

|     |   |    |
|-----|---|----|
| 1.1 | Schematic representation of linear polystannane macromolecule   | 4  |
| 1.2 | Schematic representation of the structure 15-crown-5  | 8  |
| 1.3 | (a) DSC thermograms of poly(dioctylstannane)  |    |
|     | (b) Optical microscopy images   | 22 |
| 1.4 | Molecular structures of <b>20(a-d)</b> with average Sn-Sn bond length (pm)  |    |
|     | and Sn-Sn-Sn bond angles  | 24 |
| 1.5 | Various stannanes   | 31 |
| 1.6 | $\alpha$ , $\omega$ - polystannane oligomers <b>49</b>  | 33 |
| 1.7 | Curves for the calculated (Sandorfy model C) energy differences<br>(LUMO-HUMO) and observed transition frequencies as a function<br>of chain length | 34 |
| 2.1 | The chemical structures of <b>13</b> , <b>5</b> and $[(n\text{-Bu})_2\text{Sn}]_{n=5,6}$ <b>6</b> and <b>7</b>                                      | 41 |
| 2.2 | The chemical structures of <b>45</b> , <b>50</b> and <b>42</b>  | 43 |
| 2.3 | The chemical structures of <b>29</b> , <b>30</b> and $\text{Me}_3\text{SnOH}$ <b>52</b>   | 44 |
| 2.4 | The chemical structure of inserted $(n\text{Bu}_2\text{Sn})_n$ <b>53</b>  | 46 |
| 2.5 | The chemical structures of <b>32</b> and $\text{Me}_3\text{SnCPh=CH-CH=CPhSnMe}_3$ <b>55</b>  | 47 |
| 3.1 | $^{119}\text{Sn}$ NMR spectrum of <b>7</b>  | 56 |
| 3.2 | $^{13}\text{C}$ NMR spectrum of <b>50</b>   | 58 |
| 3.3 | $^{119}\text{Sn}$ NMR spectrum of <b>50</b>   | 59 |
| 3.4 | Mass spectrum of <b>42</b>  | 60 |
| 3.5 | $^{119}\text{Sn}$ NMR spectrum of <b>42</b>   | 61 |
| 3.6 | $^{119}\text{Sn}$ NMR spectrum of the inserted <b>53</b>  | 63 |

|      |  |    |
|------|--|----|
| 3.7  | ORTEP representation of units of <b>52</b> <sup>[75]</sup> in the unit cell  | 65 |
| 3.8  | ORTEP representation of units of <b>55</b> <sup>[75]</sup> in the unit cell  | 67 |
| 3.9  | Proposed mechanism 1 for the double insertion of Phenylacetylene   | 69 |
| 3.10 | Proposed mechanism 2 for the double insertion of Phenylacetylene   | 70 |
| 3.11 | <sup>119</sup> Sn NMR spectra of the products from the dehydrocoupling of <b>43</b> at<br>A) 4h @ 200°C and B) 5h @ 200°C under static reduced pressure      | 72 |
| 3.12 | <sup>119</sup> Sn NMR spectrum of the products from the dehydrocoupling<br>of <b>43</b> and <b>44</b> at 200°C for 5h. Peaks with an asterisk are unassigned | 74 |
| 3.13 | UV-Vis (THF) spectrum of the mixture containing <b>5</b>   | 75 |

## List of Reactions

|        |  |    |
|--------|--|----|
| 1.2.1  | Wurtz-type coupling of $n\text{Bu}_2\text{SnCl}_2$ in the presence of the ether<br>15-crown-5  | 8  |
| 1.2.2  | Wurtz-type coupling of $n\text{Bu}_2\text{SnCl}_2$ in the presence of the ether<br>15-crown-5 using Na dispersion in toluene                                     | 8  |
| 1.2.3  | Synthesis of poly(dialkylstannane)s using $\text{SmI}_2/\text{HMPA-THF}$ or<br>alkali earth metal (Mg, Ca) vapour solvent cocondensates under<br>mild conditions | 9  |
| 1.2.4  | Catalytic dehydrogenation of <b>13</b> using $\text{Cp}_2\text{ZrMe}_2$  | 10 |
| 1.2.5  | Three step reaction to prepare the polymerizable tin dihydrides<br>from tetraarylstannanes   | 10 |
| 1.2.6  | Catalytic dehydrogenation of diaryltin dihydride using $\text{Cp}_2\text{ZrMe}_2$  | 11 |
| 1.2.7  | Electrochemical synthesis of poly(dibutylstannane) $[n\text{-Bu}_2\text{Sn}]_n$ and<br>poly(dioctylstannane) $[n\text{-Oct}_2\text{Sn}]_n$                       | 11 |
| 1.2.8  | Catalytic dehydropolymerization of <b>13</b> using $\text{RhCl}(\text{PPh}_3)_3$   | 12 |
| 1.2.9  | Polymerization of di( $\omega$ -alkylphenyl)stannane)s using $\text{RhCl}(\text{PPh}_3)_3$   | 13 |
| 1.2.10 | Copolymerization of $(\text{PhC}_3\text{H}_6)_2\text{SnH}_2$ and $n\text{Bu}_2\text{SnH}_2$ using $\text{RhCl}(\text{PPh}_3)_3$                                  | 13 |
| 1.2.11 | Synthesis Of <b>20(a-d)</b>  | 23 |
| 1.3.1  | Synthesis of alkylstannylene polymers by coupling of aminostannanes<br>and terminal alkynes  | 27 |
| 1.3.2  | Insertion of acetylene into the Si-Si bond of a ferrocenyldisilane using<br>$\text{Pd}(\text{PPh}_3)_4$  | 28 |
| 1.3.3  | Insertion of acetylene and 1-alkynes into hexaalkyldistannanes   | 28 |

|       |   |    |
|-------|---|----|
| 1.3.4 | Insertion of acetylenes into Si-Si bonds using Pd(dba) <sub>2</sub> -P(OCH <sub>2</sub> ) <sub>3</sub> CEt <b>34</b><br>catalyst system | 29 |
| 1.3.5 | Insertion of alkynes into tin bridged [2] ferrocenophane using Pt(0)-<br>mediated catalysis   | 30 |
| 1.4.1 | Reaction of <b>42</b> with <b>43</b>  | 32 |
| 1.4.2 | Synthesis of <b>45</b> from <b>43</b>   | 32 |
| 3.1.1 | Synthesis of <b>13</b> from <i>n</i> Bu <sub>2</sub> SnCl <sub>2</sub> <b>1</b>   | 55 |
| 3.1.2 | Synthesis of <b>5</b> from <b>13</b> using RhCl(PPh <sub>3</sub> ) <sub>3</sub>   | 55 |
| 3.1.3 | Synthesis of <b>7</b> from <b>13</b> using Pd(PPh <sub>3</sub> ) <sub>4</sub>   | 56 |
| 3.2.1 | Reaction of <b>45</b> and acetylene in toluene using Pd(PPh <sub>3</sub> ) <sub>4</sub>   | 57 |
| 3.2.2 | Reaction of <b>45</b> and acetylene in dioxane using Pd(PPh <sub>3</sub> ) <sub>4</sub>   | 58 |
| 3.2.3 | Decomposition of <b>50</b>  | 59 |
| 3.2.4 | Reaction of <b>5</b> with acetylene   | 62 |
| 3.2.5 | Synthesis of <b>30</b>  | 64 |
| 3.2.6 | Decomposition of <b>30</b>  | 65 |
| 3.2.7 | Synthesis of <b>32</b>  | 66 |
| 3.2.8 | Reaction of <b>29</b> with PhC≡CH <b>26</b> without catalyst  | 66 |
| 3.2.9 | Synthesis of hexamethyl-1,4-diphenydistannyl-1,3-butadiene <b>55</b>  | 67 |
| 3.3.1 | Thermal dehydrocoupling reaction of <b>13</b> at 160°C  | 74 |
| 3.3.2 | Thermal dehydrocoupling reaction of <b>13</b> at 200°C  | 76 |

## Abbreviations

|                               |                                     |
|-------------------------------|-------------------------------------|
| A <sup>o</sup>                | Angstrom                            |
| KJ                            | Kilojoule                           |
| Da                            | Daltons                             |
| Bu                            | Butyl                               |
| C <sub>6</sub> D <sub>6</sub> | deuterated benzene                  |
| CDCl <sub>3</sub>             | per-deuterated choloform            |
| DSC                           | Differential scanning colorimetry   |
| Dod                           | Dodecyl                             |
| eV                            | Electron volts                      |
| Et                            | Ethyl                               |
| GPC                           | Gel permeation chromatography       |
| Hex                           | Hexyl                               |
| HOMO                          | Highest occupied molecular orbital  |
| HMO                           | Hückel molecular orbital            |
| LUMO                          | Lowest unoccupied molecular orbital |
| NMR                           | Nuclear magnetic resonance          |
| Oct                           | Octyl                               |
| Pn                            | Pentyl                              |
| Ph                            | Phenyl                              |
| PDI                           | Polydispersity index                |
| Pr                            | Propyl                              |
| TGA                           | Thermogravimetric analysis          |

|       |                                 |
|-------|---------------------------------|
| UV    | Ultraviolet                     |
| UVA   | Ultraviolet absorber            |
| $M_w$ | Weight average molecular weight |

# CHAPTER ONE

## INTRODUCTION

### 1.1 Group 14 and Group 14 Polymers:

The elements of Group 14 have a clear trend from nonmetallic to metallic behaviour. While carbon is clearly non-metallic, silicon and germanium are considerably semimetallic with tin and lead being clearly metallic. Carbon atoms are unable to expand their valence shell beyond the octet, while the other elements in the family experience hypervalency due to the availability of valence shell *d* orbitals in Si and Ge and *d* and *f* orbitals for Sn and Pb. The empty orbitals are able to accept electrons from nucleophiles.

There is a significant decrease in tendency towards catenation upon descending in Group 14 from carbon to lead. This is evident by the enormous number of known linear and branched polyalkanes, numerous examples of polysilanes, some polygermanes, a few polystannanes and to date, no polyplumbanes. This significant decrease in catenation can be explained partially in terms of the decreasing strength of catenated bond; i.e., C-C = 347 kJ/mol, Si-Si = 220 kJ/mol, Ge-Ge = 170 kJ/mol, Sn-Sn = 150 kJ/mol and Pb-Pb = 86 kJ/mol.<sup>[1]</sup> Furthermore, there is decrease in the strength of single bonds between Group 14 and other elements from carbon to lead (Table 1.1).<sup>[1]</sup> The strength of Group 14 bonds to some extent is parallel to the covalent character of these bonds.

Most compounds of Group 14 elements are tetravalent with a trend towards divalency with increasing atomic number.

**Table 1.1** Electronegativities, Covalent Radii, and some mean Bond Energies (kJ/mol) for Group 14 elements <sup>[1]</sup>

|                             | <b>C</b> | <b>Si</b> | <b>Ge</b> | <b>Sn</b> | <b>Pb</b> |
|-----------------------------|----------|-----------|-----------|-----------|-----------|
| Electronegativity (Pauling) | 2.54     | 1.90      | 2.01      | 1.96      | 2.33      |
| Covalent Radius, nm         | 0.077    | 0.117     | 0.122     | 0.141     | 0.154     |
| M-H                         | 412      | 318       | 310       | 300       | ---       |
| M-C                         | 347      | 301       | 242       | ---       | ---       |
| M-Cl                        | 338      | 401       | 339       | 314       | ---       |
| M-Br                        | 276      | 310       | 280       | 270       | ---       |
| M-I                         | 238      | 230       | 210       | 190       | ---       |
| M-O                         | 360      | 466       | ---       | 540       | ---       |

Tin is the first metallic element of Group 14. It is poorly malleable and only partially oxidized in air due to the formation of a transparent oxide layer at its surface.<sup>[2]</sup> Tin is usually found with an oxidation number of +2 or +4 due to its position in the periodic table. For example, SnCl<sub>2</sub> is a stable hygroscopic compound while stannylenes, SnR<sub>2</sub> (R = alkyl or aryl), are highly reactive species similar to carbenes.

Organotin compounds have found a variety of applications as polymerization catalysts and stabilizers, herbicides or biocides<sup>[3]</sup> and selective uses in medicines though in recent years have found less favour due to environmental considerations. In industry, they are commonly used for the stabilization of poly(vinyl chloride)<sup>[10,4]</sup>, the catalytic formation of polyurethanes and the cold temperature vulcanization of silicon polymers.

Their biological properties include uses as antifouling paints on ships (now banned by legislation), in wood preservatives and as agricultural fungicides and insecticides. In medicine, several organotin compounds have shown promise in cancer therapies and in the treatment of fungal infections.<sup>[5]</sup>

The environmental interest towards the exclusion of organotin compounds in polymers is due to the federal level legislation in many countries that has largely curtailed the use of monomeric organotin compounds in paints and coatings. It is widely accepted that through migration of tin species they inhibit and kill nearby plant and animal life. Chemically bound organotin has, however been permitted by legislation. Thus there is activity to create non-migrating chemically bound organotin materials.

The commercial importance of Group 14 polymers is dominated by silicon chemistry. At this time, there are relatively few uses of Ge or Sn containing polymers<sup>[6-12]</sup> with the exception of organotin compounds that are used industrially as polymerization catalysts. Polysiloxanes represent the largest bulk use of Group 14 polymers and represent the highest worldwide sales for inorganic polymers. Pb containing polymers rank last in the Group 14 series due to their poor solubility, the lack of availability of suitable monomers and their potential toxicity.

## **1.2 Polystannanes:**

### **1.2.1 History of Tin Compounds/Polymers:**

Tin is the only metallic element reported to form organometallic polymers with a backbone consisting entirely of metal atoms covalently bonded to each other. These are referred to as polystannanes and are expected to have significant and useful electrical properties because of the delocalization of electrons along the tin backbone.<sup>[13]</sup>

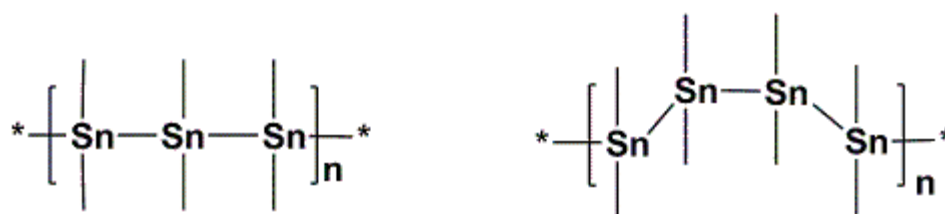


**Figure 1.1** Schematic representation of linear polystannane macromolecule

**Table 1.2** Historical timeline of polystannanes:

| Year | Development  |
|------|--|
| 1849 | Franklin created first organotin compound <sup>[14]</sup>  |
| 1852 | Löwing published first preparation of oligo- or polystannanes <sup>[15]</sup>  |
| 1858 | Cahours confirmed Löwing's results <sup>[16,17]</sup>  |
| 1870 | Ladenberg reported the presence of Sn-Sn bond <sup>[20]</sup>  |
| 1917 | Grüttner confirmed Ladenberg's results <sup>[19]</sup>   |
| 1961 | Oligomeric stannanes isolated <sup>[25]</sup>  |
| 1992 | Zhou reported the first evidence of $(n\text{Bu}_2\text{Sn})_n$ by Wurtz coupling <sup>[27]</sup>  |
| 1993 | Tilley reported polystannanes by catalytic dehydrocoupling <sup>[31]</sup>   |
| 1995 | Okano reported polystannanes by electrochemical coupling <sup>[34]</sup>   |
| 2005 | Casari <i>et al.</i> reported the synthesis of dialkyl polystannanes by using Wilkinson's catalyst <sup>[35]</sup>                                 |
| 2009 | Casari <i>et al.</i> demonstrated the cyclic free polymerization of di( $\omega$ -alkylphenyl)stannanes using Wilkinson's catalyst <sup>[36]</sup> |

Compounds containing hydrocarbon groups bonded to a central tin atom are referred to as organotin compounds or stannanes. The first organotin compound was reported by Sir Edward Frankland in 1849.<sup>[14]</sup> The first preparation of oligo- or polystannanes was published by Löwing in 1852.<sup>[15]</sup> He prepared oligo(diethylstannane)s or poly(diethylstannane)s by reacting iodoethane with Sn/K or a Sn/Na alloy. This is an exothermic reaction done in the presence of quartz sand to control the reaction rate. Cahours obtained similar products from a Wurtz type reaction.<sup>[16, 17]</sup> "Stannic ethyl" as a polymeric compound with the composition  $(\text{SnC}_2\text{H}_5)_n$  was also formulated in 1858.<sup>[18]</sup> In 1917, Grüttner<sup>[19]</sup> reinvestigated results on hexaethyldistannanes reported by Ladenberg<sup>[20]</sup> (1870) and confirmed the presence of Sn-Sn bonds. He predicted that tin could form a chain like polymeric material. Until 1900, only 37 papers were published on organotin compounds. In 1903, Pope and Peachey described the preparation of a number of simple and mixed tetraalkyl stannanes, and of triphenyltin, from Grignard reagents and tin tetrachloride or alkyltin halides.<sup>[21,22]</sup>

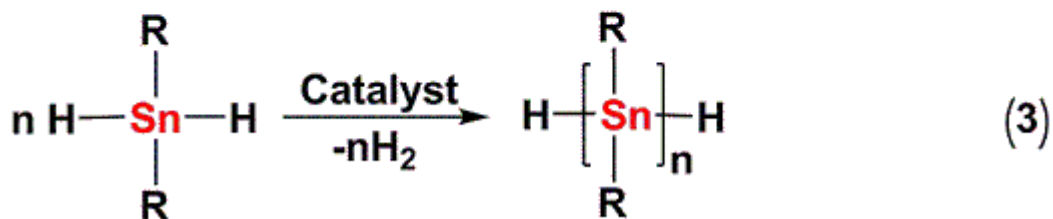
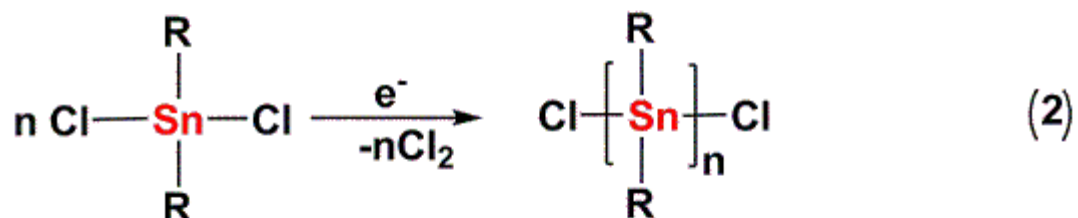
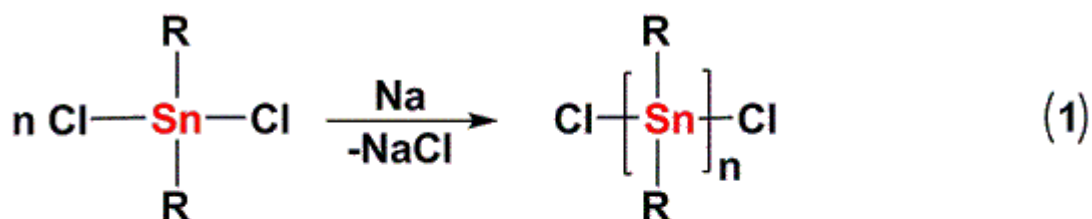
In 1943, Clauson Kass postulated that the yellow colour of diphenyltin is due to its polymeric nature.<sup>[23]</sup> A bathochromic shift of the wavelength at maximum absorption was established in the case of oligo(dibutylstannane)s having up to fifteen Sn atoms.<sup>[13,24]</sup> In 1961, the previously reported hexameric diethyltin was identified as a cyclic six-membered oligostannane.<sup>[25]</sup> After few years, the formation of crystalline cyclic-nonamers and waxy cyclic-hexamers of "diethyltin" were also isolated.<sup>[26]</sup> In 1992, the Wurtz coupling of dibutyldichlorostannane was reported to yield both linear poly(dibutylstannane) as well as oligomers.<sup>[27]</sup> In 1996 Molloy *et al.*<sup>[28]</sup> identified milder Wurtz conditions to isolate very high molecular weight polystannane.

Dräger and co-workers in 1987 showed that linear oligostannanes with up to six tin atoms can be prepared and that the  $\sigma$ - $\sigma^*$  UV-Vis transition moves dramatically to lower energy as the chain length is increased. This led him to propose the term “molecular metals” for prospective high molecular weight analogues.<sup>[29]</sup> Polystannanes are of much interest because of the involvement of their  $\sigma$ -delocalization backbone and  $\sigma$ - $\pi$  overlap when for instance they are coupled with arenes and acetylenes. Polystannanes would be expected to have more  $\sigma$  delocalized structures than polysilanes and polygermanes.

## 1.2.2 Synthesis of Polystannanes:

The following three strategies can be used for the synthesis of polystannanes:

- 1) Wurtz coupling
- 2) Catalytic dehydrogenation
- 3) Electrochemical coupling



**Scheme 1.1** Three common routes used to prepare polystannanes: (1) Polymerization of tin dichloride by Wurtz like reactions, (2) Electrochemical coupling of tin dichlorides and (3) Catalytic dehydropolymerization of tin dihydrides.

In 1992, Zou and co-workers reported the first synthesis of high molecular weight organotin polymers. This was done by using the Wurtz-type coupling of  $n\text{Bu}_2\text{SnCl}_2$  in the presence of the ether 15-crown-5.<sup>[27]</sup>

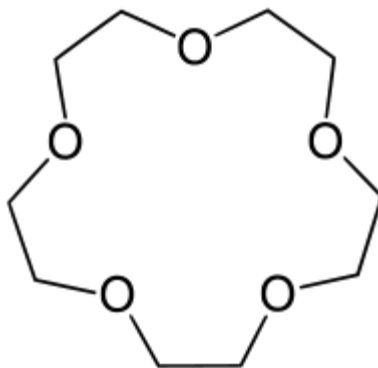
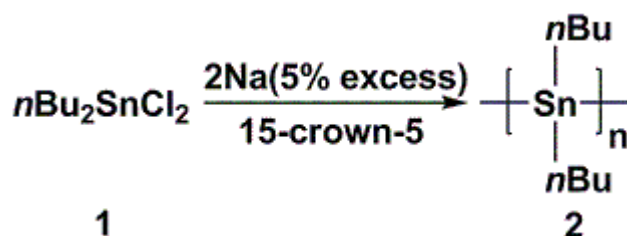


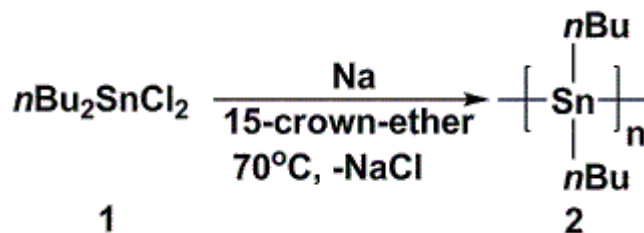
**Figure 1.2** Schematic representation of the structure of 15-crown-5

### Reaction 1.2.1



Molloy and co-workers have improved the preparation of  $[n\text{Bu}_2\text{Sn}]_n$  by carefully controlling the reaction involving  $n\text{Bu}_2\text{SnCl}_2$  with a fine sodium dispersion in the presence of 15-crown-5 in toluene at 60°C for 4 h.<sup>[28]</sup>

### Reaction 1.2.2

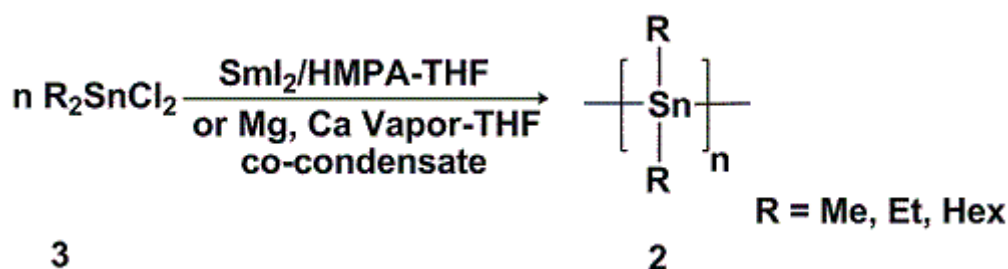


The formation of cyclic products such as  $[n\text{Bu}_2\text{Sn}]_5$  and  $[n\text{Bu}_2\text{Sn}]_6$  occur when the reaction time was increased. The polymers possessed high molecular weights ( $\sim 10^6$  Da)

as determined by GPC and were further characterized by  $^{119}\text{Sn}$  NMR which readily distinguished between polymers and higher cyclic oligomers.

Mochida *et al.*<sup>[30]</sup> synthesized polystannanes using  $\text{SnI}_2$  or alkali earth metal (Mg, Ca) vapor solvent co-condensates under mild conditions. The molecular weights for these polystannanes are typically lower than those prepared by Wurtz coupling methods.

### Reaction 1.2.3

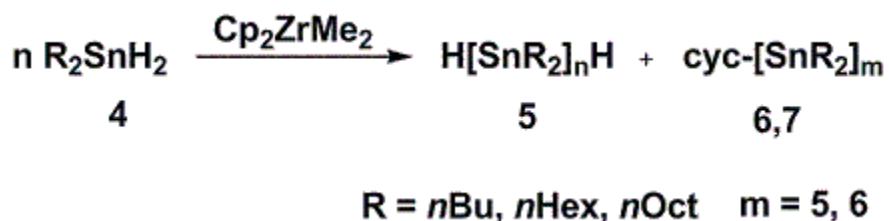


Catalytic dehydrogenation has been shown to be the most successful strategy for the monomers of the type  $\text{R}_2\text{SnH}_2$ .<sup>[31-34]</sup> These monomers are prepared by using a two step method involving the comproportionation reaction between equimolar  $\text{R}_4\text{Sn}$  and  $\text{SnCl}_4$  to produce two equivalents of  $\text{R}_2\text{SnCl}_2$  which is then reduced by  $\text{LiAlH}_4$  to yield the corresponding dihydrides. These dihydrides are typically both air and temperature sensitive.

Tilley prepared a series of poly(dialkylstannane)s from the catalytic dehydrogenation of  $\text{R}_2\text{SnH}_2$  using an organometallic zirconocene catalyst such as  $\text{Cp}_2\text{ZrMe}_2$ . The polymerization is initiated by dropwise addition of monomer to the catalyst. In these reactions, polymeric materials along with cyclic byproducts are formed. The main cyclic materials formed are the five-membered  $[\text{nR}_2\text{Sn}]_5$  along with small amounts of the six-membered  $[\text{nR}_2\text{Sn}]_6$ . The molecular weights of the

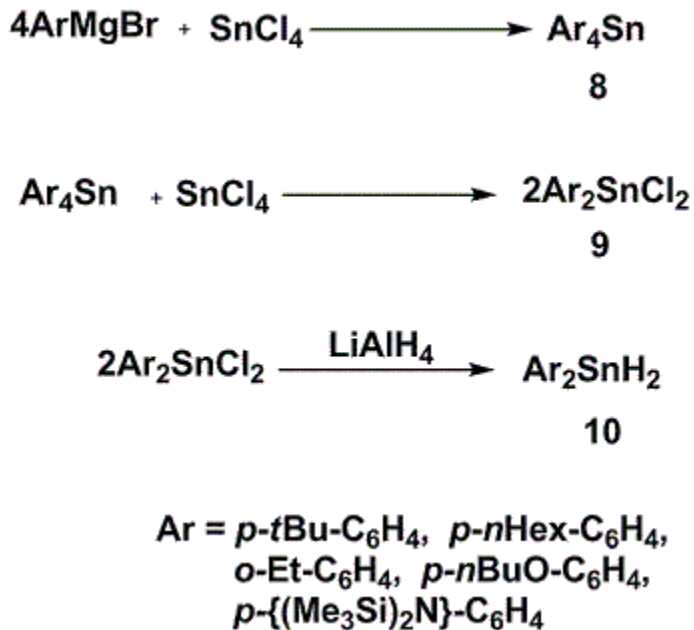
poly(dialkylstannane)s are considerably high as, for example, with  $\text{H}[n\text{Bu}_2\text{Sn}]_n\text{H}$  ( $M_w = 46,000$  Da) or  $\text{H}[n\text{Oct}_2\text{Sn}]_n\text{H}$  ( $M_w = 92,600$  Da).<sup>[31]</sup>

#### Reaction 1.2.4

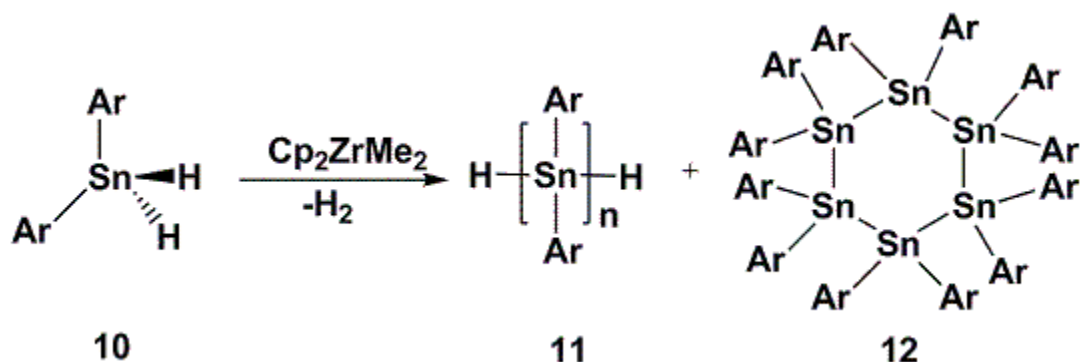


Poly(diarylstannane)s can also be synthesized by the same route as that of poly(dialkylstannane)s. This involves a three step procedure to first prepare the tetraarylstannanes, comproportionation to the dichlorostannane and finally a conversion to polymerizable tin dihydrides.

#### Reaction 1.2.5

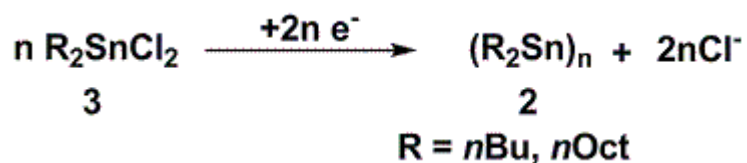


Like dialkylstannanes, dehydrogenation of diarylstannanes ( $\text{Ar}_2\text{SnH}_2$ ) is afforded by the use of metallocene catalysts. High molecular weight polymeric products along with cyclics are formed. Separation of the polymers from the cyclic rings is done by precipitation into polar solvents such as methanol.



Okano *et al.*<sup>[34]</sup> reported the first electrochemical synthesis of  $[n\text{-Bu}_2\text{Sn}]_n$  **5** and  $[n\text{-Oct}_2\text{Sn}]_n$  by using a cell consisting of a Pt cathode, Ag anode,  $[n\text{-Bu}_4\text{N}]^+[\text{ClO}_4]^-$  as supporting electrolyte and dry DME as solvent.

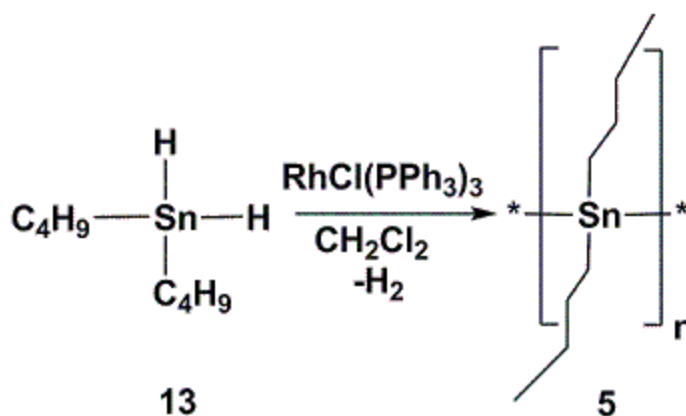
### Reaction 1.2.7



The highest molecular weight obtained by these methods for  $(n\text{-Bu}_2\text{Sn})_n$  was  $M_w = 1.09 \times 10^4$  Da (PDI = 2.6) and a  $\lambda_{\text{max}} = 381$  nm. Poly(dioctylstannane)  $[n\text{-Oct}_2\text{Sn}]_n$  was also isolated with a  $M_w = 0.59 \times 10^4$  Da (PDI = 1.7) and a  $\lambda_{\text{max}} = 378$  nm.

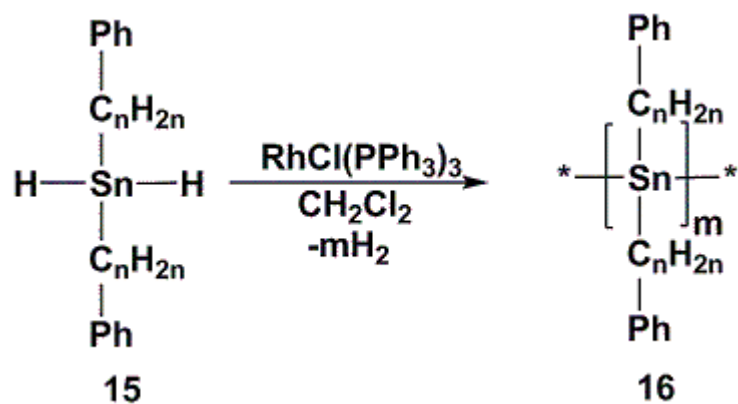
In 2005 Caseri *et al.*<sup>[35]</sup> presented a synthetic route to prepare **5** of relatively high molecular weight ( $M_w = 2.0 \times 10^4$  Da) through catalytic dehydropolymerization of **13** using  $\text{RhCl}(\text{PPh}_3)_3$  **14** as a catalyst. The polymer prepared by this method is entirely free of cyclic oligomers.

### Reaction 1.2.8



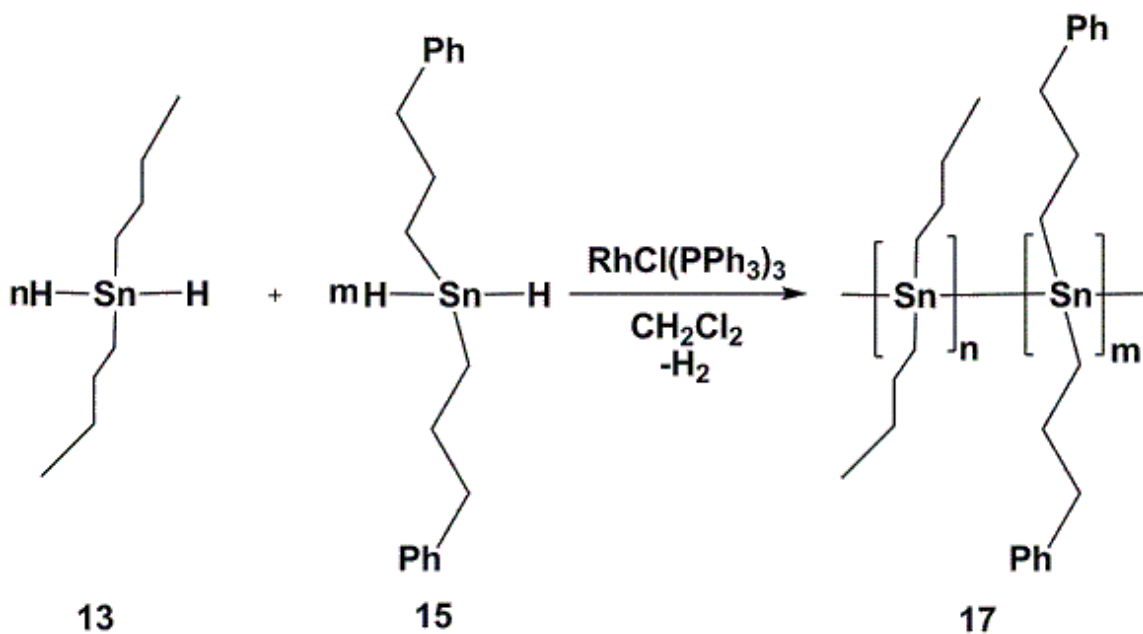
Caseri *et al.*<sup>[36]</sup> also demonstrated the polymerization of di( $\omega$ -alkylphenyl)stannane)s using **14** as catalyst, provided that the phenyl moieties are separated from the tin atom by at least two methylene groups. The poly(di( $\omega$ -alkylphenyl)stannane)s obtained were likewise free of any cyclic impurities.

### Reaction 1.2.9



A copolymer, poly(*n*-dibutylstannane-*co*-di(3-propylphenyl)stannane), was also produced from the addition of the catalyst **14** to a mixture of (PhC<sub>3</sub>H<sub>6</sub>)<sub>2</sub>SnH<sub>2</sub> **15** and **13** in CH<sub>2</sub>Cl<sub>2</sub>.

### Reaction 1.2.10



### 1.2.3 Characterization of Polystannanes:

The techniques commonly used for the characterization of polystannanes are NMR spectroscopy, gel permeation chromatography and thermal analysis.

#### 1.2.3a Nuclear magnetic resonance:

NMR spectroscopy is a useful tool for the characterization of polystannanes. Linear polymers and cyclic oligomers can be easily distinguished from each other by their distinct  $^{119}\text{Sn}$  NMR chemical shift values (Table 1.3).  $^{119}\text{Sn}$  NMR chemical shifts for the poly(dialkylstannane)s are typically around -190 ppm with the exception of poly(diethylstannane)s with a resonance at -172.2 ppm. The chemical shift values for the corresponding cyclic oligomers are shifted to higher field by approximately 10 ppm. The  $^{119}\text{Sn}$  NMR shifts for the poly(diarylstannane)s are also found  $\approx$  -190 ppm except for  $\text{H}[(o\text{-Et-}p\text{-}n\text{BuO-C}_6\text{H}_4)_2\text{Sn}]_n\text{H}$  which gives a resonance located at -125 ppm (Table 1.5).

**Table 1.3**  $^{119}\text{Sn}$  NMR spectroscopic data for poly(dialkylstannane)s

| Polymer  | $^{119}\text{Sn}$ ( $\delta$ ) ppm<br>(Linear chain) | $^{119}\text{Sn}$ ( $\delta$ ) ppm<br>(Cyclics) | Ref.<br>No. |
|--|--|---|-------------|
| $(\text{Et}_2\text{Sn})_n^a$                                     | -172.2   |   | 33          |
| $(\text{Pr}_2\text{Sn})_n^b$                                     | -194.8   |   | 33          |
| $(n\text{Bu}_2\text{Sn})_n^c$<br>$(n\text{Bu}_2\text{Sn})_n^b$   | -189.6<br>-190.6                                     | -200.9, -202.1<br>-201.9, -202.9                | 31<br>33    |
| $(n\text{Pn}_2\text{Sn})_n^b$                                    | -192.0   |   | 33          |
| $(n\text{Hex}_2\text{Sn})_n^c$<br>$(n\text{Hex}_2\text{Sn})_n^a$ | -190.9<br>-192.5                                     | -202.1, -202.7                                  | 31<br>33    |
| $(n\text{Oct}_2\text{Sn})_n^c$<br>$(n\text{Oct}_2\text{Sn})_n^a$ | -190.7<br>-192.1                                     | -201.8, -202.4                                  | 31<br>33    |
| $(n\text{Dod}_2\text{Sn})_n^b$                                   | -189.0   |   | 33          |

<sup>a</sup> Measured in dichloromethane- $d_2$ , <sup>b</sup> Measured in toluene- $d_8$ , <sup>c</sup> Measured in benzene- $d_6$

**Table 1.4**  $^1\text{H}$  NMR spectroscopic data for poly(dialkylstannane)s

| <b>Polymer</b>                          | <b><math>-\text{CH}_3</math><br/><math>^1\text{H}(\delta)</math> ppm</b> | <b><math>-\text{CH}_2</math><br/><math>^1\text{H}(\delta)</math> ppm</b> | <b><math>\text{Sn}-\text{CH}_2-</math></b> | <b><math>\text{Sn}-\text{CH}_2-</math></b> | <b>Ref.<br/>No.</b> |
|---|--|--|--|--|---------------------|
| $(\text{Et}_2\text{Sn})_n^{\text{a}}$   |  |  |  | m, 10H, 1.34                               | 33                  |
| $(\text{Pr}_2\text{Sn})_n^{\text{c}}$   | t, 6H, 1.2   | m, 4H, 1.54  | m, 4H, 1.87                                |  | 33                  |
| $(n\text{Bu}_2\text{Sn})_n^{\text{b}}$  | t, 6H, 1.13  | m, 8H, 1.62  | m, 4H, 1.80                                |  | 33                  |
| $(n\text{Pn}_2\text{Sn})_n^{\text{c}}$  | t, 6H, 1.10  | m, 12H, 1.63   | m, 4H, 0.97                                |  | 33                  |
| $(n\text{Hex}_2\text{Sn})_n^{\text{a}}$ | t, 6H, 0.81  | m, 16H, 1.22   | m, 4H, 1.45                                |  | 33                  |
| $(n\text{Oct}_2\text{Sn})_n^{\text{a}}$ | t, 6H, 0.90  | m, 24H, 1.30   | m, 4H, 1.55                                |  | 33                  |
| $(n\text{Dod}_2\text{Sn})_n^{\text{c}}$ | m, 6H, 0.96  | m, 40H, 1.38   | m, 4H, 1.97                                |  | 33                  |

<sup>a</sup> Measured in dichloromethane- $d_2$ , <sup>b</sup> Measured in benzene- $d_6$ , <sup>c</sup> Measured in toluene- $d_8$

**Table 1.5**  $^{119}\text{Sn}$  NMR spectroscopic data for poly(diarylstannane)s

| Polymer   | $^{119}\text{Sn}$ ( $\delta$ ) ppm | $^{119}\text{Sn}$ ( $\delta$ ) ppm<br>(Cyclics) | Ref. No. |
|---|------------------------------------|---|----------|
| $\text{H}[(p\text{-}^t\text{Bu-C}_6\text{H}_4)_2\text{Sn}]_n\text{H}^{\text{a}}$              | -197                               | -221  | 32       |
| $\text{H}[(p\text{-}^n\text{Hex-C}_6\text{H}_4)_2\text{Sn}]_n\text{H}^{\text{a}}$             | -196                               |   | 32       |
| $\text{H}[(p\text{-}^n\text{BuO-C}_6\text{H}_4)_2\text{Sn}]_n\text{H}^{\text{a}}$             | -183                               |   | 32       |
| $\text{H}[(o\text{-Et-}p\text{-}^n\text{BuO-C}_6\text{H}_3)_2\text{Sn}]_n\text{H}^{\text{a}}$ | -125                               | -180  | 32       |
| $\text{---}[(\text{PhC}_2\text{H}_4)_2\text{Sn}]_n\text{---}^{\text{b}}$                      | -187                               |   | 36       |
| $\text{---}[(\text{PhC}_3\text{H}_6)_2\text{Sn}]_n\text{---}^{\text{b}}$                      | -192.12                            |   | 36       |
| $\text{---}[(\text{PhC}_4\text{H}_8)_2\text{Sn}]_n\text{---}^{\text{b}}$                      | -190.48                            |   | 36       |

<sup>a</sup> Measured in benzene- $d_6$ , <sup>b</sup> Measured in dichloromethane- $d_2$

### 1.2.3b Gel Permeation Chromatography:

GPC using a RI detector is an efficient method for estimating the molar mass of the polystannanes relative to that of polystyrene standards. Table 1.6 shows typical values for polystannanes prepared by dehydrocoupling, Wurtz coupling and electrochemical

**Table 1.6** Molecular weight data of polystannanes

| Compound   | $M_w$<br>[g/mol] | $M_n$<br>[g/mol] | Polymerization Method                  | Ref. |
|--|------------------|------------------|--|------|
| (Me <sub>2</sub> Sn) <sub>n</sub>  | 1,120            |                  | SmI <sub>2</sub> in HMPA-THF           | 30   |
| (Et <sub>2</sub> Sn) <sub>n</sub>  | 31,000           | 13,000           | catalytic dehydrogenation <sup>a</sup> | 33   |
|  | 4,820            |                  | SmI <sub>2</sub> in HMPA-THF           | 30   |
|  | 4,100            |                  | Mg in THF                              | 30   |
|  | 3,700            |                  | Ca in THF                              | 30   |
| (Pr <sub>2</sub> Sn) <sub>n</sub>  | 27,000           | 10,000           | catalytic dehydrogenation <sup>a</sup> | 33   |
| (nBu <sub>2</sub> Sn) <sub>n</sub>   | 91,000           | 36,000           | catalytic dehydrogenation <sup>a</sup> | 33   |
|  | 17,500           | 7,800            | catalytic dehydrogenation <sup>b</sup> | 31   |
|  | 46,000           | 13,900           | catalytic dehydrogenation <sup>c</sup> | 31   |
|  | 10,900           |                  | Electrochemical synthesis              | 34   |
|  | 1,495,000        | 1,150,000        | Wurtz coupling                         | 28   |
| (nPe <sub>2</sub> Sn) <sub>n</sub>   | 48,000           | 19,000           | catalytic dehydrogenation <sup>a</sup> | 33   |
| (nHex <sub>2</sub> Sn) <sub>n</sub>  | 76,000           | 31,000           | catalytic dehydrogenation <sup>a</sup> | 33   |
|  | 36,800           | 15,300           | catalytic dehydrogenation <sup>b</sup> | 31   |
|  | 2,770            |                  | SmI <sub>2</sub> in HMPA-THF           | 30   |
| (nOct <sub>2</sub> Sn) <sub>n</sub>  | 97,000           | 40,000           | catalytic dehydrogenation <sup>a</sup> | 33   |
|  | 95,700           | 14,300           | catalytic dehydrogenation <sup>b</sup> | 31   |
|  | 92,600           | 21,700           | catalytic dehydrogenation <sup>c</sup> | 31   |
|  | 5,900            |                  | Electrochemical synthesis              | 34   |
| (nDod <sub>2</sub> Sn) <sub>n</sub>  | 28,000           | 19,000           | catalytic dehydrogenation <sup>a</sup> | 33   |
| H[( <i>p</i> - <sup><i>t</i></sup> Bu-C <sub>6</sub> H <sub>4</sub> ) <sub>2</sub> Sn] <sub>n</sub> H                | 56,000           | 16,700           | catalytic dehydrogenation <sup>c</sup> | 32   |
| H[( <i>p</i> - <sup><i>n</i></sup> Hex-C <sub>6</sub> H <sub>4</sub> ) <sub>2</sub> Sn] <sub>n</sub> H               | 48,200           | 20,000           | catalytic dehydrogenation <sup>c</sup> | 32   |
| H[( <i>p</i> - <sup><i>n</i></sup> BuO-C <sub>6</sub> H <sub>4</sub> ) <sub>2</sub> Sn] <sub>n</sub> H               | 12,000           | 7,000            | catalytic dehydrogenation <sup>c</sup> | 32   |
| H[( <i>o</i> -Et- <i>p</i> - <sup><i>n</i></sup> BuO-C <sub>6</sub> H <sub>4</sub> ) <sub>2</sub> Sn] <sub>n</sub> H | 4,400            | 4,000            | catalytic dehydrogenation <sup>c</sup> | 32   |

<sup>a</sup> Wilkinson's catalyst RhCl(PPh<sub>3</sub>)<sub>3</sub>

<sup>b</sup> CpCp\*Zr[Si(SiMe<sub>3</sub>)<sub>3</sub>Me

<sup>c</sup> Cp<sub>2</sub>ZrMe<sub>2</sub>

coupling. While Wurtz coupling typically yields higher molecular weight polymers, the distribution is often bimodal. By comparison dehydrocoupling and electrochemical

methods produced polydialkylstannanes of lower molecular weight, but more narrowly dispersed.

### 1.2.3c Thermal analysis:

Thermal properties are important as functional polymers are expected to work at various temperatures. The instruments typically used to study the thermal behaviour of materials are thermogravimetric analysis (TGA) and differential scanning calorimetry (DSC).

All polystannanes are reasonably thermally stable. They show a maximum rate of decomposition between 280-300°C in N<sub>2</sub> atmosphere, but in air the temperature range was 240-300°C (Table 1.7). Thermal stability of poly(dialkylstannane)s does not depend on the length of the alkyl chain.

**Table 1.7** TGA data of poly(dialkylstannane)s<sup>[31]</sup> and poly(diarylstannane)s<sup>[33]</sup>

| Polymer   | Atmosphere     | Onset temp for decomp.(°C) | % Ceramic yield      |
|---|----------------|----------------------------|----------------------|
| (nBu <sub>2</sub> Sn) <sub>n</sub> <sup>a</sup>   | N <sub>2</sub> | 255                        | 18                   |
|   | air            | 239                        | 53                   |
|   | O <sub>2</sub> | 196                        | 66                   |
| (nHex <sub>2</sub> Sn) <sub>n</sub> <sup>a</sup>  | N <sub>2</sub> | 265                        | 24                   |
|   | air            | 220                        | 50                   |
| (nOct <sub>2</sub> Sn) <sub>n</sub> <sup>a</sup>  | N <sub>2</sub> | 271                        | 34                   |
|   | air            | 245                        | 44                   |
| H[( <i>p</i> - <sup><i>t</i></sup> Bu-C <sub>6</sub> H <sub>4</sub> ) <sub>2</sub> Sn] <sub>n</sub> H <sup>b</sup>  | N <sub>2</sub> | 303                        | 30 (31) <sup>c</sup> |
|   | O <sub>2</sub> | 227                        | 39 (39) <sup>d</sup> |
| H[( <i>p</i> - <sup><i>n</i></sup> Hex-C <sub>6</sub> H <sub>4</sub> ) <sub>2</sub> Sn] <sub>n</sub> H <sup>b</sup> | N <sub>2</sub> | 313                        | 21 (27) <sup>c</sup> |
|   | O <sub>2</sub> | 188                        | 40 (34) <sup>d</sup> |
| H[( <i>o</i> -Et- <i>p</i> -C <sub>6</sub> H <sub>4</sub> ) <sub>2</sub> Sn] <sub>n</sub> H <sup>b</sup>            | N <sub>2</sub> | 203                        | 22 (36) <sup>c</sup> |
|   | O <sub>2</sub> | 209                        | 46 (46) <sup>d</sup> |
| H{[( <i>p</i> -(Me <sub>3</sub> Si)-C <sub>6</sub> H <sub>4</sub> ) <sub>2</sub> Sn] <sub>n</sub> H <sup>b</sup>    | N <sub>2</sub> | 214                        | 38 (20) <sup>c</sup> |
|   | O <sub>2</sub> | 194                        | 46 (26) <sup>d</sup> |
| H[( <i>p</i> - <sup><i>n</i></sup> BuO-C <sub>6</sub> H <sub>4</sub> ) <sub>2</sub> Sn] <sub>n</sub> H <sup>b</sup> | N <sub>2</sub> | 327                        | 28 (29) <sup>c</sup> |
|   | O <sub>2</sub> | 183                        | 43 (36) <sup>d</sup> |

<sup>a</sup> at 400°C. <sup>b</sup> at 550°C <sup>c</sup>Theoretical yield for tin metal. <sup>d</sup>Theoretical yield of SnO<sub>2</sub>.

The polymer  $H[(p\text{-}^n\text{Hex-C}_6\text{H}_4)_2\text{Sn}]_n\text{H}$  was stable up to 250 °C but incurred a 79% weight loss between 265-310 °C. The polymer  $H[(o\text{-Et-}p\text{-C}_6\text{H}_4)_2\text{Sn}]_n\text{H}$  was stable to 200 °C but showed a rapid weight loss between 330-390 °C. Comparatively  $H[(p\text{-}^n\text{BuO-C}_6\text{H}_4)_2\text{Sn}]_n\text{H}$  was stable below 214 °C, with 22% of its mass lost between 214-270 °C followed by a second weight loss of up to 40% between 275-400 °C.

### Differential scanning calorimetry (DSC) of the polystannanes:

Polystannanes with shorter side chains ( $\text{C}_2\text{-C}_4$ ) showed one thermally reversible phase glass transition ( $T_1$ ) but polystannanes with longer alkyl chain show a second thermally reversible liquid crystalline phase transition ( $T_2$ ) in the temperature range between -50 and +120 °C (Fig. 1.3a, Table 1.8).

**Table 1.8** Transition temperatures of poly(dialkylstannane)s<sup>[33]</sup>

| Polymer   | Transition temp (°C) |                   |
|---|----------------------|-------------------|
|   | First transition     | Second transition |
| $(\text{Et}_2\text{Sn})_n$ heating<br>cooling   | 1.5<br>6             |                   |
| $(n\text{Pr}_2\text{Sn})_n$ heating<br>cooling  | 93<br>63             |                   |
| $(n\text{Bu}_2\text{Sn})_n$ heating<br>cooling  | 1<br>-26             |                   |
| $(n\text{Pn}_2\text{Sn})_n$ heating<br>cooling  | 6<br>-16             | 57<br>42          |
| $(n\text{Hex}_2\text{Sn})_n$ heating<br>cooling | 34<br>21             | 68<br>43          |
| $(n\text{Oct}_2\text{Sn})_n$ heating<br>cooling | 29<br>13             | 74<br>58          |
| $(n\text{Dod}_2\text{Sn})_n$ heating<br>cooling | 55<br>39             | 91<br>80          |

It was commonly observed for polymeric species that the transition temperatures recorded upon cooling were lower (10-30 °C) than those transitions found during heating

and  $T_2$  increased as the length of the alkyl group increased, but there was no systematic trend in  $T_1$ .

Qualitative determination of the phase transitions of polystannanes were studied using a cross polarized optical microscope. The selected polystannanes were also investigated with X-ray diffraction. All polymers showed birefringent film behaviour below the first phase transition temperature. There was no evidence of change in birefringence upon heating above the first phase transition of thin films of poly(alkylstannane)s with C<sub>2</sub>-C<sub>5</sub> alkyl chain even up to 100°C. (*n*Hex<sub>2</sub>Sn)<sub>n</sub> and (*n*Dod<sub>2</sub>Sn)<sub>n</sub>, showed significantly weaker birefringence above the first transition temperature and completely disappeared for (*n*Oct<sub>2</sub>Sn)<sub>n</sub> above  $T_1$ . For (*n*Hex<sub>2</sub>Sn)<sub>n</sub> and (*n*Dod<sub>2</sub>Sn)<sub>n</sub>, birefringence was not seen above the second transition temperatures. (*n*Hex<sub>2</sub>Sn)<sub>n</sub>, (*n*Oct<sub>2</sub>Sn)<sub>n</sub> and (*n*Dod<sub>2</sub>Sn)<sub>n</sub> became significantly birefringent only at the temperatures lower than the first phase transition (Table 1.7).

It can be concluded from the optical microscope images that all samples, except (*n*Oct<sub>2</sub>Sn)<sub>n</sub>, still retain some order after the first phase transition. Heating above  $T_2$  caused a loss in orientation, which was unrecoverable by cooling. The initial orientation was unchanged when the sample was heated above the first transition temperature. The transition temperatures obtained for (*n*Hex<sub>2</sub>Sn)<sub>n</sub>, (*n*Oct<sub>2</sub>Sn)<sub>n</sub> and (*n*Dod<sub>2</sub>Sn)<sub>n</sub> were in general agreement with transition temperatures found in DSC thermograms.

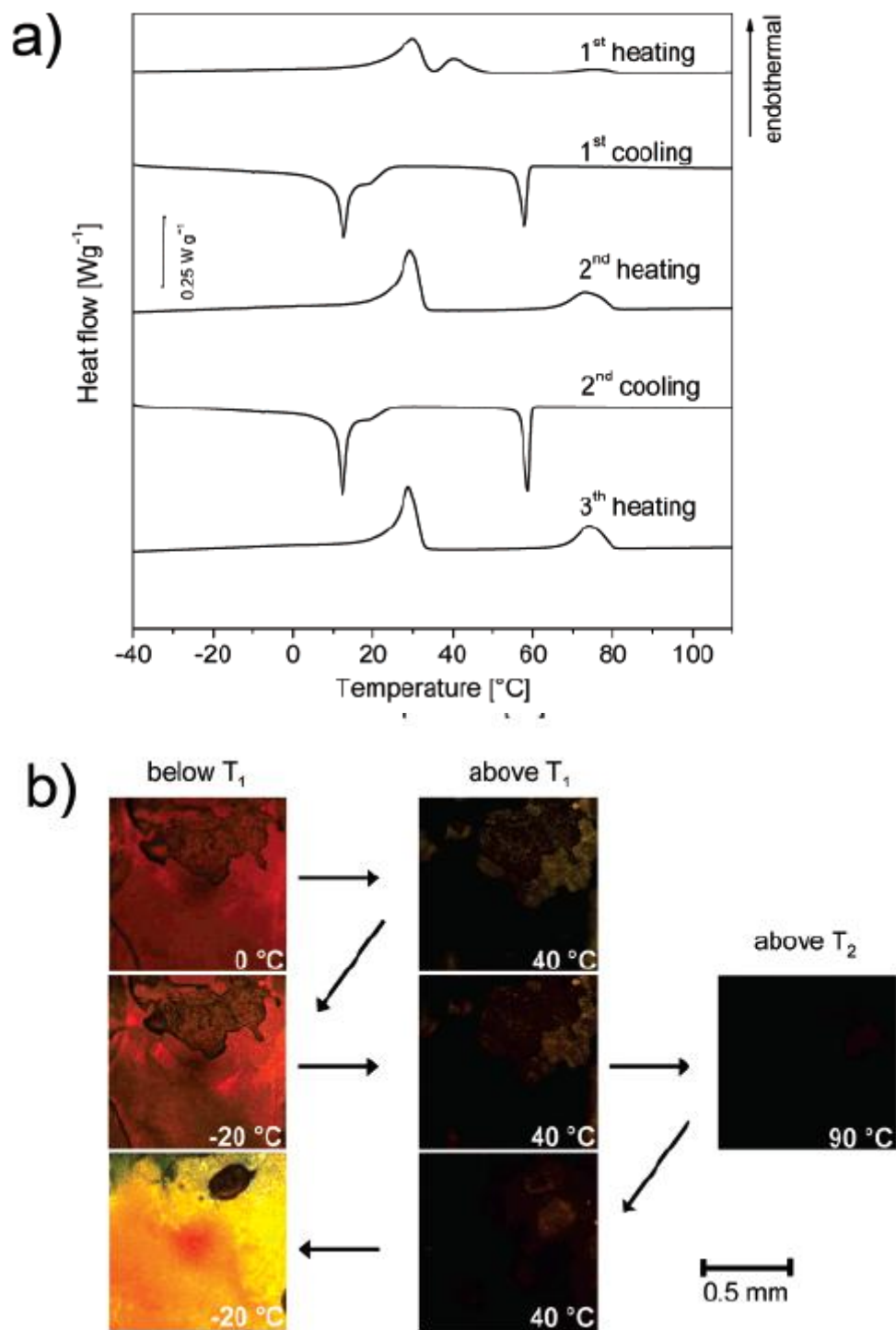
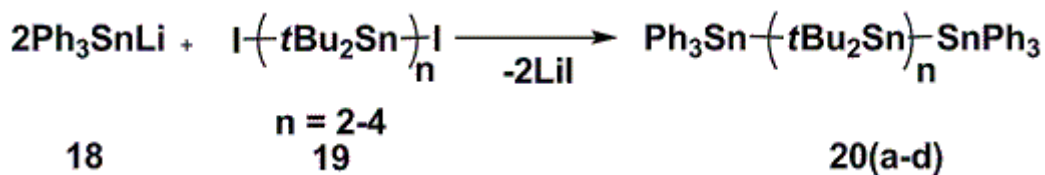


**Figure 1.3** (a) DSC thermograms of  $(n\text{Oct}_2\text{Sn})_n$ ; recorded for subsequent heating /cooling cycles (under  $\text{N}_2$ , rate  $5\text{ }^{\circ}\text{C}/\text{min}$ ). (b) Optical microscopy images of the sample at the various temperatures indicated; crossed polarizers. The sequence of the heating/cooling steps proceeded is indicated with the arrows (under argon, rate  $5\text{ }^{\circ}\text{C}/\text{min}$ ).<sup>[33]</sup>

### 1.2.4 Structural and electronic properties of Polystannanes

The term “Molecular metals” for polystannanes was first proposed by Adams and Dräger <sup>[29]</sup> in 1987. This is based on the study of a series of oligomers **20(a-d)** (Fig 1.4).

#### Reaction 1.2.11



They isolated the tri-**20a**, tetra-**20b**, penta-**20c** and hexastannanes **20d** by varying the molar ratio of the starting materials, solvent and the concentration. X-ray structure analysis showed that bulky, electron rich substituents on the Sn-Sn units causes an increase in bond length. The Sn-Sn bond length for the central bond in **20d** is 296.6 pm (Fig.1.4), the longest reported for an oligostannane. A strong absorption maximum with a reasonable red shift was exhibited by UV spectra with increasing chain length. The increase in chain length decreases the HOMO/LUMO energy difference.

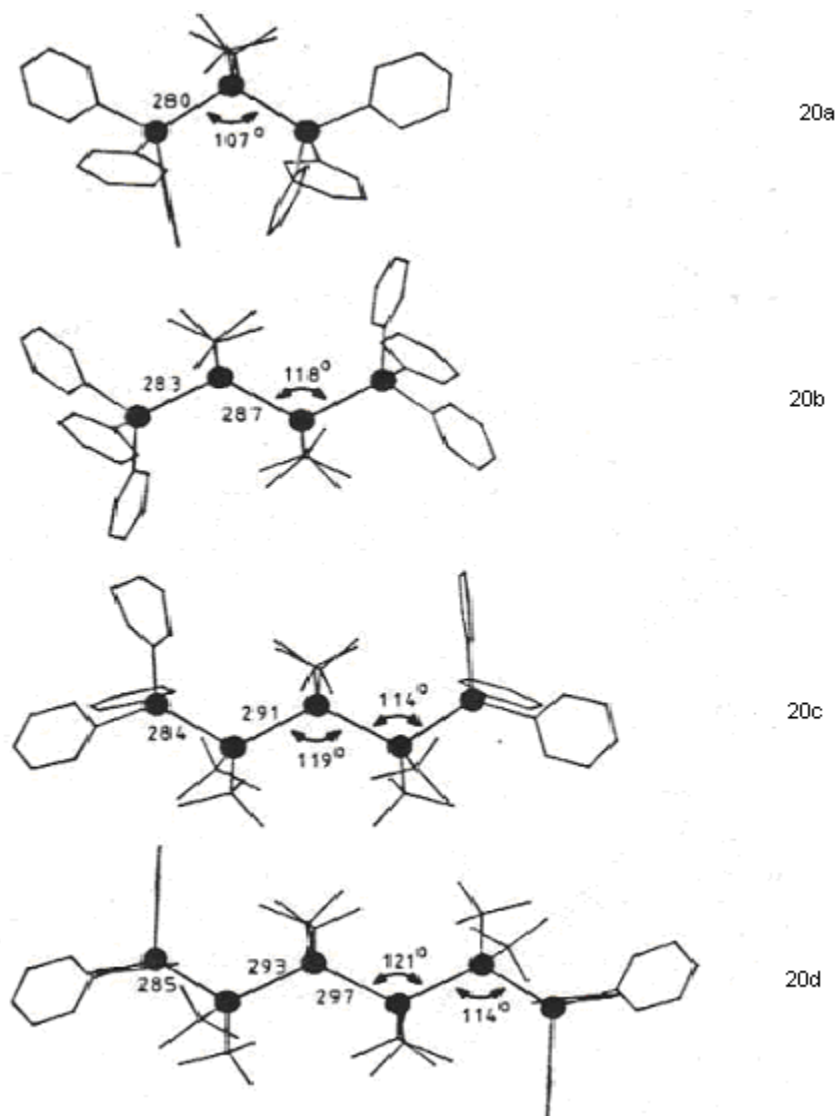


**Figure 1.4** Molecular structures of **20(a-d)** with average Sn-Sn bond length (pm) and Sn-Sn bond angles.<sup>[29]</sup>

A comparison of the bonding nature of polymers with heavier tin atoms in the backbone to the polysilanes showed that they have more diffuse bonding orbitals than silicon in polysilanes. Polystannanes are expected to exhibit the following properties due to greater  $\sigma$ -conjugation.

- a) Narrower band gaps (4 eV for polysilanes)
- b) Increased metallic character

c) Enhanced photochemical and thermochromic behaviours

d) Lower Sn-Sn bond strength vs. Si-Si <sup>[37]</sup>

Poly(dialkylstannane)s have  $\lambda_{\max}$  absorbance values in the range of 380-400 nm from the  $\sigma\text{-}\sigma^*$  transitions along its backbone. The  $\lambda_{\max}$  value of poly(dialkylstannane)s increases as the molecular weight increases up to a limiting value. The comparison of poly(dialkylstannane)s with corresponding polysilanes showed that  $\sigma\text{-}\sigma^*$  transitions for poly(dialkylstannane)s are 70 nm red shifted <sup>[32]</sup>.

It is evident from the  $\lambda_{\max}$  values (Table 1.9) for poly(diarylstannane)s that they are 50 nm red shifted with respect to poly(dialkylstannane)s. This is likely due to the presence of  $\sigma\text{-}\pi$  mixing between the aryl ligands and tin atoms.

**Table 1.9** UV spectroscopic data for polystannanes <sup>[31, 32]</sup>

| Polymer  | $\lambda_{\max}(\text{nm})$ |
|--|-----------------------------|
| H[( <i>p</i> - <sup><i>t</i></sup> Bu-C <sub>6</sub> H <sub>4</sub> ) <sub>2</sub> Sn] <sub>n</sub> H                | 432(THF)                    |
| H[( <i>p</i> - <sup><i>n</i></sup> Hex-C <sub>6</sub> H <sub>4</sub> ) <sub>2</sub> Sn] <sub>n</sub> H               | 436(THF)                    |
| H[( <i>o</i> -Et- <i>p</i> -C <sub>6</sub> H <sub>4</sub> ) <sub>2</sub> Sn] <sub>n</sub> H                          | 468(film)                   |
| H[( <i>p</i> - <sup><i>n</i></sup> BuO-C <sub>6</sub> H <sub>4</sub> ) <sub>2</sub> Sn] <sub>n</sub> H               | 448(THF)                    |
| H[( <i>o</i> -Et- <i>p</i> - <sup><i>n</i></sup> BuO-C <sub>6</sub> H <sub>3</sub> ) <sub>2</sub> Sn] <sub>n</sub> H | 506(THF)                    |
| H{[( <i>p</i> -(Me <sub>3</sub> Si) <sub>2</sub> -C <sub>6</sub> H <sub>4</sub> ) <sub>2</sub> Sn] <sub>n</sub> H    | 450(THF)                    |
| ( <i>n</i> Bu <sub>2</sub> Sn) <sub>n</sub> <sup>[31]</sup>  | 384(THF)                    |
| ( <i>n</i> Bu <sub>2</sub> Sn) <sub>n</sub>  | 365(THF)                    |
| ( <i>n</i> Hex <sub>2</sub> Sn) <sub>n</sub> <sup>[31]</sup>   | 384(THF)                    |
| ( <i>n</i> Oct <sub>2</sub> Sn) <sub>n</sub>   | 388(THF)                    |

The reversible thermochromic behaviour of polystannanes is visibly evident as a discoloration of the material occurs upon warming above room temperature. UV-vis spectrometry showed a change in the absorption maximum between 384 to 369 nm moving from 30 and 40°C, respectively in a toluene solution.

Tilley<sup>[31]</sup> and co-workers measured the conductivity of poly(alkylstannane)s at room temperature by doping the film of H(*n*Bu<sub>2</sub>Sn)<sub>n</sub>H and H(*n*Oct<sub>2</sub>Sn)<sub>n</sub>H by exposure to

SbF<sub>5</sub> vapour for 3 and 30 h, respectively. The conductivities measured by four-point probe method were 10<sup>-2</sup> and 0.3 Scm<sup>-1</sup>, respectively. These results may be improved by using a milder dopant such as SbF<sub>3</sub> which is less corrosive towards the Sn-Sn bonds.

Matthijis P. de Haas<sup>[38]</sup> and co-workers measured charge mobility of **5** in the crystalline solid and mesophase by using the pulse-radiolysis time-resolved microwave conductivity technique. The values of mobility were 0.027 and 0.097cm<sup>2</sup>V<sup>-1</sup>s<sup>-1</sup> for meso (M) and crystalline solid phase (K) respectively. The decrease in mobility at the transitions from K to M is due to the structural disorder on melting of the alkyl side chain.

Caseri<sup>[36]</sup> and co-workers measured the conductivity of the poly(di( $\omega$ -alkylphenyl)stannane)s. At 300K the conductivity of poly(di-(3-propylphenyl)stannane) was  $3 \times 10^{-8}$  Scm<sup>-1</sup>. An increase in the conductivity was observed by increasing the temperature, characteristic of a semi-conducting material.

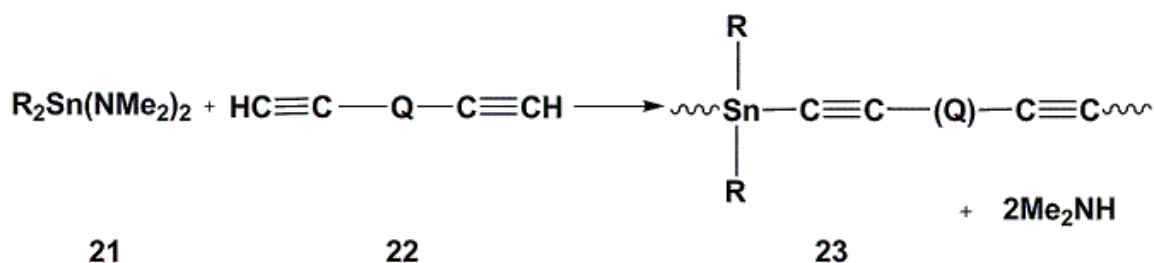
### 1.3 Insertion of alkynes into Sn-Sn bonds

Most organometallic metal-metal bonds are not as stable as their elemental forms. The reasons for this may be due to the poor overlap of the atomic orbitals and low electronegativity. In case of tin, its large size and low electronegativity result in Sn-Sn bonds that are sensitive to moisture and light.

The backbone of polystannanes may be stabilized by inserting alkynes between tin atoms. Van der Kerk *et al.* prepared a series of organotin polymers with Sn-C bonds in the main chain through the polyaddition of organotin dihydrides with dienes or diynes.<sup>[39-42]</sup> These polymers have poor overall physical properties like low glass transition temperatures and poor solubilities.

The preparation of polymers containing tin-alkyne bonds in the backbone are interesting as these bonds are known to be quite weak. Labadie *et al.* synthesized alkylstannylene polymers by coupling of aminostannanes and terminal alkynes.<sup>[43]</sup>

#### Reaction 1.3.1



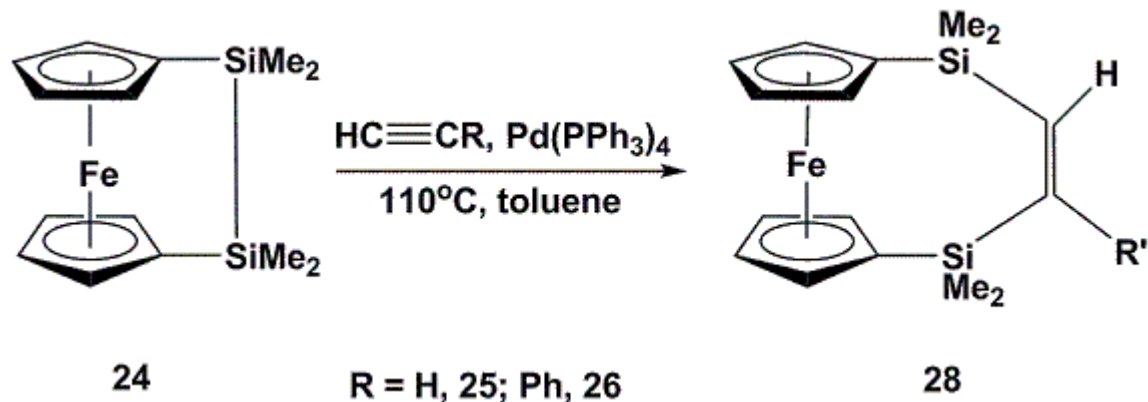
R = *n*-Bu, Ph

R = *n*-Bu, Ph; Q = -(CH<sub>2</sub>)<sub>2</sub>-

R = *n*-Bu; Q = -(CH<sub>2</sub>)<sub>5</sub>-

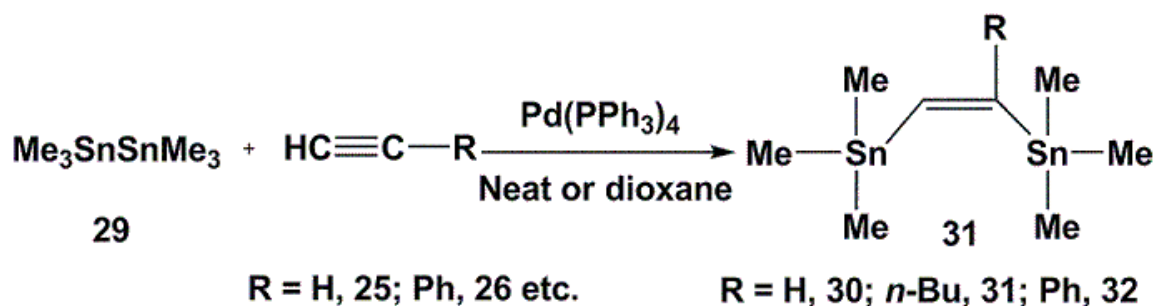
Precedents for the insertion of olefins and alkynes into Group 14 bond was demonstrated by Manners and co-workers who inserted acetylene into the Si-Si bond of a ferrocenyldisilane in the presence of catalytic amount of Pd(PPh<sub>3</sub>)<sub>4</sub>.<sup>[44]</sup>

### Reaction 1.3.2



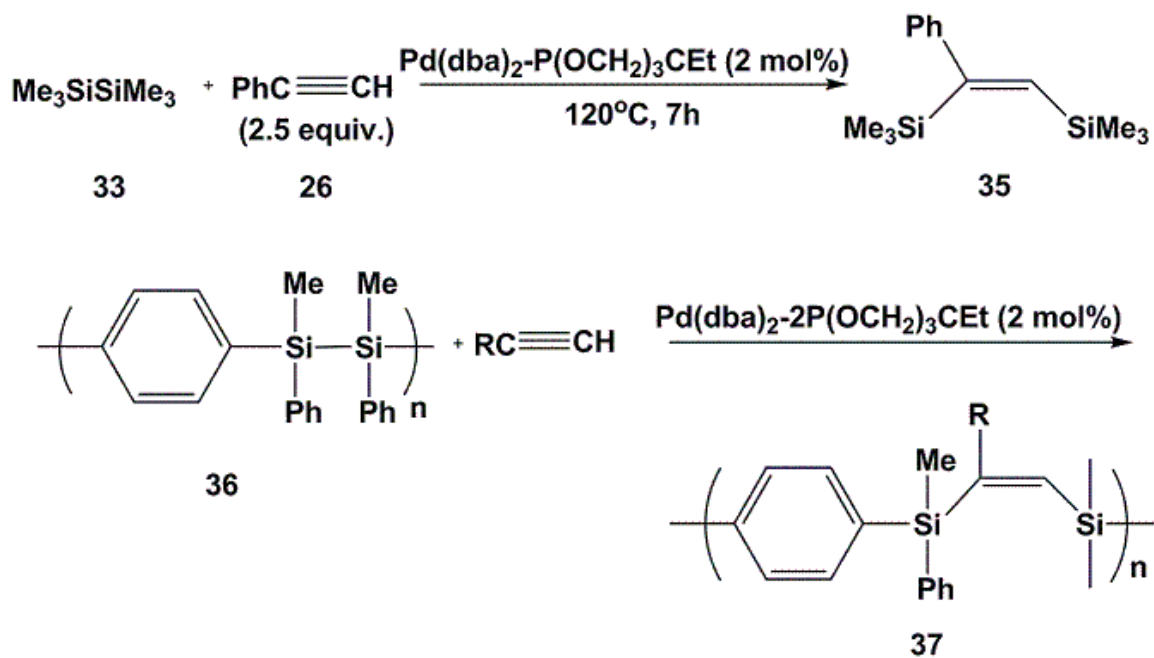
Mitchell *et al.*<sup>[45]</sup> reported the  $\text{Pd(PPh}_3)_4$  (**27**) catalyzed addition of hexaalkylditins  $\text{R}_6\text{Sn}_2$  ( $\text{R} = \text{Me, Et, } n\text{-Bu}$ ) to acetylene and 1-alkynes. The solvent used for acetylene insertion reactions was dioxane.

### Reaction 1.3.3



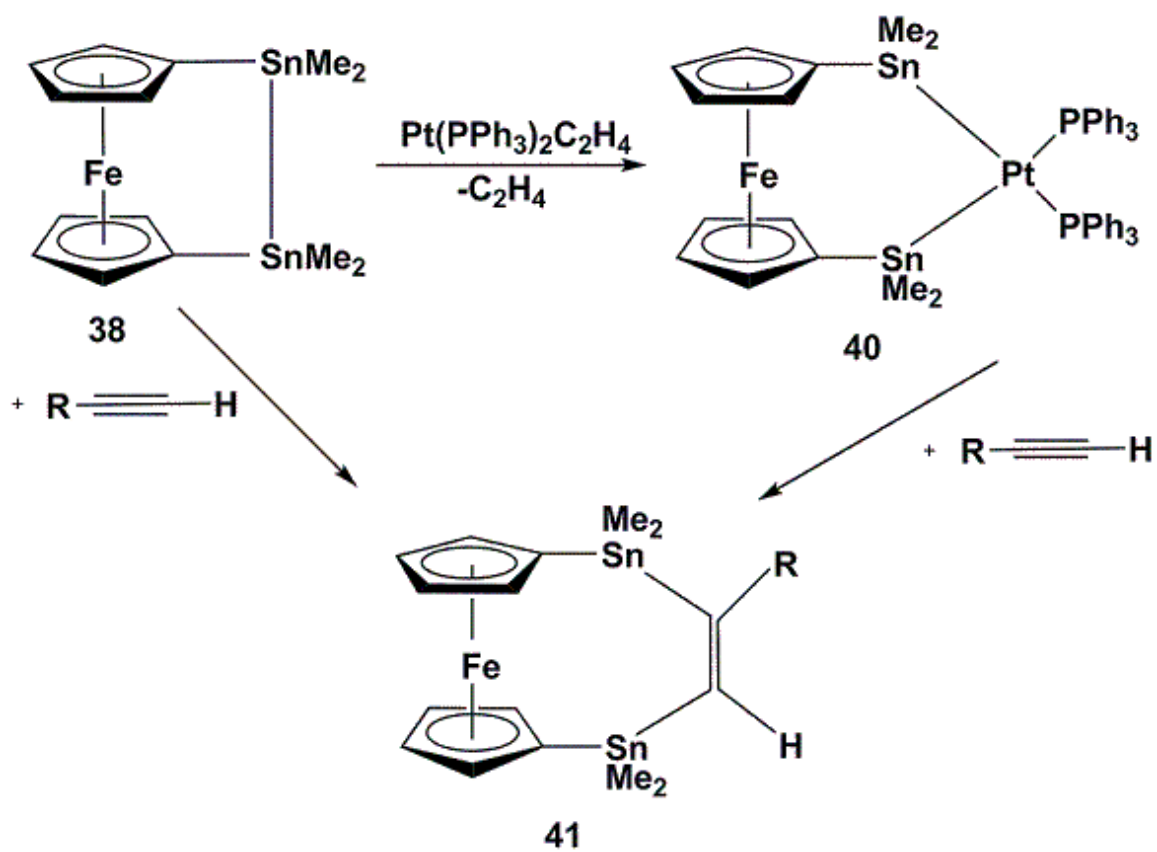
Yamashita *et al.*<sup>[46]</sup> reported the use of the  $\text{Pd(dba)}_2\text{-P(OCH}_2)_3\text{CEt}$  (**34**) catalyst system for the insertion of acetylenes into Si-Si bonds of non-activated disilanes or trisilanes.

### Reaction 1.3.4



Max Herberhold *et al.*, carried out distannation of non-terminal alkynes which provides an elegant route for the insertion of alkynes between the tin atoms of a tin bridged [2] ferrocenophane. Distannation of many alkynes has been shown to proceed under mild conditions by employing Pt(0)-mediated **39** catalysis.<sup>[47]</sup>

Reaction 1.3.5



## 1.4 Distannanes and Oligostannanes

Hexaorganodistannanes are a convenient source of stannyl radicals and have found applications in organic chemistry in a variety of reduction reactions<sup>[48]</sup> in addition to their utility in palladium-catalyzed cross-coupling processes.<sup>[49]</sup> Distannanes also serve as useful models for polystannanes.<sup>[29]</sup> Industrially, distannanes show considerable bacterial and fungicidal activity and were previously used as wood preservatives.<sup>[50]</sup> The distannane class of compounds are the tin analogues of ethanes but possess a Sn-Sn bond that is comparatively weaker (154 kJ/mol vs. 356 kJ/mol) and longer (2.80 vs. 1.54 Å) than typical C-C bonds.<sup>[51,52]</sup> Organodistannanes are generally thermally stable but are chemically sensitive to the presence of oxygen (more so than that of water, mild acids or alkalis) and can readily decompose to form stannoxanes (i.e. R<sub>3</sub>Sn-O-SnR<sub>3</sub>) such as **42** (Figure 1.5).<sup>[53]</sup>

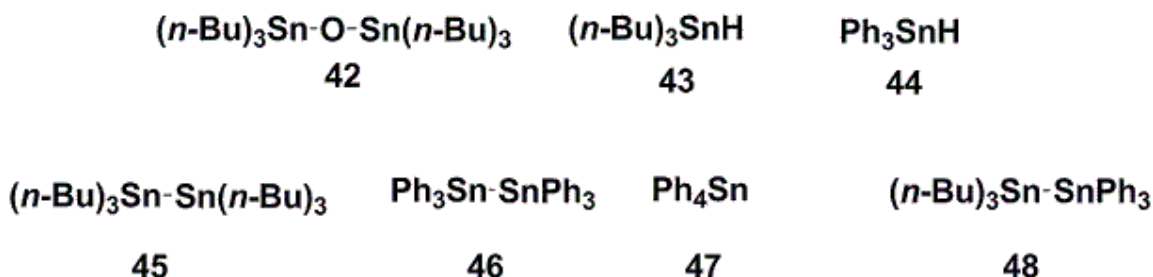
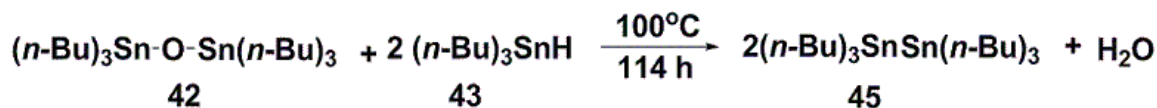


**Figure 1.5** Various Stannanes

Distannanes can be synthesized directly from the dehydrogenative dimerization of tin hydrides (e.g., **43**, **44**) with either amines or alkoxides acting as the catalyst.<sup>[54]</sup> Organotin hydrides can also be dehydrogenatively coupled using transition metal catalysts such as Pd(PPh<sub>3</sub>)<sub>4</sub>, PdCl<sub>2</sub>(NCMe)<sub>2</sub><sup>[55]</sup> or ruthenium-allenylidene complexes.<sup>[56]</sup> Electrochemical preparations of R<sub>3</sub>SnSnR<sub>3</sub> (e.g., R = *n*-C<sub>4</sub>H<sub>9</sub> **45**, C<sub>6</sub>H<sub>5</sub> **46**, *p*-CH<sub>3</sub>C<sub>6</sub>H<sub>4</sub>-, C<sub>6</sub>H<sub>5</sub>CH<sub>2</sub>-) compounds involving the reduction of R<sub>3</sub>SnX (X = Cl, NO<sub>3</sub>, H, SPh, OCHO,

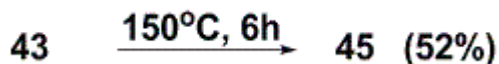
OCOCH<sub>3</sub>, etc.) have also been reported.<sup>[57,58]</sup> Chemically, **46** can be prepared via the reductive coupling of triphenyltin derivatives (Ph<sub>3</sub>SnX where X = Cl, I, or OH) in a THF/aq. NH<sub>4</sub>Cl solution containing Zn metal.<sup>[59,60]</sup> The first high yield synthesis of **45** was reported by Sawyer<sup>[61]</sup> from the treatment of distannoxane **42** with **43** at 100°C for several days (Reaction 1.4.1).

#### Reaction 1.4.1



Alternative methods for the synthesis of **45** from **42** include reactions with formic acid<sup>[62]</sup>, or reductions utilizing Mg, Na, or K metal in THF<sup>[63]</sup> solution; NaBH<sub>4</sub><sup>[64]</sup> or SmI<sub>2</sub><sup>[65]</sup> in HMPA has also been used. Recently, an improvement in the synthesis of **45**<sup>[66]</sup> was reported which involves a high temperature (200°C) catalyst free protocol using **42** and **43** at a molar ratio of 1:2.2. This method gives **45** in a quantitative yield. Interestingly, these same authors also reported a lower yield (52%) of **45** by simply heating **43** at a lower temperature (150°C) for 6 h under vacuum (Reaction 1.4.2).

#### Reaction 1.4.2

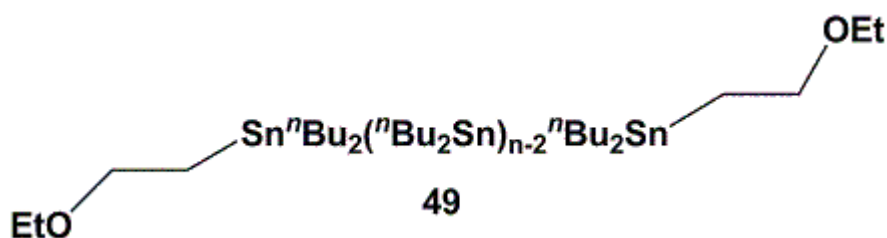


## 1.5 Molecular Modeling of Oligostannanes:

Polystannanes consist of a backbone of  $\sigma$ -bonded Sn atoms. They are of considerable interest due to their unusual electronic properties. Short chain oligostannanes ( $n \leq 6$ ) which can be used as models for polystannanes have been both synthesized and characterized.

Sita *et al.* <sup>[67]</sup> isolated and collected the experimental data of  $\alpha$ ,  $\omega$ -difunctional polystannane oligomers represented by  $X-(\text{Bu}_2\text{Sn})_n-X$  ( $X = 2$ -ethoxyethyl,  $n = 3-15$ ). The experimental data in this report was used for comparison with the calculated data obtained by Sandorfy using the Hückel molecular orbital (HMO) approximation at the semiempirical level. It revealed that the HMO theory developed for conjugated organic systems was a poor choice for oligo- and polystannanes. A modified Sandorfy HMO theory was then employed by setting  $m = 0.75$  ( $m$  is the measure of degree of delocalization of the molecular orbitals of the backbone,  $m = \beta_{\text{gem}}/\beta_{\text{vic}}$ ). A good correlation was found between the observed transition frequency ( $\text{cm}^{-1}$ ) curve of  $\alpha$ ,  $\omega$ -polystannane oligomers **49** and a plot of calculated HOMO and LUMO energy difference with the increasing chain length.

Figure 1.6



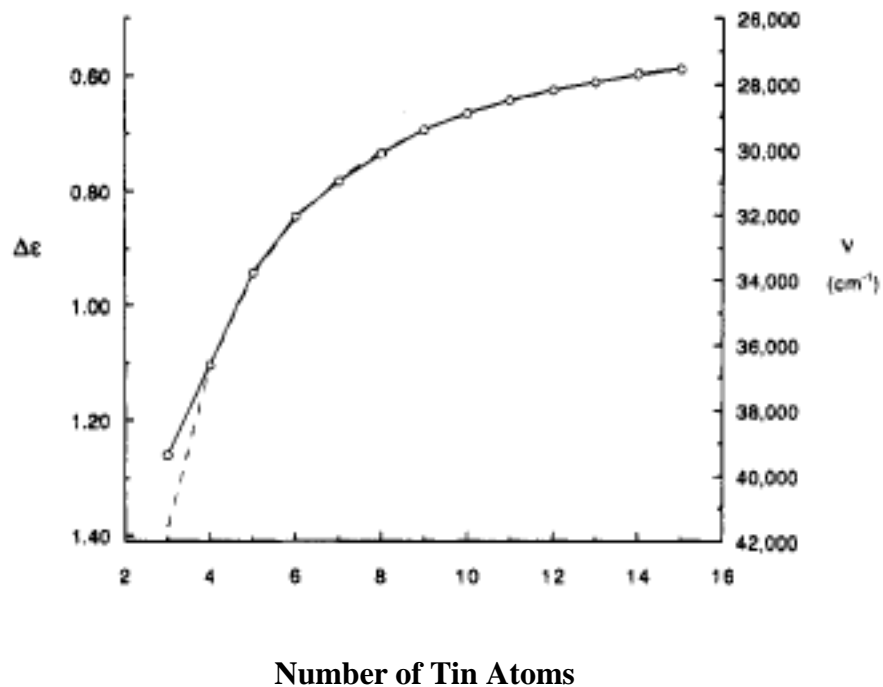


**Figure 1.7** Curves for the calculated (Sandorfy model C) energy differences (LUMO-HOMO) (dashed line) and observed transition frequencies (circles and solid line) as a function of chain length.<sup>[67]</sup>

Sita *et al.* successfully applied the Sandorfy HMO approximation to model the electronic structure of long chain polystannane.

## 1.6 Molecular Modeling Approaches:

Various models can be used for the geometrical optimization of equilibrium geometries of molecules including

1. Density functional model (DFT)
2. Semi-empirical model (PM3, AM1) and
3. Molecular Mechanic model [Merck Molecular Force Field (MMFF)]

The above models have been typically used for the optimization of various organic and inorganic structures with energies of the molecules were calculated only by density functional method.

### **1.6.1 Density Functional Model:**

The density functional theory is based on the fact that the sum of the exchange and correlation energies of a uniform electron gas can be calculated exactly knowing only its density. Density functional models are applicable to molecules of moderate size (50-100 atoms).

#### **Pseudopotentials:**

Calculations can be simplified by only considering the valence electrons and replacing the core electrons by some form of potential. This technique is used for calculations of molecules having one or more heavy elements, particularly transition metals.

### **1.6.2. Semi-Empirical Models:**

Semi-empirical models are based on Hartree-Fock models. In these models the size of the problem is reduced, first because the treatment is restricted to valence electrons only and the core electrons are ignored. Next, the basis set is restricted to a minimal valence only representation. Parameters for PM3 for transition metals are used for the reproduction of equilibrium geometries. The AM1 and PM3 models have different parameters but use the same approximations.

### **1.6.3. Molecular Mechanic model:**

Molecular mechanics (MM) consider the molecules as “bonded atoms”, which ideal geometry have been distorted due to non-bonded van der Waals and Coulombic

interactions. This is a fundamental difference between the MM models and quantum chemical models, because in quantum chemical models there is no reference to chemical bonding. The two reasons for the success of molecular mechanics are the high degree of transferability of geometrical parameters from one molecule to another and predictable dependence of the parameters on atomic hybridization. A more complex force field calculation known as MMFF, was developed at Merck Pharmaceuticals. This method provides a better quantitative account of molecular geometry and conformation. However, it is limited in scope to common organic systems and biopolymers.

MMF is a simple model and the molecular mechanics calculations can conveniently be performed on molecules composed of several thousand atoms. MM calculations are less time consuming, which permits extensive conformational searching on molecules having between 100-200 atoms, such as polymers. This is one of the most important applications of this model. MMF is limited to the description of equilibrium geometries and equilibrium conformations, and does not provide any information about atomic bonding. Currently available force fields are not able to handle non-equilibrium forms, especially reaction transition states. The success of MM models would be doubtful in describing the structures and conformations of “new” molecules which are outside the range of parameterization.

#### **1.6.4 Calculated (gas phase) Vs Crystallographic Data:**

Equilibrium geometries for a large number of molecules have been determined in the solid (crystalline) phase by X-ray diffraction.<sup>[68, 69]</sup> These have more uncertainties than the gas-phase structures due to thermal motions in the crystal. These calculations are reliable for bond lengths and angles to within  $\pm 0.02$  Å and one or two degrees,

respectively. In case of geometrical parameters involving hydrogen atoms, the X-ray experiment actually locates areas of high electron density and for hydrogen atoms these are not precisely the same as their nuclear positions. Often it shortens the bonds involving hydrogen by one or two tenths of an Å.

It should also be considered that the geometries of molecules in crystals are not the same as those of isolated molecules in the gas phase. In case of crystals, the molecules will be influenced by intermolecular crystal packing forces. Finally, it needs to be stated that calculated geometries are also subject to errors in precision. The reason of this error may be the incomplete convergence of the geometric optimization procedure. Within these limits, comparisons between the experimental and calculated values can be used to judge the quality of the calculations, although there is always the chance of error in the experimental structure.

## 1.7 Objectives:

The main objectives of this thesis are to synthesize light, air and moisture stable tin containing model compounds and polymers.

Target compounds of this research include:

- i) Preparation of tin polymers
- ii) Preparation of alkyne inserted model dimer compounds
- iii) Preparation of an alkyne inserted polycarbostannanes
- iv) Investigate the catalyst free dehydrocoupling reactions of stannanes

The proposed steps to achieve the objectives are as follows:

- 1) Synthesize and characterize polydibutylstannane
- 2) Insert acetylene and acetylene derivatives into the Sn-Sn bonds to stabilize the polymer.
- 3) Explore thermal and catalyst free dehydrocoupling of simple model stannanes
- 4) Model oligostannanes by using different methods of optimization

For the modelling effort, the purpose of this study is to calibrate molecular modelling approaches for oligostannanes **20(a-d)** using the available structural data for comparison. By utilizing the optimized geometries, the electronic structure of oligostannanes will then be investigated using density functional method.

## CHAPTER TWO

### Experimental

#### 2.1 General:

$^1\text{H}$  NMR,  $^{13}\text{C}$   $\{^1\text{H}\}$  NMR and  $^{119}\text{Sn}$   $\{^1\text{H}\}$  NMR spectra were recorded on a Bruker Avance 400 MHz NMR spectrometer.  $^1\text{H}$  spectra were referenced to the residual solvent peaks in the deuterated solvents while the  $^{13}\text{C}$  spectra are referenced internally to the deuterated solvent resonances which are in turn referenced to  $\text{SiMe}_4$  ( $\delta = 0$  ppm), while  $^{119}\text{Sn}$  was referenced to  $\text{SnMe}_4$  ( $\delta = 0$  ppm). UV-Vis measurements were carried out in THF solutions using a Perkin Elmer Lambda 40 spectrometer. Molecular weights of the polymers were determined by gel permeation chromatography (GPC) using a Viscotek Triple Model 302 Detector system equipped with a Refractive Index Detector (RI), a four capillary differential viscometer (VISC), a right angle ( $90^\circ$ ) laser light scattering detector ( $\lambda_0 = 670$  nm) and a low angle ( $7^\circ$ ) laser light scattering detector. GPC columns were calibrated versus polystyrene standards (American Polymer Standards). A flow rate of 1.0 mL/min. was used with ACS grade THF as the eluent. GPC samples were prepared using 3-10 mg of each polymer per mL THF, and filtered using a  $0.45\ \mu\text{m}$  filter. All samples were run with and without UVA (conc.  $\approx 0.001$  M) for comparison. All reactions were carried out under a nitrogen atmosphere using Schlenk techniques unless otherwise described. Bruker-Nonius Kappa-CCD diffractometer was used to obtain the X-ray information of the crystal structures. Thermally driven de-hydrocoupling reactions were performed under a variety of conditions in Schlenk flasks, including in an inert  $\text{N}_2$  atmosphere or in a sealed Schlenk flask placed under a static reduced pressure (closed) or

finally in a Schlenk flask exposed to dynamic reduced pressure (open). Pressures were measured using a mercury manometer attached to the Schlenk line.

## 2.2 Materials:

$\text{Me}_3\text{SnSnMe}_3$  (**29**: 98%),  $\text{C}_6\text{H}_5\text{CH}\equiv\text{CH}$  (**26**: 98%),  $\text{C}_2\text{H}_2$  (**25**),  $\text{Pd}(\text{PPh}_3)_4$  (**27**: 99%),  $\text{RhCl}(\text{PPh}_3)_3$  (**14**: 99.99%),  $(n\text{-Bu})_3\text{SnH}$  (**43**: 99%),  $\text{Ph}_3\text{SnH}$  (**44**: 97%),  $(n\text{-Bu})_2\text{SnCl}_2$  (**1**: 97%),  $\text{LiAlH}_4$  (1.0 M in ether) and anhydrous  $\text{CaCl}_2$  were purchased commercially and used without further purification.  $(n\text{-Bu})_6\text{Sn}_2$  (**45**) and  $\text{Ph}_6\text{Sn}_2$  (**46**) were purchased from Strem and used as reference samples.  $(n\text{-Bu})_2\text{SnH}_2$  (**13**) was prepared from **1** and  $\text{LiAlH}_4$  according to published literature preparations.<sup>[31,70]</sup> Solvents were dried by standard procedures prior to use.

## 2.3 Polystannanes:

### 2.3.1 Synthesis of $(n\text{-Bu})_2\text{SnH}_2$ **13**:

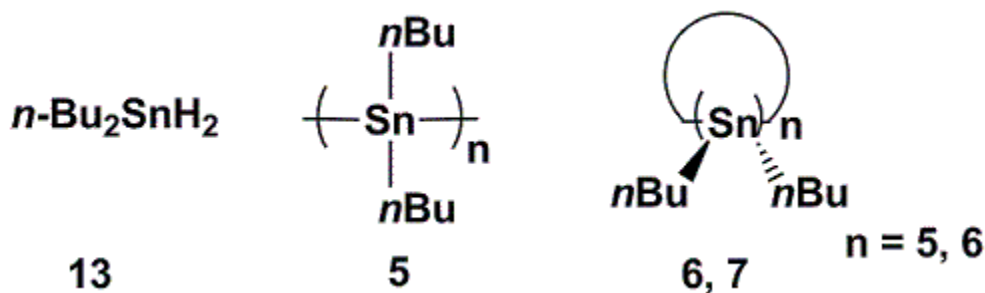
This reaction was carried out in an inert  $\text{N}_2$  atmosphere. A sample of  $n\text{-Bu}_2\text{SnCl}_2$  **1** (7.8 g, 25.67 mmol) was weighed in glove box and then dissolved in ether. To a suspension of  $\text{LiAlH}_4$  in diethyl ether at  $0^\circ\text{C}$ , was added drop-wise, an ether solution of **1** over a 30 min time period. The reaction mixture was then stirred for an additional 2 h. The ice bath was removed and the reaction mixture quenched with 50 mL of chilled de-oxygenated water. The contents of the reaction flask were then transferred to a separatory funnel and the organic layer separated. The aqueous layer was then washed with  $3 \times 20$  mL of ether. All the organic layers were then collected and dried over  $\text{CaCl}_2$  (2 h),

filtered and the ether removed *in vacuo*. The product obtained was a colourless liquid. (Yield was 83%, 5.0g). Analysis by  $^1\text{H}$ ,  $^{13}\text{C}$  and  $^{119}\text{Sn}$  NMR spectroscopy revealed peaks identical to those provided in the literature.<sup>[31,35, 69]</sup>

$^1\text{H}$  NMR (400 MHz,  $\text{C}_6\text{D}_6$ )  $\delta$  (ppm): 0.86 (t, 6H,  $\text{CH}_3$ ), 0.96 (t, 4H,  $\text{SnCH}_2-$ ), 1.29 (dt, 4 H,  $-\text{CH}_2\text{CH}_3$ ), 1.49 (m, 2H,  $\text{SnCH}_2\text{CH}_2-$ ), 4.76 (q, 2H,  $^3J_{\text{H,H}} = 2.1$  Hz,  $^1J^{119}_{\text{Sn,H}} = 1672$  Hz,  $^1J^{117}_{\text{Sn,H}} = 1596$  Hz).  $^{13}\text{C}$  { $^1\text{H}$ } NMR ( $\text{C}_6\text{D}_6$ )  $\delta$  (ppm): 7.1, 13.8, 27.1, and 30.7.  $^{119}\text{Sn}$  { $^1\text{H}$ } NMR ( $\text{C}_6\text{D}_6$ )  $\delta$  (ppm): -203.4.

### 2.3.2 Polymerization of 13:

Figure 2.1



This reaction was carried out in a glove box in the absence of light. Catalyst **14** (10 mg, 0.011 mmol) was placed in a 50 mL Schlenk tube and thereafter dissolved in 4 mL of  $\text{CH}_2\text{Cl}_2$ . The reaction flask was wrapped with black soft cloth and subsequently with aluminum foil to protect the contents of reaction flask from ambient light. Compound **13** (125 mg, 0.54 mmol) was dissolved in 5 mL of  $\text{CH}_2\text{Cl}_2$  added drop-wise via syringe, over a 30 min period. The reaction mixture was then stirred for an additional 2 h. The  $\text{CH}_2\text{Cl}_2$  was removed under reduced pressure. The bright yellow coloured waxy product was obtained. The  $^1\text{H}$  and  $^{119}\text{Sn}$  NMR spectroscopic analysis of the product obtained was identical to that given in literature.<sup>[31, 35]</sup>

$^1\text{H}$  NMR (400 MHz,  $\text{C}_6\text{D}_6$ )  $\delta$  (ppm): 1.02 (t,  $\text{CH}_3$ , cyclic), 1.12 (t,  $\text{CH}_3$ , polymer), 1.45-1.53 (m,  $2\text{CH}_2$ , cyclic), 1.54-1.66 (m,  $2\text{CH}_2$ , polymer), 1.77-1.83 (m,  $\text{CH}_2$ , cyclic), 1.87-1.95 (m,  $\text{CH}_2$ , polymer).  $^{119}\text{Sn}$  { $^1\text{H}$ } NMR ( $\text{C}_6\text{D}_6$ )  $\delta$  (ppm): -190.06 (polymer)

### 2.3.3 Polymerization of **13** using $\text{Pd}(\text{PPh}_3)_4$ **27**:

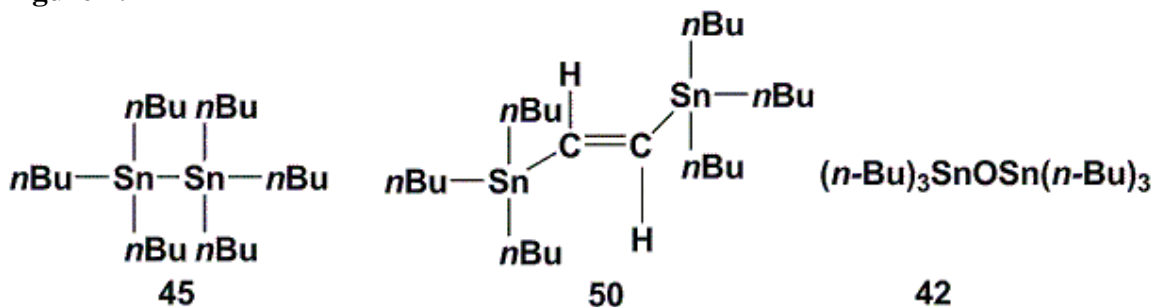
The reaction was completed in an inert atmosphere ( $\text{N}_2$ ) in glove box and in the absence of light. Catalyst **27** (35 mg, 0.030 mmol) was placed in a 50 mL Schlenk tube thereafter dissolved in 4 mL of  $\text{CH}_2\text{Cl}_2$ . The reaction flask was wrapped with black soft cloth and subsequently with aluminum foil to protect the contents of reaction flask from ambient light. Compound **13** (528 mg, 2.26 mmol) was dissolved in 5 mL  $\text{CH}_2\text{Cl}_2$  and added drop-wise via syringe over a 30 min time period. The reaction mixture was then stirred for additional 2 h. The solvent was removed under reduced pressure and analyzed by NMR spectroscopy. The  $^{119}\text{Sn}$  NMR spectrum shows only one resonance at -201.85 ppm and attributed to the presence of the cyclic compound **7** only.

$^1\text{H}$  NMR (400 MHz,  $\text{C}_6\text{D}_6$ )  $\delta$  (ppm): 1.01 (t,  $\text{CH}_3$ , cyclic), 1.45-1.57 (m,  $2\text{CH}_2$ , cyclic), 1.74-1.81 (m,  $\text{CH}_2$ , cyclic).  $^{119}\text{Sn}$  { $^1\text{H}$ } NMR ( $\text{C}_6\text{D}_6$ )  $\delta$  (ppm): -201.7.

## 2.4 Insertion of alkynes into Sn-Sn bond:

### 2.4.1 Synthesis of hexabutyldistannyl ethylene 50:

Figure 2.2



#### 2.4.1a Reaction of 45 with C<sub>2</sub>H<sub>2</sub> in toluene:

Compound **45** (1.08 g, 1.86 mmol) was weighed in glove box and diluted with toluene (10 mL). Then catalyst **27** (43.8 mg, 0.04 mmol) was then added to the solution. The reaction mixture was refluxed at 85°C and acetylene gas **25** bubbled through the reaction mixture for ≈100 h. The solvent was removed under reduced pressure. The <sup>119</sup>Sn NMR revealed no peak attributed to **50**.

#### 2.4.1b Reaction of 45 with 25 in 1,4-dioxane:

Compound **45** (1.2 g, 2.06 mmol) and **27** (40 mg, 0.035 mmol) were weighed and transferred into the reaction flask in the glove box. Reaction mixture was then diluted with 20 mL 1,4-dioxane. The reaction mixture was warmed to 85°C and acetylene bubbled through the reaction mixture for ≈100 h. The solvent was removed under reduced pressure. The reddish brown oily product obtained was analyzed by NMR spectroscopy which confirmed the presence of **50**.

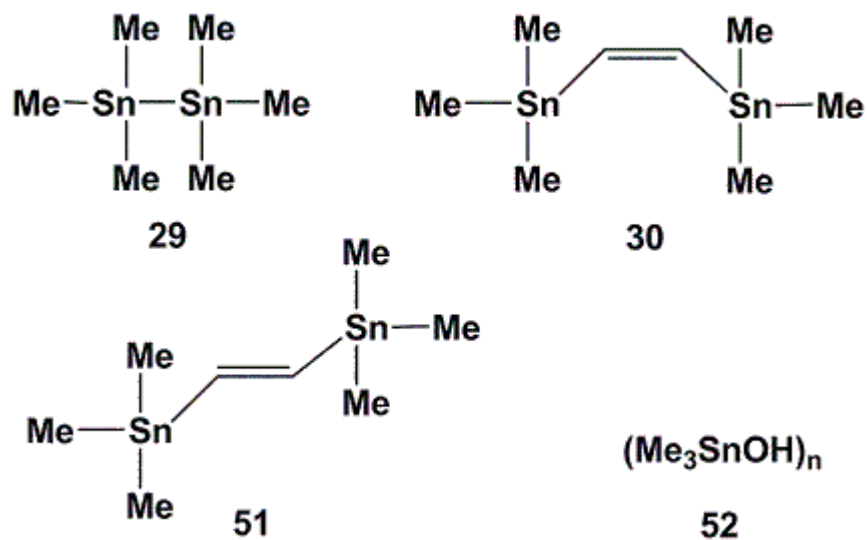
<sup>1</sup>H NMR (C<sub>6</sub>D<sub>6</sub>) δ (ppm): 1.08 (t, 3H, CH<sub>3</sub>CH<sub>2</sub>CH<sub>2</sub>CH<sub>2</sub>-Sn), 1.20 (m, 2H, CH<sub>3</sub>CH<sub>2</sub>CH<sub>2</sub>CH<sub>2</sub>-Sn), 1.53 (m, 2H, CH<sub>3</sub>CH<sub>2</sub>CH<sub>2</sub>CH<sub>2</sub>-Sn), 1.77 (m, 2H,

CH<sub>3</sub>CH<sub>2</sub>CH<sub>2</sub>CH<sub>2</sub>-Sn), 7.58 (s, 2H,  $^2J^{119}_{Sn-H}(-Sn-CH=) = 35.3$  Hz and  $^2J^{117}_{Sn-H}(-Sn-CH=) = 37.2$  Hz).  $^{13}C \{^1H\}$  NMR (C<sub>6</sub>D<sub>6</sub>)  $\delta$  (ppm): 10.77 ( $^1J_{C-Sn}(CH_3CH_2CH_2CH_2-Sn) = 157.5$  Hz and  $^2J_{C-Sn}(CH_3CH_2CH_2CH_2-Sn-Sn) = 165$  Hz), 13.99(CH<sub>3</sub>CH<sub>2</sub>CH<sub>2</sub>CH<sub>2</sub>-Sn), 27.91 ( $^3J_{C-Sn}(CH_3CH_2CH_2CH_2-Sn) =$  Hz), 29.75 ( $^2J_{C-Sn}(CH_3CH_2CH_2CH_2-Sn) = 10.35$  Hz), 154.24( $^1J_{C-Sn}(-Sn-CH=) = 17.13$  Hz).  $^{119}Sn \{^1H\}$  NMR (C<sub>6</sub>D<sub>6</sub>)  $\delta$  (ppm): -68.3 ( $J^{119}_{Sn-^{117}Sn} = 111.14$  Hz).

The sample used for NMR analysis was then sent for mass spectrometry analysis. The mass spectrum showed that the product had decomposed to **42** with no evidence of **50**.  $^{119}Sn$  NMR analysis of the sample remaining after mass spectrometry showed that a chemical transformation had taken place. This indicates that product **50** is stable to light but not to an air/moisture environment.

### 2.4.2 Synthesis of 30:

Figure 2.3



The distannane **29** (1.05 g, 3.2 mmol) and Pd(PPh<sub>3</sub>)<sub>4</sub> (10 mg, 0.0086 mmol) was transferred to the reaction flask in the glove box. The reaction mixture was diluted with 20 mL dioxane (CH<sub>2</sub>CH<sub>2</sub>O)<sub>2</sub>. The reaction mixture was warmed to 60°C and acetylene passed through the reaction mixture for 4 h. The contents of the flask turned brown. The solvent was removed under reduced pressure. A reddish brown oily product was obtained and analyzed by NMR spectroscopy. <sup>1</sup>H and <sup>119</sup>Sn NMR<sup>[45]</sup> in C<sub>6</sub>D<sub>6</sub> showed the presence of **30**.

<sup>1</sup>H NMR (C<sub>6</sub>D<sub>6</sub>) δ (ppm): 0.15 (s, 18H, <sup>2</sup>J<sub>Sn-H</sub>(Sn-CH<sub>3</sub>) = 25.75 Hz), 7.39 (s, <sup>2</sup>J<sub>Sn-H</sub>(=CH-Sn) = 40.48 Hz), <sup>119</sup>Sn { <sup>1</sup>H } NMR (C<sub>6</sub>D<sub>6</sub>) δ (ppm): -61.36 (*J*<sup>119</sup><sub>Sn-<sup>117</sup>Sn</sub> = 234.8 Hz)

The product mixture containing **30** was dissolved in ether, filtered and left to evaporate in open atmosphere. Crystals were isolated and analyzed by X-ray crystallography to be compound **52**.<sup>[71]</sup> Further analysis of the crystals by <sup>119</sup>Sn NMR spectroscopy showed a new peak at -35.7 ppm attributed **52** along with **30**.

<sup>119</sup>Sn { <sup>1</sup>H } NMR (C<sub>6</sub>D<sub>6</sub>) δ (ppm): -35.7

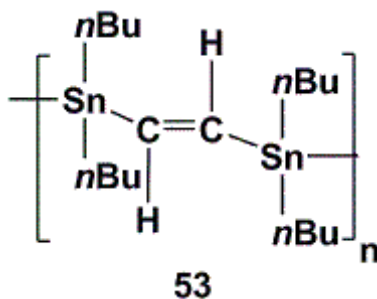
### 2.4.3 Reaction of **7** with acetylene:

The cyclic product obtained in 2.3.3, compound **7** was then dissolved in dioxane and acetylene bubbled through the solution at 85°C for 100 h. The solvent was removed under reduced pressure. A dark brown coloured semi-solid was obtained. A <sup>119</sup>Sn NMR analysis of this product reveals one new resonance at -176 ppm along with the starting oligomer compound **7** and another unassigned peak at -202.95 ppm.

<sup>119</sup>Sn { <sup>1</sup>H } NMR (C<sub>6</sub>D<sub>6</sub>) δ (ppm): -176.0, -201.7, -202.95

#### 2.4.4 Reaction of **5** with acetylene:

Figure 2.4



The experiment was carried out in an inert atmosphere and in the absence of light. Compound  $(n\text{-Bu})_2\text{SnH}_2$  **13** was polymerized by using the method described in section 2.2. The polymer was dissolved in dioxane and transferred to a 3-neck flask. Catalyst **27** (40 mg, 0.035 mmol) was then added and acetylene was bubbled through the reaction mixture and refluxed at 85°C for  $\approx 100$  h. The solvent was removed under reduced pressure. A dark brown coloured semi-solid was obtained and analyzed by NMR spectroscopy. The  $^{119}\text{Sn}$  NMR spectrum revealed resonances at 68.51 ppm, -50.23 ppm, -66.57 ppm, -176.83 ppm, with no evidence of a peak for the parent polymer **5** ( $\approx -190$  ppm).

An attempt to isolate the product in  $\text{CH}_2\text{Cl}_2$  using dry ice/acetone (-78°C) bath was unsuccessful and nothing precipitated out. Half of the product was dissolved in small amount of  $\text{CH}_2\text{Cl}_2$  and added drop wise into the non-solvent MeOH. A hazy solution was obtained and the flask was placed in glove box freezer. The solution was decanted and solvent was removed under reduced pressure.  $^{119}\text{Sn}$  NMR analysis revealed a single peak at -66.5 ppm for **53**.

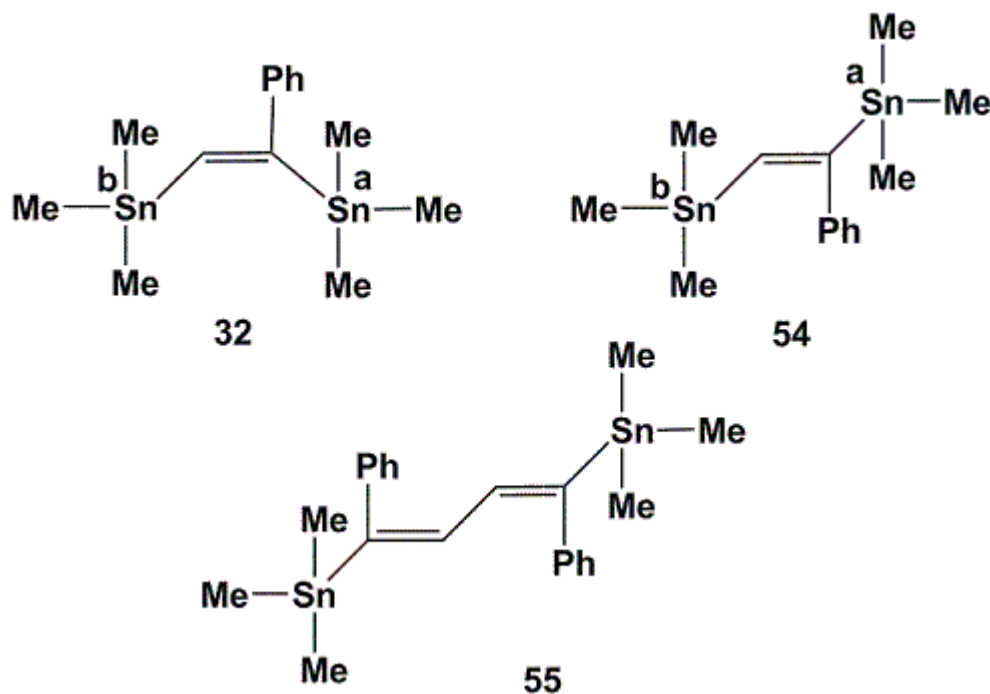
$^{119}\text{Sn}\{^1\text{H}\}$  NMR ( $\text{C}_6\text{D}_6$ )  $\delta$  (ppm): -66.5.

The supernatant from methanol precipitation was recovered by first removing solvent *in vacuo* followed by  $^{119}\text{Sn}$  NMR ( $\text{C}_6\text{D}_6$ ).

$^{119}\text{Sn}$  { $^1\text{H}$ } NMR ( $\text{C}_6\text{D}_6$ )  $\delta$  (ppm): 68.5, -176.83.

#### 2.4.5 Reaction of compounds **29** with **26**:

Figure 2.5



#### 1:1 ratio of compounds **29** and **26**:

$\text{Me}_3\text{SnSnMe}_3$  **29** (4.7 mmol, 1.55 g), Phenylacetylene (483 mg, 4.7 mmol) **26** and **27** (10mg, 0.0086mmol) were weighed and transferred to a reaction flask in the glove box. The solvent free reaction mixture was refluxed at  $80^\circ\text{C}$  for 72 h.  $^{119}\text{Sn}$  NMR analysis revealed resonances for **32** and **54** that agreed with known values from the literature.<sup>[45]</sup>

$^1\text{H}$  NMR ( $\text{C}_6\text{D}_6$ )  $\delta$  (ppm): 0.20 (s, 9H,  $^2J_{\text{Sn-H}}(\text{Sn-CH}_3) = 26.6$  Hz), 0.23 (s, 9H,  $J_{\text{Sn-H}}(\text{C}_6\text{H}_5\text{-C-Sn-CH}_3) = 25.9$  Hz), 7.03- 7.18 (m, 5H,  $\text{C}_6\text{H}_5$ -), 6.92 [7.37] (s, 2H,  $=\text{CH}$ ),

$^{119}\text{Sn}\{^1\text{H}\}$  NMR ( $\text{C}_6\text{D}_6$ )  $\delta$  (ppm): -45.7 ( $^3J_{^{119}\text{Sn}-^{117}\text{Sn}} = 175.5 \text{ Hz}$ ) [-38.97]<sup>a</sup>, -59.66 ( $^3J_{^{119}\text{Sn}-^{117}\text{Sn}} = 176.2 \text{ Hz}$ ) [62.76]<sup>a</sup>

<sup>a</sup> Values for trans isomer in square brackets

### 1:2 ratios of compounds **29** and **26**:

The above experiment was repeated with 1:2 ratio of compound **29** and **26**. The reaction mixture was analyzed after 3d but analysis by  $^{119}\text{Sn}$  NMR showed the presence of untreated **29**. The reaction mixture was heated at 80°C for further 3d. Analysis by NMR spectroscopy showed complete conversion to **32**. The product was crystallized in the NMR tube after few weeks. The  $^{119}\text{Sn}$  NMR spectrum showed only one peak at -44.0 ppm. An X-ray crystallographic analysis of these crystals revealed a compound with a structure containing two phenylacetylene units inserted between the tin atoms instead of one. The crystalline product was hexamethyl-1,4-diphenyldistannyl-1,3-butadiene **55**.

$^1\text{H}$  NMR ( $\text{C}_6\text{D}_6$ )  $\delta$  (ppm): 0.25 (s, 18H,  $^2J_{\text{Sn-H}}(\text{Sn-CH}_3) = 25.9 \text{ Hz}$ ), 7.18- 7.22 (m, 5H,  $\text{C}_6\text{H}_5$ -), 7.41 (s, 2H, =CH),  $^{119}\text{Sn}\{^1\text{H}\}$  NMR ( $\text{C}_6\text{D}_6$ )  $\delta$  (ppm): -44.0

### 1:5 ratios of compounds **29** and **26**:

In a separate reaction the ratios between the reactants was changed to 1:5.  $^{119}\text{Sn}$  NMR spectrum showed the same peaks but the peaks for cis isomer at -45.7 ppm and -59.66 ppm are more intense than for trans at -38 ppm and -62 ppm. The physical appearance of this product thick, viscous and black wax was entirely different from the product obtained from 1:1 and 1:2 ratios.

$^1\text{H}$  NMR ( $\text{C}_6\text{D}_6$ )  $\delta$  (ppm): 0.32 (s, 9H,  $^2J_{\text{Sn-H}}(\text{Sn-CH}_3) = 26.6 \text{ Hz}$ ), 0.34 (s, 9H,  $J_{\text{Sn-H}}(\text{C}_6\text{H}_5\text{-C-Sn-CH}_3) = 27.0 \text{ Hz}$ ), 7.22- 7.27 (m, 10H,  $\text{C}_6\text{H}_5$ -), 7.82 (s, 2H, =CH),  $^{119}\text{Sn}\{^1\text{H}\}$  NMR ( $\text{C}_6\text{D}_6$ )  $\delta$  (ppm): -45.7, -59.6.

## 2.5 Distannanes and Oligostannanes

### 2.5.1 Large scale thermal dehydrocoupling of (*n*-Bu)<sub>3</sub>SnH **43** under reduced pressure (open system)

The tin hydride **43** (50 g, 0.17 mol) was added to a 100 mL round bottom flask connected to a long path (13 cm) distillation condenser and the volatile components distilled at 200°C under reduced pressure ( $\approx 1 \times 10^{-2}$  mmHg). The product of this distillation was then analyzed by NMR spectroscopy. The <sup>1</sup>H and <sup>119</sup>Sn NMR spectra revealed that **43** had been consumed and converted (Recovered yield: 97%) into (*n*-Bu)<sub>3</sub>SnSn(*n*-Bu)<sub>3</sub> **45**. The NMR data provided here are in good agreement with literature values. [64, 66, 72]

### 2.5.2 Small scale thermal dehydrocoupling of **43** under reduced pressure (open system)

To a 25 mL round bottom flask equipped with long path reflux condenser (20 cm), was added tin hydride **43** (1.0 g, 3.44 mmol). The sample was heated to reflux temperature (200°C) under reduced pressure ( $\approx 2 \times 10^{-2}$  mmHg) for 6h. *In situ* analysis (<sup>1</sup>H and <sup>119</sup>Sn NMR spectroscopy) revealed 75% conversion of **43** into **45**, while the remainder was unreacted **43**. Additional heating for 6 h under these conditions showed no further reactant conversion (NMR).

### 2.5.3 Small scale thermal dehydrocoupling of **43** under reduced pressure (closed system)

Compound **43** (530 mg, 1.82 mmol) was added to a 25 mL Schlenk flask equipped with a glass stopper. The neat hydride was placed under static reduced pressure

( $\approx 5 \times 10^{-1}$  mmHg), the vessel was then sealed, and subsequently heated (200°C) for 5 h. Analysis ( $^1\text{H}$  and  $^{119}\text{Sn}$  NMR spectroscopy) showed that the majority of **43** had been consumed and was converted to **45** (Recovered yield: 95%).

#### 2.5.4 Small scale thermal dehydrocoupling of **43** under inert atmosphere (open system)

Compound **43** (530 mg, 1.82 mmol) was added to a 25 mL Schlenk flask equipped with a long path (20 cm) reflux condenser which was open to a  $\text{N}_2(\text{g})$  atmosphere. The flask was then heated (200°C) for 6 h. *In situ* analysis ( $^1\text{H}$  and  $^{119}\text{Sn}$  NMR spectroscopy) indicated that **43** had been consumed and was converted to **45** (Recovered Yield: 97%).

$^1\text{H}$  NMR ( $\text{C}_6\text{D}_6$ )  $\delta$  (ppm): 0.97 (3H, t,  $\text{CH}_3\text{CH}_2\text{CH}_2\text{CH}_2\text{-Sn}$ ), 1.16 (2H, m,  $\text{CH}_3\text{CH}_2\text{CH}_2\text{CH}_2\text{-Sn}$ ), 1.42 (2H, m,  $\text{CH}_3\text{CH}_2\text{CH}_2\text{CH}_2\text{-Sn}$ ), 1.66 (2H, m,  $\text{CH}_3\text{CH}_2\text{CH}_2\text{CH}_2\text{-Sn}$ ).  $^{13}\text{C}\{^1\text{H}\}$  NMR ( $\text{C}_6\text{D}_6$ )  $\delta$  (ppm): 10.49 ( $^1J_{\text{C-Sn}}(\text{CH}_3\text{CH}_2\text{CH}_2\text{CH}_2\text{-Sn}) = 120.3$  Hz and  $^2J_{\text{C-Sn}}(\text{CH}_3\text{CH}_2\text{CH}_2\text{CH}_2\text{-Sn-Sn}) = 19.6$  Hz), 14.01( $\text{CH}_3\text{CH}_2\text{CH}_2\text{CH}_2\text{-Sn}$ ), 27.98 ( $^3J_{\text{C-Sn}}(\text{CH}_3\text{CH}_2\text{CH}_2\text{CH}_2\text{-Sn}) = 26.5$  Hz), 31.23 ( $^2J_{\text{C-Sn}}(\text{CH}_3\text{CH}_2\text{CH}_2\text{CH}_2\text{-Sn}) = 8.1$  Hz) ppm.  $^{119}\text{Sn}\{^1\text{H}\}$  NMR ( $\text{C}_6\text{D}_6$ )  $\delta$  (ppm): -83.6 ( $J^{119}_{\text{Sn}-^{117}\text{Sn}} = 1280$  Hz).

#### 2.5.5 Small scale thermal dehydrocoupling of $\text{Ph}_3\text{SnH}$ **44** under reduced pressure (open system)

Compound **44** (471 mg, 1.34 mmol) was added to a 25 mL round bottom flask equipped with long path reflux condenser (20 cm). The sample was heated (200°C) under reduced dynamic pressure ( $\approx 1 \times 10^{-3}$  mmHg) for 6 h. During this time period, clear and colourless crystals formed on the sides of the reaction flask which were then collected and analyzed ( $^1\text{H}$  and  $^{119}\text{Sn}$  NMR spectroscopy). These data indicated that a considerable

fraction of **44** (41%) was unreacted. Approximately 59% of **44** was consumed and was converted to both **46** (31%),<sup>[73]</sup> **47** (24%)<sup>[74]</sup> and Sn metal (4%).

Major Product **46**: <sup>1</sup>H NMR (CDCl<sub>3</sub>) δ (ppm): 7.28-7.36 (12H, m), 7.39-7.52 (12H, m), 7.60-7.63 (6H, m). <sup>13</sup>C{<sup>1</sup>H} NMR (CDCl<sub>3</sub>) δ (ppm): 139.24 (C1), 137.61 (C2, C6), 128.82 (C3, C5), 128.94 (C4). <sup>119</sup>Sn{<sup>1</sup>H} (CDCl<sub>3</sub>) δ (ppm):-143.7.

### **2.5.6 Small scale thermal dehydrocoupling of 44 under reduced pressure (closed system)**

To a 50 ml Schlenk flask equipped with a glass stopper, was added **44** (394 mg, 1.12 mmol). The neat hydride was kept under static reduced pressure ( $\approx 5 \times 10^{-1}$  mmHg), the flask sealed and heated (200°C) for 4 h. *In situ* analysis (<sup>1</sup>H and <sup>119</sup>Sn NMR) indicated that **44** had been consumed and was converted to both **47** (Yield: 87%),<sup>[74]</sup> **46** (Yield: 10%)<sup>[73]</sup> and Sn metal (3%).

Major Product **47**: <sup>13</sup>C{<sup>1</sup>H} NMR (CDCl<sub>3</sub>) δ (ppm): 138.04 (C1), 137.39 (C2, C6), 128.79 (C3, C5), 128.28 (C4). <sup>119</sup>Sn {<sup>1</sup>H} NMR (CDCl<sub>3</sub>) δ (ppm): -129.6.

### **2.5.7 Small scale thermal dehydrocoupling of 43 and 44 under reduced pressure (closed system)**

To a 50 ml Schlenk flask equipped with a glass stopper was added **43** (291 mg, 1.00 mmol) and **44** (351 mg, 1.00 mmol). Neat tin hydrides were then placed under static reduced pressure ( $\approx 5 \times 10^{-1}$  mmHg), sealed and heated (200°C) for 5 h. *In situ* analysis (<sup>1</sup>H and <sup>119</sup>Sn NMR) indicated the conversion of **43** and **44** into a mixture containing **45** (12%), **46** (37%), **47** (13%) and **48** (37%)<sup>[72]</sup> and trace of elemental tin (1%).

### 2.5.8 Small scale thermal dehydrocoupling of (*n*-Bu)<sub>2</sub>SnH<sub>2</sub> **13** under nitrogen (open system)

To a 50 ml Schlenk flask equipped with a glass stopper was added **13** (428 mg, 1.82 mmol). The flask containing **13** was then placed under an atmosphere of N<sub>2</sub> and heated (160°C) for 6h. *In situ* analysis (<sup>1</sup>H and <sup>119</sup>Sn NMR spectroscopy) indicated the conversion of **13** to a mixture containing **58**<sup>[75]</sup>, **5**<sup>[70]</sup>, **6** and **7**<sup>[31,76]</sup> along with unassigned oligomers. <sup>119</sup>Sn {<sup>1</sup>H} NMR (C<sub>6</sub>D<sub>6</sub>) δ (ppm): (**5**: -189.3), (**7**: -202.1), (**13**: -203.2), (**56**: -207.9), (others: -195.6, -209.5, -220.1). Analysis by GPC revealed a molecular weight of  $M_w = 1.8 \times 10^4$  Da, PDI = 6.9. UV-Vis:  $\lambda_{max} = 370$  nm.

### 2.5.9 Small scale thermal dehydrocoupling of **13** under reduced pressure (Open system)

To a 50 ml Schlenk flask equipped with a glass stopper was added **13** (500 mg, 2.12 mmol). The flask containing **13** was then placed under an atmosphere of N<sub>2</sub> and heated (200°C) for 6h. *In situ* analysis (<sup>1</sup>H and <sup>119</sup>Sn NMR spectroscopy) indicated the conversion of **13** to a mixture containing **43**, **45**, **58** and **57**<sup>[62]</sup> along with other unassigned peaks. <sup>119</sup>Sn {<sup>1</sup>H} NMR (C<sub>6</sub>D<sub>6</sub>) δ (ppm): (**57**: -75.3, -213.4), (**58**: -76.2, -227.0), (**45**: -83.2), (**43**: -87.3), (others: +155.9, -57.7, -66.6, -210.2).

## 2.6 Molecular Modeling of Oligostannanes:

The molecular modeling was done for the Dräger oligostannanes **20(a-d)**, distannanes and alkyne inserted distannanes using different methods of geometric optimization. The energy calculation of these molecules was performed using density functional method (DFT).

The basis set used in all calculations was the LACVP\* basis set (Spartan 08 V1.1.1) in corresponding the LAN2DZD core potentials (pseudopotential) on heavy atoms and 6-31G\* basis set on lighter atoms. The density function form used was B3LYP. Geometry optimization and energy calculations were carried out at the same level of theory.

## CHAPTER THREE

### Results and Discussion

To achieve the objectives of this research, polydibutylstannane **5** was synthesized from di-*n*-butylstannane **13** using a previously reported method.<sup>[35]</sup> To reach the eventual goal of a stabilized inserted polystannane, alkyne inserted model distannanes were explored and successfully prepared using literature routes. The same method was also successfully explored for the insertion of acetylene into **5**.

A further objective was to explore the radically driven dehydrocoupling of simple stannanes as a potential route to dimer and polymer.

The final objective was to re-examine the series of compounds that Dräger prepared and model the structures using DFT method.

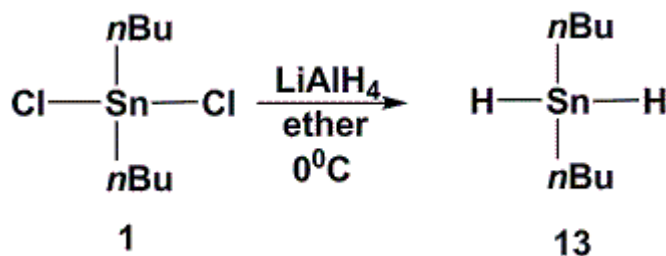
The results obtained during this research are described below in detail.

### 3.1 Polystannanes:

#### 3.1.1 Di-*n*-butylstannane **13**:

Compound **13** was obtained in good yield using the preparation method (Reaction 3.1.1) described by Tilley's group.<sup>[31,70]</sup> During this synthesis, it was observed that CaCl<sub>2</sub>, used as drying agent should be granular in nature and of the highest grade available. When commercial grade CaCl<sub>2</sub> was used, <sup>1</sup>H and <sup>119</sup>Sn NMR spectra (<sup>1</sup>H, <sup>119</sup>Sn) of the resulting product indicated additional unwanted resonances.

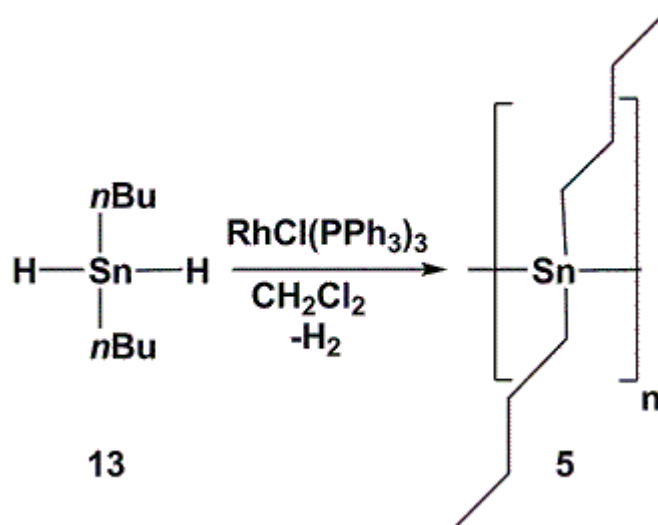
### Reaction 3.1.1



### 3.1.2 Poly di-*n*-butylstannane **5**:

The method used for the polymerization of **13** was the same as described in the recent literature.<sup>[35]</sup> This involved the polymerization of **13** to **5** by catalytic dehydrogenation using Wilkinson's catalyst (Reaction 3.1.2).

### Reaction 3.1.2



Due to the unstable nature (ambient light degradation) of the resulting polymer, we were unsuccessful in establishing the absolute molecular weight of this polymer when using a triple detector GPC instrument. Sensitivity to the laser sources of the RI and light scattering detector promoted photolysis. However, when benzotriazole-5-carboxylic

acid was added as a UV absorber to the THF solution, the absolute molecular weight of this polymer could be determined ( $M_w$   $5.1 \times 10^4$  Da).

The polymerization of **13** was also attempted using  $\text{Pd}(\text{PPh}_3)_4$  **27** as the catalyst. The  $^{119}\text{Sn}$  NMR spectrum (Figure 3.1) of this reaction mixture revealed only the formation of cyclic oligomer(s) **7** and no evidence for polymer **5**.

### Reaction 3.1.3

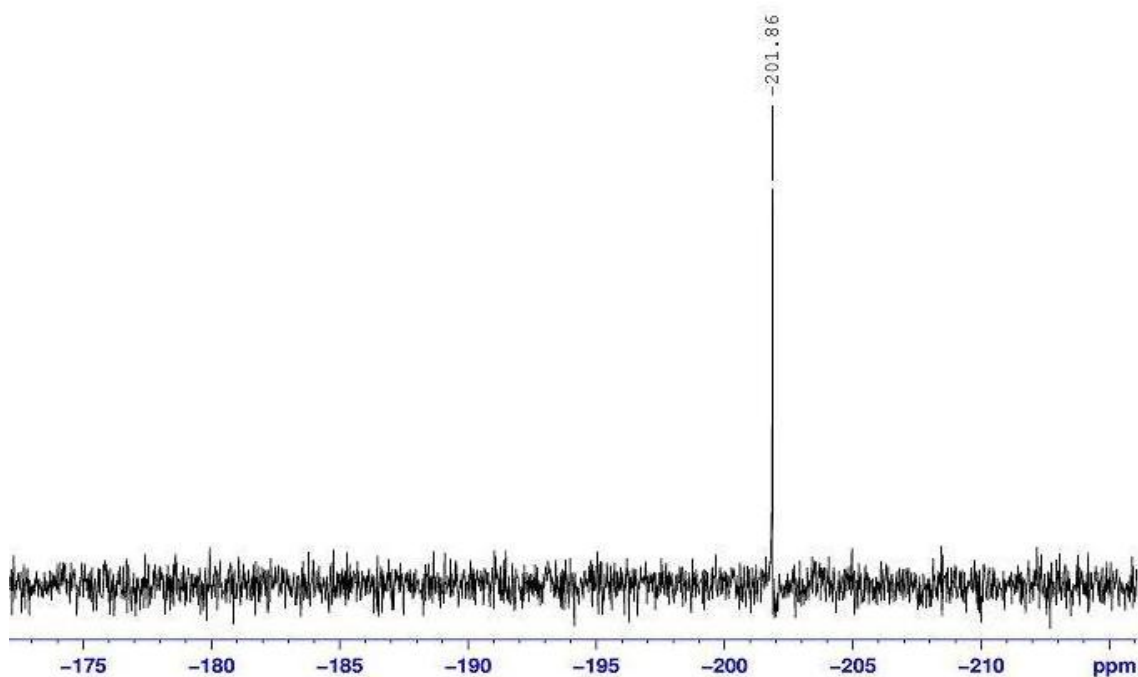
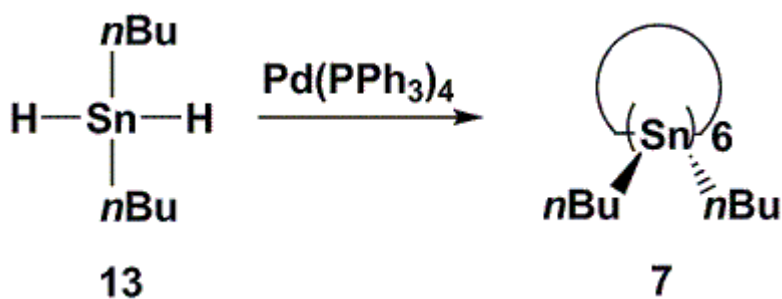


**Figure 3.1**  $^{119}\text{Sn}$  NMR spectrum of **7**

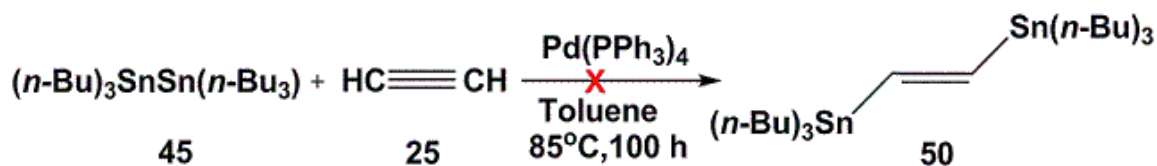
## 3.2 Inserted distannanes and oligostannanes

This part of the chapter describes the synthesis of tin oligomers as models of larger polymer-like materials. These materials are obtained via Sn-alkyne insertion reactions.

### 3.2.1 Hexa-*n*-butyldistannyl ethylene **50**:

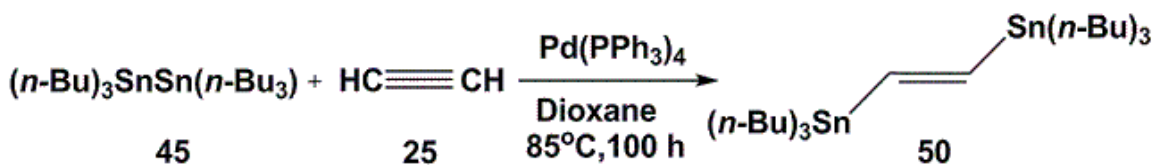
An initial attempt to synthesize compound **50** was carried out by bubbling acetylene (C<sub>2</sub>H<sub>4</sub>) gas through a solution of **45** in toluene using **27** as catalyst was unsuccessful. The reaction mixture was analyzed after 60 h but no change in the contents of the reaction mixture was observed (NMR). The reason for this inactivity may be a result of the poor solubility of acetylene in toluene.

#### Reaction 3.2.1

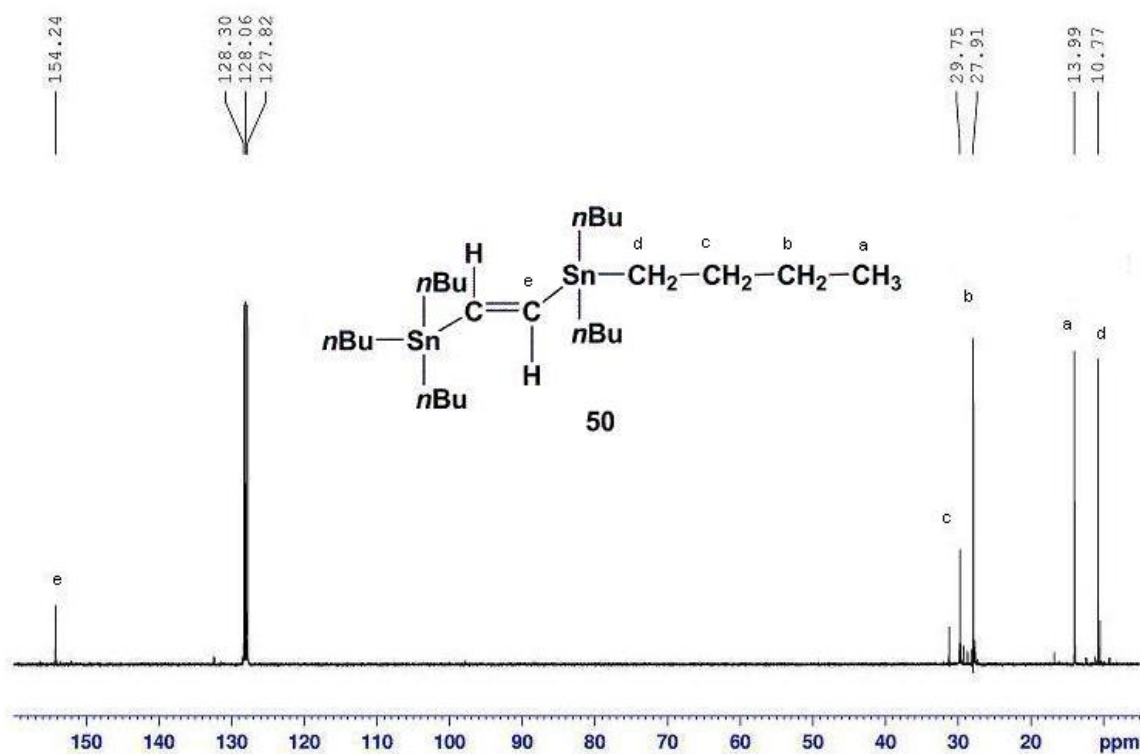


The reaction was repeated using dioxane as a solvent employing protocols first described by Mitchell *et al.*<sup>[45]</sup> Over the 100 h reaction period, the mixture turned orange brown in colour and was then filtered through a glass frit (Reaction 3.2.2). The solvent was removed under reduced pressure and an orange brown coloured oily products **50** was obtained.

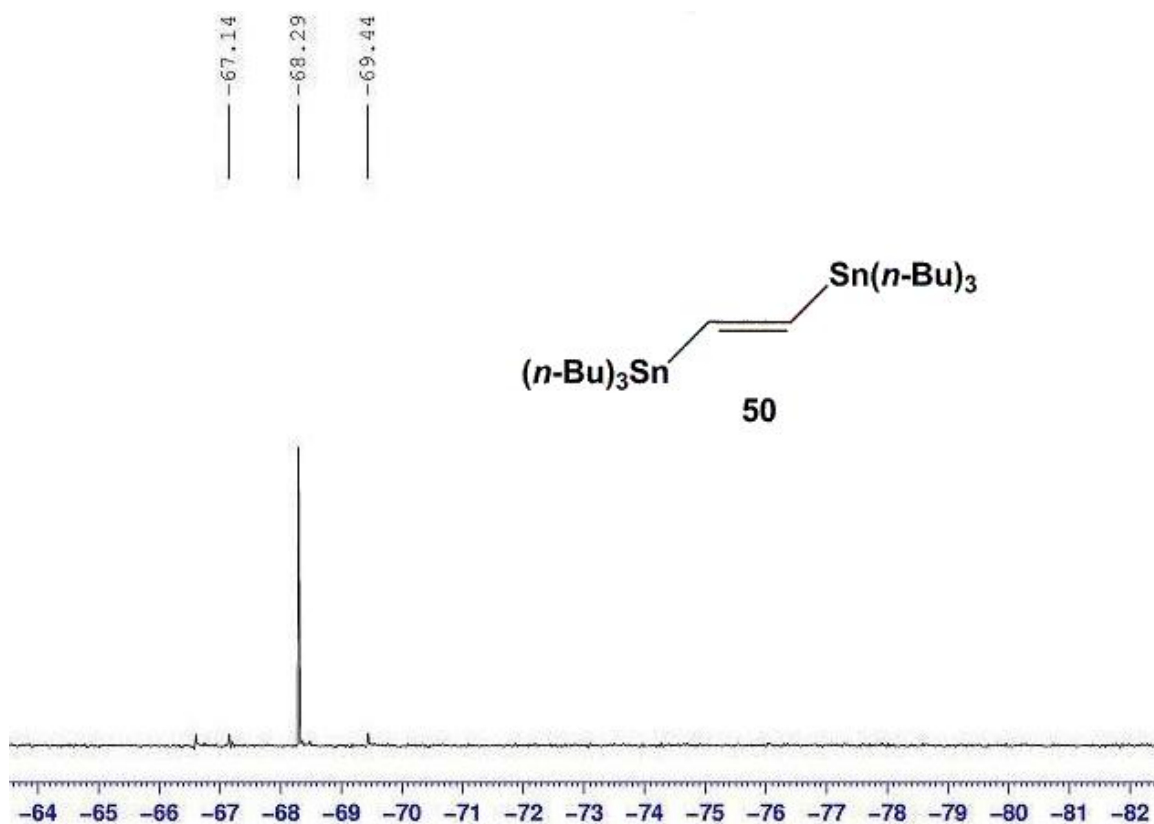
### Reaction 3.2.2



The  $^{119}\text{Sn}$  NMR spectrum for the reaction products showed a significant shift of the chemical resonance from -83.5 ppm for **45** to -68.3 ppm for **50**.  $^{13}\text{C}$ -NMR spectrum also showed a signal assigned to the olefin bridging carbon -CH=CH- carbons resonating at 154.2 ppm. This product was then re-dissolved in hexane and filtered. Unfortunately, our attempts to crystallize this material at  $-70^\circ\text{C}$  were not successful.



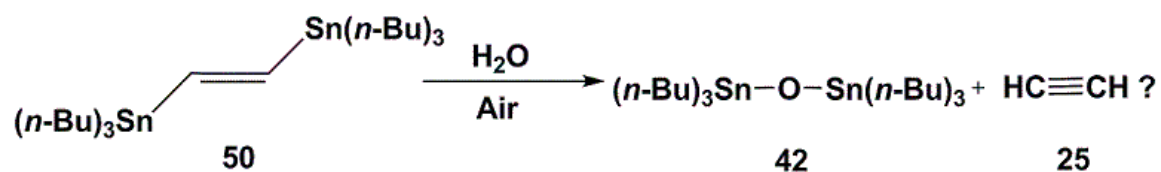
**Figure 3.2**  $^{13}\text{C}$  NMR spectrum of **50**



**Figure 3.3**  $^{119}\text{Sn}$  NMR spectrum of **50**

A sample of **50** was sent for analysis by mass spectrometry (MS). These results revealed that the only product present was distannaxone **42** instead of the desired **50**. This likely indicates a high degree of sensitivity of compound **50** to exposure to moist solvents and/or light.

### Reaction 3.2.3



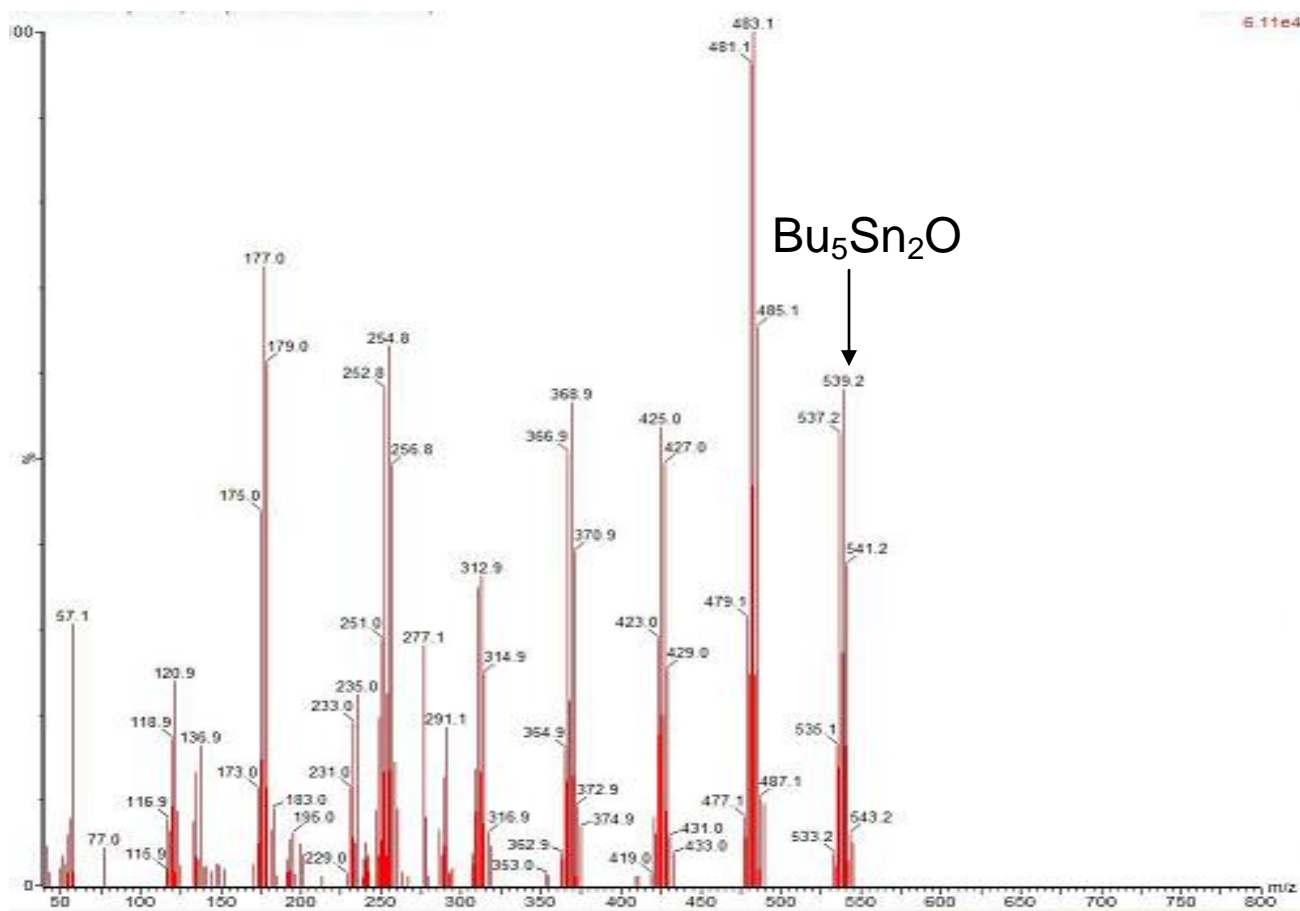


**Figure 3.4** Mass spectrum of **42**

Analysis of the sample used for MS by  $^{119}\text{Sn}$  NMR spectrum showed a peak at 69.0 ppm corresponding to the stannoxane **42** instead of -68.3 ppm **50**.

**Table 3.1** Fragmentation of **42**

| M/z   | fragment ion                         | Fragment lost         |
|-------|--------------------------------------|-----------------------|
| 539.3 | $[\text{Bu}_5\text{Sn}_2\text{O}]^+$ | [Bu]                  |
| 481.1 | $[\text{Bu}_4\text{Sn}_2\text{O}]^+$ | [Bu <sub>2</sub> ]    |
| 425   | $[\text{Bu}_3\text{Sn}_2\text{O}]^+$ | [Bu <sub>3</sub> ]    |
| 368.9 | $[\text{Bu}_2\text{Sn}_2\text{O}]^+$ | [Bu <sub>4</sub> ]    |
| 312.9 | $[\text{BuSn}_2\text{O}]^+$          | [Bu <sub>5</sub> ]    |
| 254.8 | $[\text{Sn}_2\text{O}]^+$            | [Bu <sub>6</sub> ]    |
| 136.9 | $[\text{SnO}]^+$                     | [Bu <sub>6</sub> Sn]  |
| 120.9 | $[\text{SnH}]^+$                     | [Bu <sub>6</sub> SnO] |

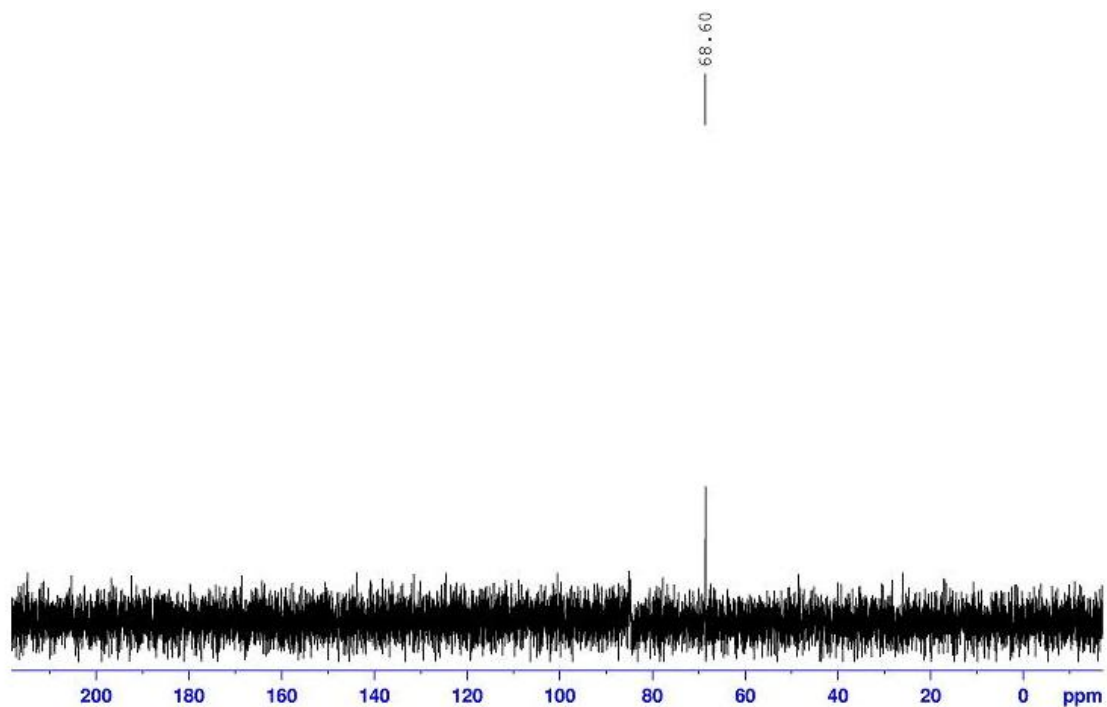


**Figure 3.5**  $^{119}\text{Sn}$  NMR ( $\text{C}_6\text{D}_6$ ) spectrum of **42**

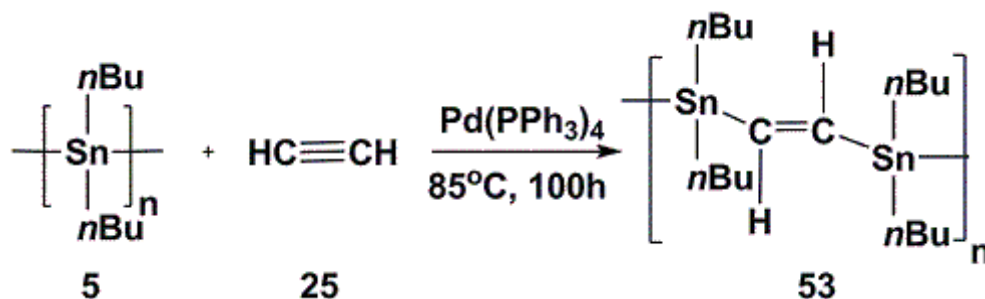
The product obtained at the end of Reaction 3.2.2 was different from that detected by MS (Figure 3.4) which suggests that oxygen inserts and replaces the -CH=CH- group.

There are two likely causes for the insertion of oxygen in the product. The first is that there is simple exchange and insertion of oxygen when the sample is open to the atmosphere and second may be due to bond breakage between Sn-C atoms and Sn-O formation during mass spectrometric analysis. Subsequent testing has shown that samples of **50** left exposed to moist air will convert to stannoxanes.

### 3.2.2 Insertion of acetylene in **5**:

The insertion of acetylene into the backbone of  $[(n\text{-Bu})_2\text{Sn}]_n$  **5** was attempted. All work was done in an inert atmosphere on the basis of the previous experience from Reaction 3.2.2. Polymer **5** was synthesized using the same route as described in section 2.3.2

#### Reaction 3.2.4



Analysis by  $^{119}\text{Sn}$  NMR spectrum shows only one peak at  $\delta = -66.6$  ppm. This is similar to the chemical shift found for the acetylene inserted distannane **50** ( $\delta = -68.3$  ppm). Absent in this spectrum is a peak at  $-190$  ppm for the starting material **5**. NMR spectrum also revealed additional peaks at  $68.5$  ppm,  $-50.23$  ppm and  $-176.83$  ppm. These peaks were assigned on the basis of other experiments which were performed both prior to and after this experiment. The peak at  $-66.6$  ppm was assigned to polymer **5** with

inserted acetylenic groups between the Sn atoms. The peak at  $\delta = -176.8$  ppm can be assigned to the  $-\text{CH}=\text{CH}-$  inserted cyclic product and one at  $\delta = 68.5$  ppm is likely **42**. However, the resonance at  $\delta = -50.23$  ppm is currently unknown. The viscous product(s) obtained from the above reaction mixture was dark brown in colour. This mixture was subsequently re-dissolved in  $\text{CH}_2\text{Cl}_2$  and the solution filtered. An attempt to reprecipitate the product(s) from the solution in  $\text{CH}_2\text{Cl}_2$  in dry ice and acetone was unsuccessful. However, this product was successfully isolated via a methanol precipitation process at  $-33^\circ\text{C}$ . The precipitated product showed only one resonance at  $\delta = -66.5$  ppm ( $^{119}\text{Sn}$  NMR). Presumably, the other reaction products are completely soluble in the methanol used to precipitate the desired material.

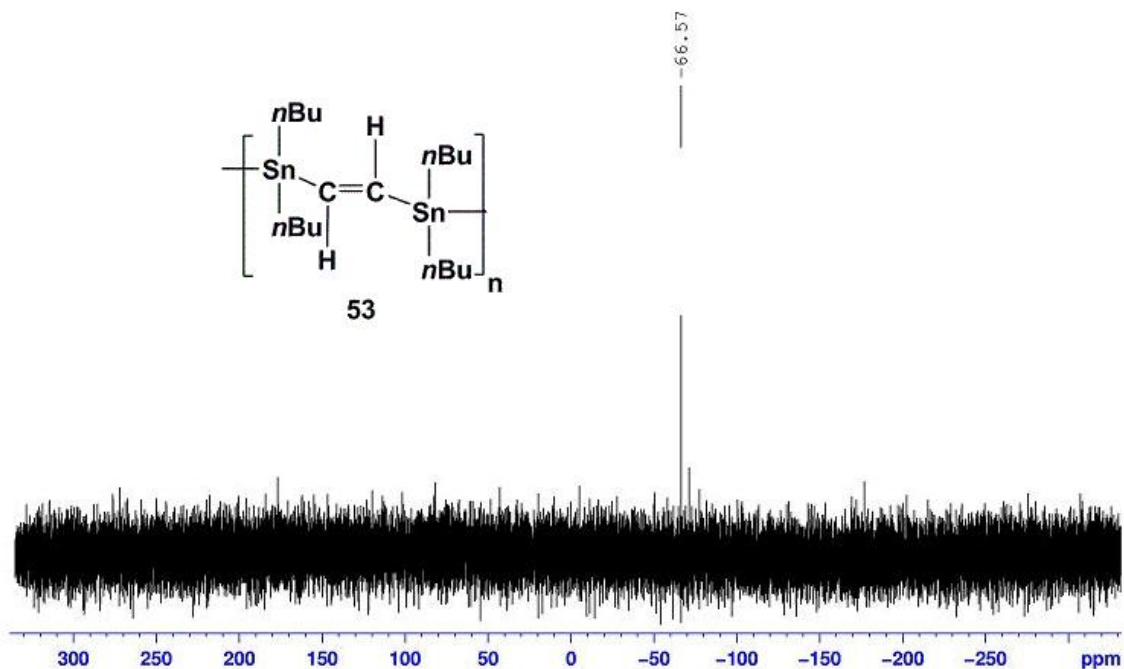


**Figure 3.6**  $^{119}\text{Sn}$  NMR ( $\text{C}_6\text{D}_6$ ) spectrum of the inserted  $(\text{nBu}_2\text{Sn})_n$  **53**

### 3.2.3 Hexamethyldistannyl ethylene 30:

Compound **29** was diluted with dioxane containing  $\text{Pd}(\text{PPh}_3)_4$  and heated ( $60^\circ\text{C}$ ) while passing acetylene gas through the reaction mixture (4 h). Analysis by  $^{119}\text{Sn}$  NMR in  $\text{C}_6\text{D}_6$  showed the presence of both **30** and **51**.

#### Reaction 3.2.5

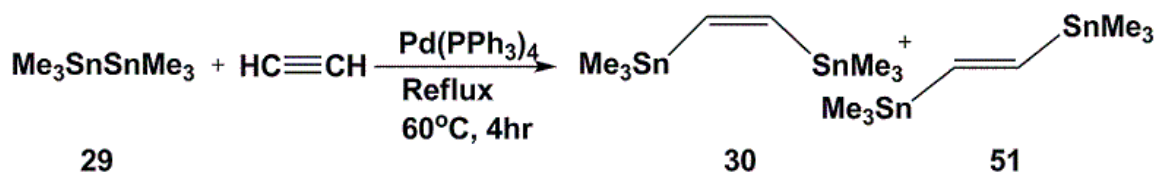


**Table 3.2**  $^{119}\text{Sn}$  NMR data of **30** and **51**

| Isomer | Chemical shift( $\delta$ ) ppm<br>found | Chemical shift( $\delta$ ) ppm<br>Literature value <sup>[45]</sup> |
|--------|---|--|
| Cis    | -61.3                                   | -60.6  |
| Trans  | -54.7                                   | -52.3  |

An attempt to crystallize the product from hexane was unsuccessful. To induce crystallization, the product was diluted in ether, filtered and evaporated in an open atmosphere. This led to the formation of crystals suitable for X-ray diffraction. The analysis of the crystal unit cell data revealed the material to be the one dimensional hydroxyl bridged polymer  $(\text{Me}_3\text{SnOH})_n$  **52**. This known compound was not further analyzed.  $^{119}\text{Sn}$  NMR analysis of these crystals showed a new peak at -35 ppm attributed to **52** along with peaks assigned to **30** and **51**.

Reaction 3.2.6

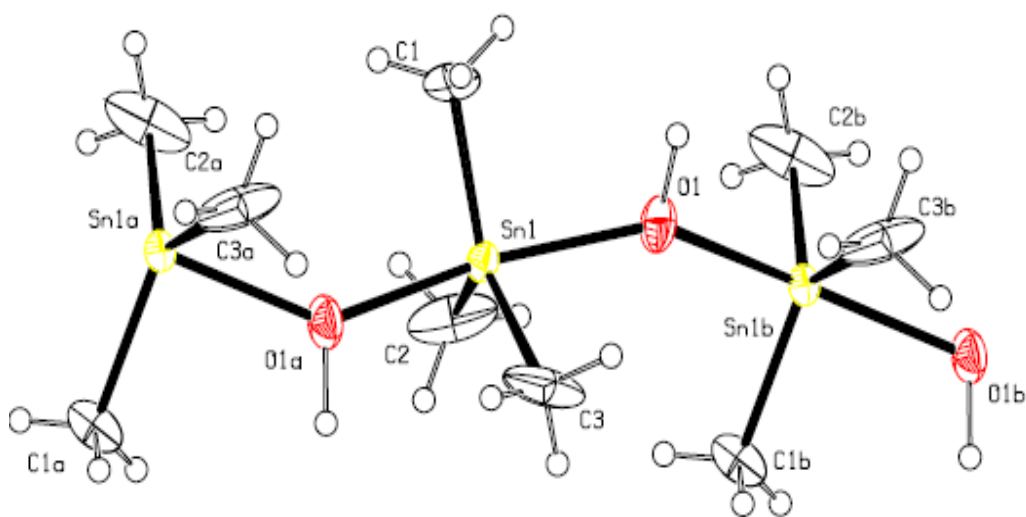
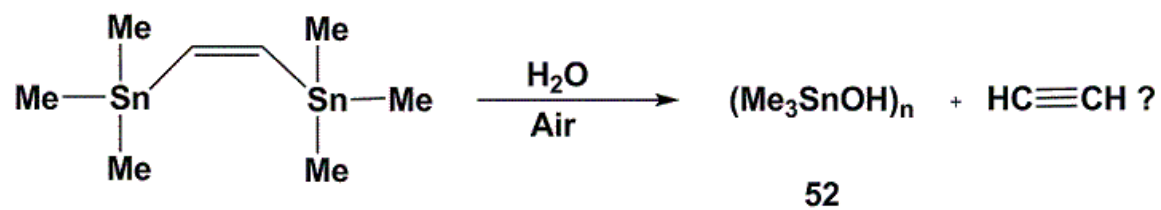


**Figure 3.7** ORTEP representation of units of **52**<sup>[71]</sup> in the unit cell

### 3.2.4 Hexamethyl-1-phenyldistannyl ethylene 32, 54:

The hexamethyldistannane **29** and phenylacetylene **26** with  $\text{Pd}(\text{PPh}_3)_4$  was refluxed at  $80^\circ\text{C}$  for 72h. A  $^{119}\text{Sn}$  NMR analysis showed the presence of both cis and trans isomers of **32** and **54** respectively.

#### Reaction 3.2.7

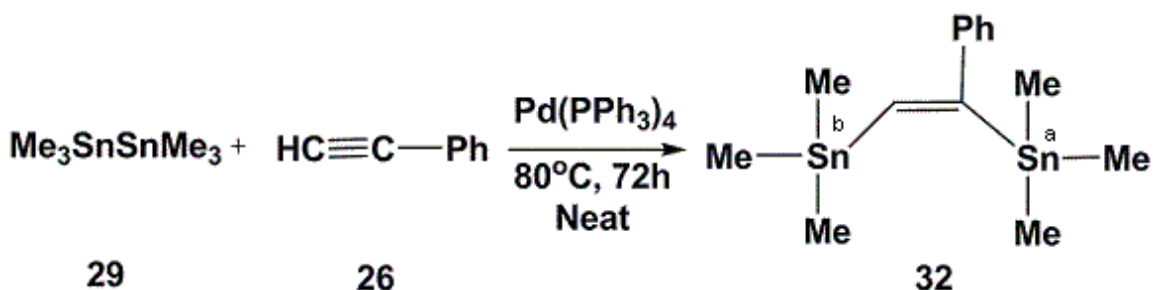
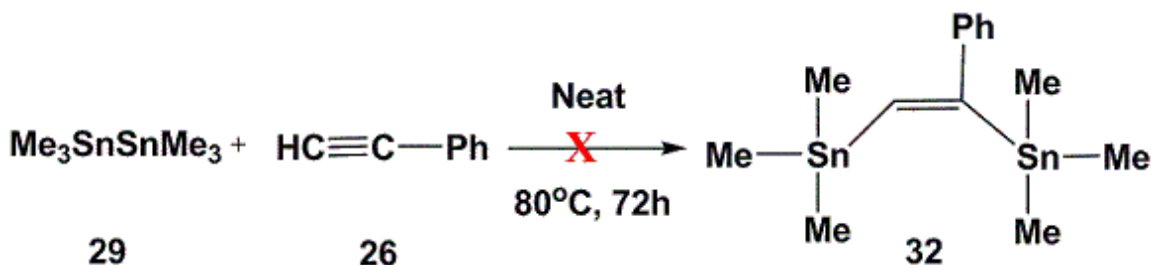


**Table 3.3**  $^{119}\text{Sn}$  NMR data of **32** and **54**

| Isomer | $\delta(\text{Sn}^a)$ ppm |                            | $\delta(\text{Sn}^b)$ ppm |                            |
|--------|---------------------------|----------------------------|---------------------------|----------------------------|
|        | observed                  | Literature <sup>[45]</sup> | observed                  | Literature <sup>[45]</sup> |
| Cis    | -45.7                     | -45.9                      | -59.7                     | -59.4                      |
| Trans  | -38.9                     | -39.0                      | -62.7                     | -62.0                      |

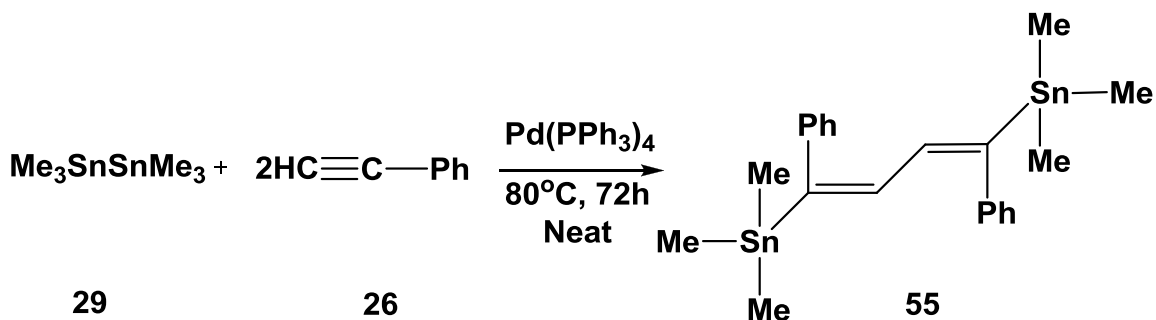
When this experiment was repeated in the absence of catalyst, no reaction was observed.

#### Reaction 3.2.8



The above experiment was repeated with a 1:2 ratio of **29** to **26**.

### Reaction 3.2.9



The product was crystallized in an NMR tube after a few weeks. Analysis of the crystals by  $^{119}\text{Sn}$  NMR showed only one peak at -44 ppm. An X-ray structure determination of these crystals reveals a head to head insertion of two phenylacetylene units between the tin atoms forming the unexpected hexamethyl-1,4-diphenyldistannyl-1,3-butadiene **55**.

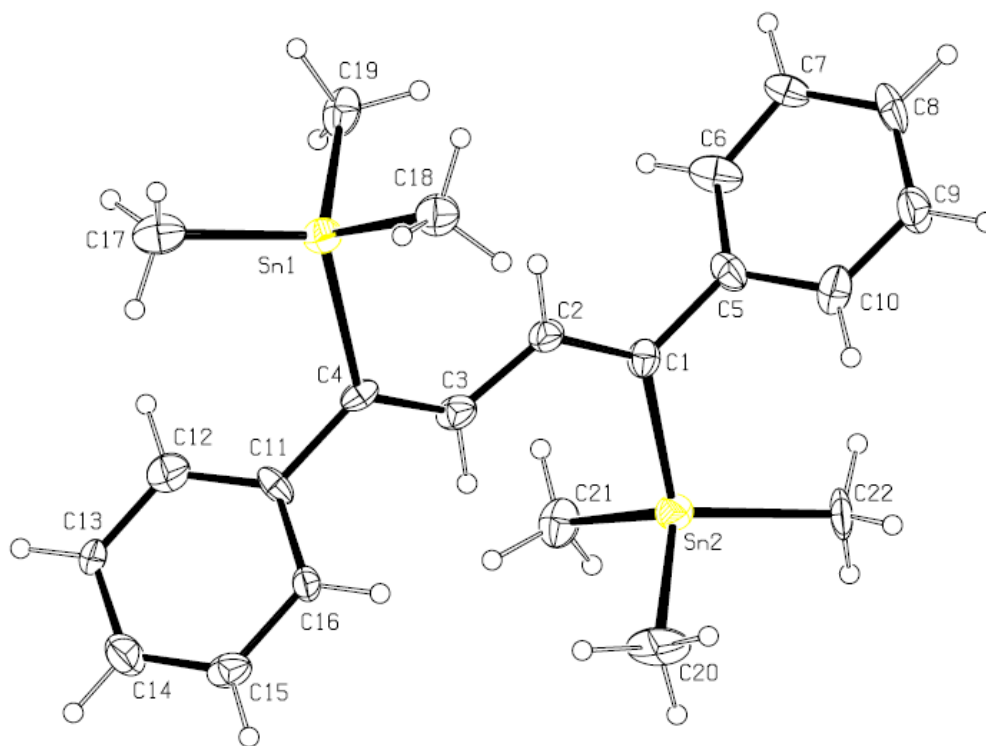


**Figure 3.8** ORTEP representation of units of **55** in the unit cell

The experiment was repeated with a 1:5 ratio of **29** to phenylacetylene **26**. The  $^{119}\text{Sn}$  NMR spectrum showed the same products as found in the previous experiments with **29** and **26** (1:2 ratio). The physical appearance of the product oil was black in colour and highly viscous; in other words different to that of the product obtained by using 1:2 ratio of **29** to phenylacetylene **26**. Crystals developed after few weeks in the NMR tube and in the reaction flask and have yet to be fully analyzed.

The proposed mechanism for the formation of **55** (Reaction 3.2.7) follows a free radical mechanism 1 or insertion of the second phenylacetylene unit by proposed Mechanism 2.

### Proposed Mechanism 1:

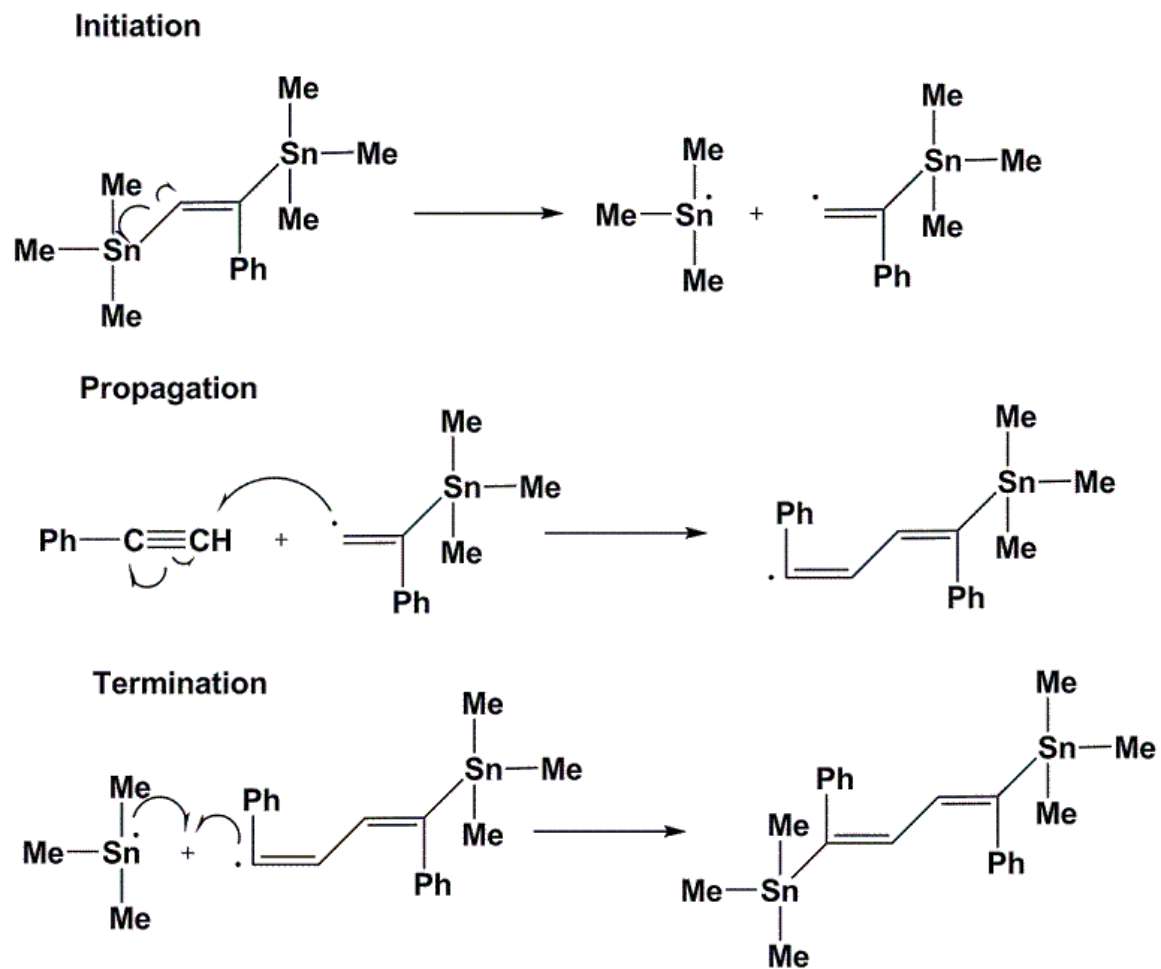


**Figure 3.9** Proposed mechanism 1 for the double insertion of phenylacetylene

## Mechanism 2:

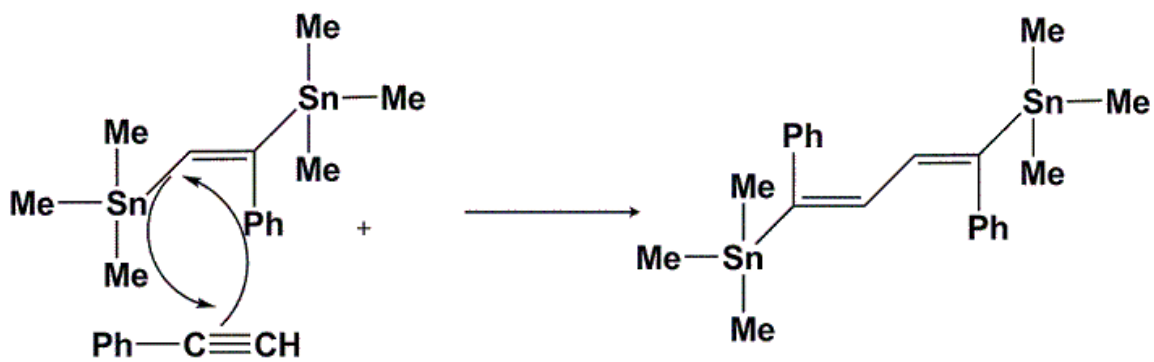


**Figure 3.10** Proposed mechanism 2 for the double insertion of phenylacetylene

### 3.3 Distannanes and oligostannanes:

The reaction conditions that were used to produce distannanes **45** and **46** from **43** and **44** respectively are listed in Table 1. An attempt to distill crude commercial **43** (200°C: *vacuo*) using a long path distillation condenser was initiated with the intention to further purify **43**. Surprisingly, the product of this distillation was not **43**, but a nearly quantitative (97%) conversion ( $^1\text{H}$  and  $^{119}\text{Sn}$  NMR) to distannane **45**. We investigated the impact of heating **43** to reflux temperature (200°C) under reduced pressure using a long path reflux condenser. After 6h, analysis by  $^1\text{H}$  and  $^{119}\text{Sn}$  NMR indicated a 75% conversion of **43** to **45**. The sample was further heated (6h) under these conditions but NMR analysis showed virtually no change in the proportions of the product to that of the starting material. A plausible reason for this observation is that the more volatile hydride is retained by the cool portion of the reflux condenser rather than in close proximity to the heat source. To improve this conversion, **43** was heated (200°C) under static vacuum conditions in a sealed Schlenk flask. *In situ* analysis ( $^{119}\text{Sn}$  NMR) of the reaction mixture taken every hour revealed that after 5h, **43** had completely converted to the distannane **45**. The reaction was also carried out in a sealed flask under a nitrogen atmosphere. Analysis by  $^{119}\text{Sn}$  NMR showed a small peak for **43** after 5h, which was completely consumed after heating for one additional hour (Fig.3.11). There was no evidence of redistribution products, which were reported when **43** was thermally dehydrocoupled in the presence of Group 4 or 6 transition metal complexes.<sup>[76]</sup>

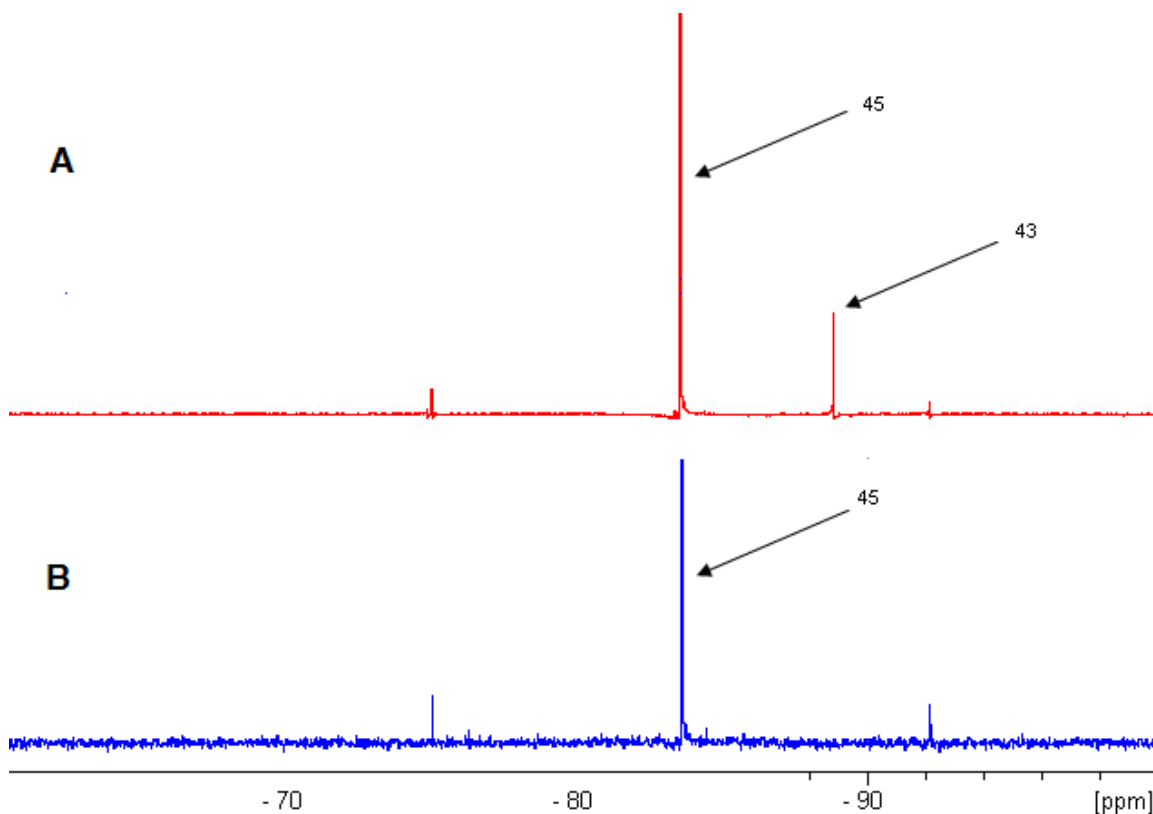


**Figure 3.11**  $^{119}\text{Sn}$  NMR spectra of the products from the dehydrocoupling of **43** at **A**) 4h @ 200°C and **B**) 5h @ 200°C under static reduced pressure.

Similar, presumably radical in origin, dehydrocoupling conditions were used for hydride **44**. After 6h at reflux (200°C) under reduced pressure, approximately 31% of the starting material had converted to distannane **46**, with most of the remainder represented by the starting material **44** in addition to a significant fraction (24%) of the redistribution product  $\text{Ph}_4\text{Sn}$  **47**. Product **46** precipitated from the reaction mixture as a crystalline solid as it cooled and could be easily recovered from the starting material by recrystallization. The reaction was also repeated in a heated (200°C) and sealed Schlenk flask under static vacuum. The  $^{119}\text{Sn}$  NMR spectrum of this mixture showed evidence for a thermal redistribution reaction with the bulk of the material converted (87%) to **47**, a considerably

lower fraction of **46** (10%) in addition to a trace of grayish sediment which was attributed to elemental tin.

**Table 3.4 Catalyst and solvent-free thermal couplings of tin hydrides**

| Starting material | Reaction conditions             | Reaction time | Product       | Yield (%) |
|-------------------|---------------------------------|---------------|---------------|-----------|
| <b>43</b>         | 200°C, N <sub>2</sub>           | 6h            | <b>45</b>     | 97        |
|                   | 200°C, Reflux/ reduced pressure | 12h           | <b>45</b>     | 75        |
|                   | 200°C, Static/reduced pressure  | 5h            | <b>45</b>     | 95        |
| <b>44</b>         | 200°C, Reflux/reduced pressure  | 6h            | <b>46, 47</b> | 31, 24    |
|                   | 200°C, Static/reduced pressure  | 4h            | <b>46, 47</b> | 10, 87    |
| <b>43 and 44</b>  | 200°C, Static/reduced pressure  | 5h            | <b>45</b>     | 12        |
|                   |                                 |               | <b>46</b>     | 37        |
|                   |                                 |               | <b>47</b>     | 13        |
|                   |                                 |               | <b>48</b>     | 37        |

Utilizing closed, reduced pressure reaction conditions, an equimolar mixture reaction of the **43** and **44** were heated (200°C) for 5h. Analysis by <sup>119</sup>Sn NMR spectroscopy (Fig.3.12: below) revealed resonances at  $\delta = -145.8$  and  $-67$  ppm. These chemical shift values are consistent with the formation of **48**.<sup>[72]</sup> Traces of the starting materials, along with **45** and **46**, the redistribution product **47**, and two unassigned peaks were also noted. These unidentified materials may be other higher molecular weight redistribution products.

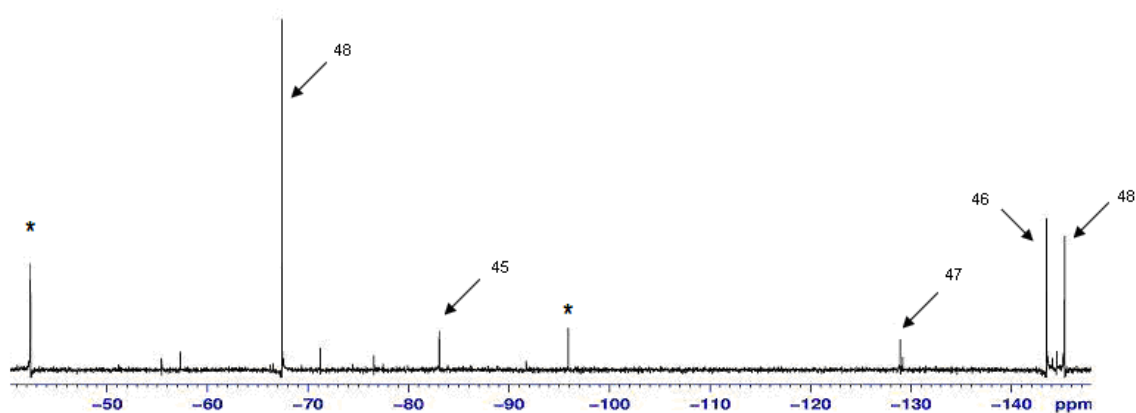
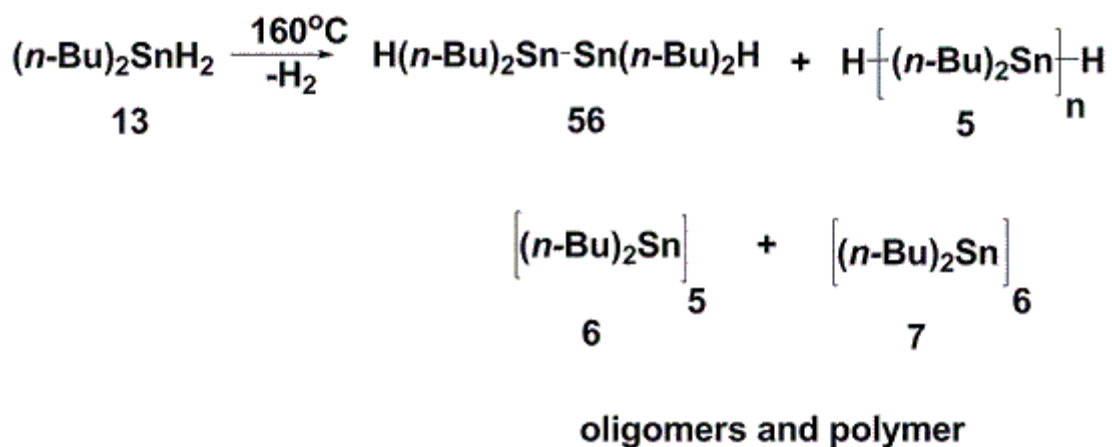


**Figure 3.12**  $^{119}\text{Sn}$  NMR spectrum of the products from the dehydrocoupling of **43** and **44** at 200°C for 5h. Peaks with an asterisk are unassigned.

The solvent-free, catalyst-free reaction  $\text{N}_2(\text{g})$  conditions were also employed with the secondary stannane,  $(n\text{-Bu})_2\text{SnH}_2$  (**13**; Reaction 3.3.1). After 6h of heating (160°C),  $^{119}\text{Sn}$  NMR spectroscopic analysis of the brightly yellow coloured oily solid material revealed a multitude of resonances.

### Reaction 3.3.1



Clearly identifiable in this spectrum however was a resonance at  $\delta \approx -208$  ppm, which is attributed to the hydride terminated distannane  $(n\text{Bu}_2\text{SnH})_2$  **56**.<sup>[75]</sup> Additionally, a resonance at  $\delta \approx -189$  ppm can be assigned to linear dibutylpolystannane **5**.<sup>[70]</sup> Two

cyclic species **6** and **7** were identified by comparison with the literature  $^{119}\text{Sn}$  chemical shift values.<sup>[29,74]</sup> The assignments of the rest of the minor signals has not yet been made but these are likely due to the presence of higher molecular weight hydride terminated oligomers (e.g.  $n\text{-Bu}_2\text{SnH}(n\text{-Bu}_2\text{Sn})_n\text{SnH}n\text{-Bu}_2$ ). Analysis of this material by GPC showed a broad polymer distribution and a modest molecular weight polystannane ( $M_w = 1.8 \times 10^4$  Da, PDI = 6.9) along with a considerable fraction of lower molecular weight linear and cyclic products. A UV-Vis spectrum (Fig. 3.13) of the mixture containing the polymer **5** displayed a broad absorbance with a  $\lambda_{\text{max}}$  centered at  $\approx 370$  nm. This absorbance can be attributed to the  $\sigma\text{--}\sigma^*$  of the polystannane which is in good agreement with reported values.<sup>[69]</sup>

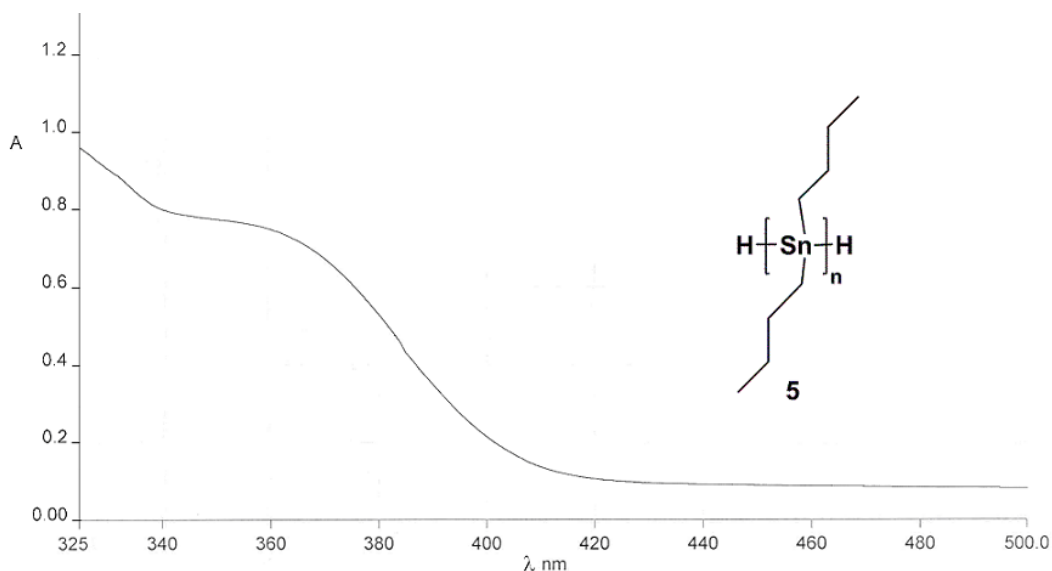
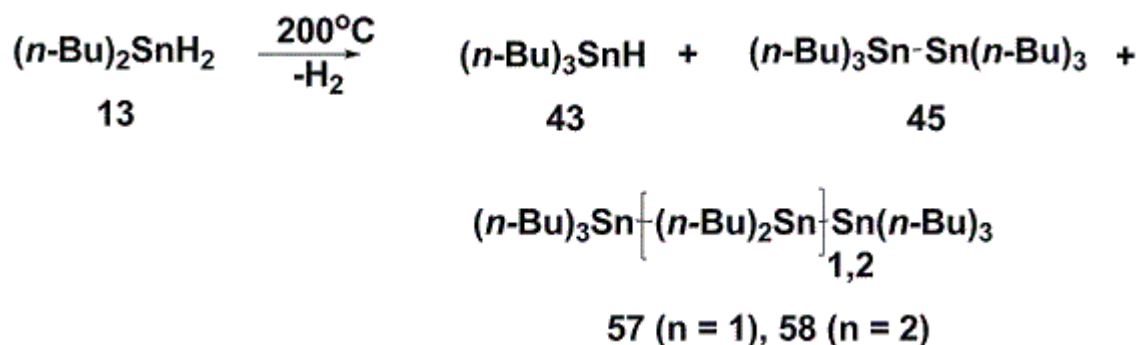


**Figure 3.13** UV-Vis (THF) spectrum of the mixture containing **5**

When the dehydrocoupling of **13** was attempted at a higher temperature (200°C: 6h), evidence of multitude of alkyl redistribution products was found (Reaction 3.3.2). Analysis by  $^{119}\text{Sn}$  NMR spectroscopy showed resonances attributed to **43** as well as to

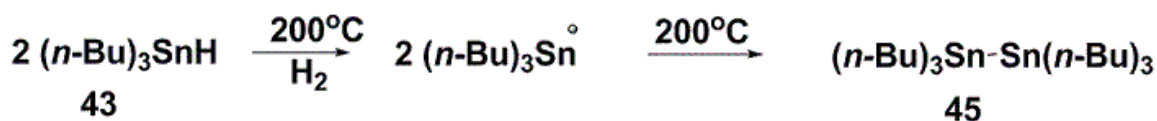
dimeric **45** and higher tributylstannane terminated oligomers i.e. **57**, **58** identified by comparison to literature values.<sup>[62]</sup> One strong and unassigned resonance was observed at +156 ppm. There is, however, no evidence of cyclic products or hydride terminated oligomers.

### Reaction 3.3.2



The catalyst and solvent-free, presumably radically driven, dehydrocoupling reactions described herein are apparently activated through the thermolysis of the relatively weak Sn-H bonds of R<sub>3</sub>SnH (R = *n*-Bu, Ph).

### Scheme 3.3.1



In the case of **44**, additional redistribution reactions to yield products such as **47** also occur. The Sn-aryl bonds also appear to be thermally labile at 200°C and redistribution chemistry is competitive with dehydrogenation. In contrast, trialkyl

stannanes seem less active towards such redistributions at this temperature. In order to maximize yields of distannanes and reduce the potential of unwanted redistribution products, it is essential to identify the optimum reaction conditions (*e.g.*, temperature and duration of the reaction). Closed reaction vessels under slight reduced pressure produce the highest yields for all products **45**, **46** and **48**. A likely driving force in these reactions is the liberation of H<sub>2</sub>(*g*) along with formation of the persistent tin alkyl and aryl radicals that later combine to form distannanes. Attempts to carry out dehydrocoupling reactions at higher temperatures (200°C) resulted in the decomposition of the starting materials and/or lower product yields. Reaction of the secondary stannane **13** at lower temperatures (160°C) resulted in the formation of linear and cyclic polystannane species including a modest molecular weight polymer **5**. The broad polydispersity found for this sample is typical of other radical polymers prepared from an uncontrolled polymerization process. The mechanism of propagation for this species is unclear, but may occur through the coupling of two growing oligomeric species which contain active radical end groups. When a sample of **13** was heated at 200°C, redistribution to tributylstannyl terminated species are the dominant process and no evidence for cyclics or polymer was noted.

### 3.4 Modelling of oligostannanes and alkyne inserted stannanes:

The crystallographic structural and electronic spectral data for Dräger's oligostannanes **20(a-d)** provide a useful reference set for a molecular modeling study of tin oligomers. The work presented in this thesis represents the first such modeling study for these compounds. Based on these results, the most successful of the modeling methods have been extended to other compounds (distannanes and alkyne inserted distannanes) prepared in the lab, not all of which have been fully characterized with respect to structure or electronic properties.

**Table 3.5** Calculated and experimental Bond angles  $\alpha(\text{Sn-Sn}^x\text{-Sn})$  and bond lengths  $d(\text{Sn}^x\text{-Sn}^y)$  of Dräger oligomers **20(a-d)** and compound **46**.

| No.        | Compound  | Method of optimization | Pos.x | $\alpha[^\circ]$<br>Calc. | $\alpha[^\circ]$<br>Exp. | Pos.<br>x y | d[pm]<br>Calc. | d[pm]<br>Exp.     |
|------------|---|------------------------|-------|---------------------------|--------------------------|-------------|----------------|-------------------|
| <b>46</b>  | $\text{R}_3\text{Sn}^1\text{-Sn}^1\text{R}_3$   | MMF                    |       |                           |                          | 1-1         | 280.8          | $277.0^{[78,79]}$ |
| <b>20a</b> | $\text{R}_3\text{Sn}^1\text{-Sn}^2\text{R}_2\text{-Sn}^1\text{R}_3$   | MMF                    | 2     | 112.4                     | 106.9                    | 1-2         | 282.0          | $279.8^{[29]}$    |
|            |   | PM3                    |       | 114.0                     |                          | 1-2         | 267.3          |                   |
|            |   | DF                     |       | 109.7                     |                          | 1-2         | 287.7          |                   |
| <b>20b</b> | $\text{R}_3\text{Sn}^1\text{-Sn}^2\text{R}_2\text{'-Sn}^2\text{R}_2'\text{-Sn}^1\text{R}_3$   | MMF                    | 2     | 110.4                     | 117.8                    | 1-2         | 283.8          | $282.5^{[29]}$    |
|            |   |                        |       |                           |                          | 2-2         | 287.9          | 286.8             |
|            |   | PM3                    | 2     | 108.01                    |                          | 1-2         | 282.6          |                   |
|            |   |                        |       |                           |                          | 2-2         | 285.2          |                   |
|            |   | DF                     | 2     | 113.89                    |                          | 1-2         | 291.3          |                   |
|            |   |                        |       |                           |                          | 2-2         | 294.4          |                   |
| <b>20c</b> | $\text{R}_3\text{Sn}^1\text{-Sn}^2\text{R}_2\text{'-Sn}^3\text{R}_2'\text{-Sn}^2\text{R}_2'\text{-Sn}^1\text{R}_3$                        | MMF                    | 2     | 112.79                    | 113.9                    | 1-2         | 285.8          | $284.0^{[29]}$    |
|            |   |                        | 3     | 117.63                    | 118.9                    | 2-3         | 292.3          | 291.2             |
|            |   | PM3                    | 2     | 117.78                    |                          | 1-2         | 269.9          |                   |
|            |   |                        | 3     | 119.3                     |                          | 2-3         | 276.6          |                   |
|            |   | DF                     | 2     | 112.66                    |                          | 1-2         | 294.05         |                   |
|            |   |                        | 3     | 120.61                    |                          | 2-3         | 303.0          |                   |
| <b>20d</b> | $\text{R}_3\text{Sn}^1\text{-Sn}^2\text{R}_2\text{'-Sn}^3\text{R}_2'\text{-Sn}^3\text{R}_2'\text{-Sn}^2\text{R}_2'\text{-Sn}^1\text{R}_3$ | MMF                    | 2     | 111.04                    | 113.7                    | 1-2         | 287.4          | $284.5^{[29]}$    |
|            |   |                        | 3     | 117.85                    | 121.0                    | 2-3         | 283.75         | 292.5             |
|            |   |                        |       |                           |                          | 3-3         | 295.0          | 296.6             |
|            |   | PM3                    | 2     | 112.56                    |                          | 1-2         | 272.7          |                   |
|            |   |                        | 3     | 113.95                    |                          | 2-3         | 282.7          |                   |
|            |   |                        |       |                           |                          | 3-3         | 305.0          |                   |

R= Ph, R' = *t*Bu

The modeling studies began with geometric optimization for each molecule, using the algorithm supplied with the Spartan program. Optimizations were based on energies calculated using molecular mechanics (MMF), semi-empirical (PM3), and density functional methods. MMF is a quick method; geometrical optimizations were completed in several minutes or less. DF methods were the slowest and required days, even weeks, for completion. Geometric optimizations by DF failed for oligomeric chains having more than five Sn atoms, probably due to the large number of degrees of freedom in the extended chain.

Table 3.5 presents a comparison of calculated and experimental bond lengths and angles for the Dräger oligomers determined using the different methods of optimization. The PM3 semi-empirical method did not provide reasonable results for any of the compounds. The bond lengths obtained from MMF optimization are in reasonable agreement with the experimental values for compounds **46**, **20a** and **20b**, but poor agreement with **20c**, **20d**. The bond angles determined by DF optimization are in fair agreement for the four molecules for which optimization succeeded. For each molecule, the MMF molecular mechanics method provided excellent agreement for both bond lengths and angles. This suggests that the MMF force fields supplied with Spartan can accurately treat the bonding and steric interactions in the Dräger oligomers. This is an important finding, because DF geometrical optimization is not feasible for longer oligomers while MMF should be.

**Table 3.6** Calculated and experimental values  $\lambda_{\max}$  of polytin species

| No.        | Compound  | Method of geometry optimization | $\lambda_{\max}$ Calcu. B3LYP/LACVP* | $\lambda_{\max}$ Exp. | $\lambda_{\max}$ Calcu. From HOMO-LUMO energy difference |
|------------|---|---------------------------------|--------------------------------------|-----------------------|--|
| <b>46</b>  | $R_3Sn^1-Sn^1R_3$                                     | MMF                             | 246.93                               | $247.5^{[80,81]}$     | 226  |
|            |   | PM3                             | 268.26                               |                       |  |
|            |   | DF                              | 252.46                               |                       |  |
| <b>20a</b> | $R_3Sn^1-Sn^2R'_2-Sn^1R_3$                            | MMF                             | 264.12                               | $267^{[29]}$          |  |
|            |   | PM3                             | 284.05                               |                       |  |
|            |   | DF                              | 268.66                               |                       |  |
|            |   | AM1                             | 261.52                               |                       |  |
| <b>20b</b> | $R_3Sn^1-Sn^2R'_2-Sn^2R'_2-Sn^1R_3$                   | MMF                             | 285.11                               | $295^{[29]}$          | 265  |
|            |   | PM3                             | 301.6                                |                       |  |
|            |   | DF                              | 296.02                               |                       |  |
| <b>20c</b> | $R_3Sn^1-Sn^2R'_2-Sn^3R'_2-Sn^2R'_2-Sn^1R_3$          | MMF                             | 301.78                               | $328^{[29]}$          | 300  |
|            |   | PM3                             | 318.64                               |                       |  |
|            |   | DF                              | 334.2                                |                       |  |
|            |   | AM1                             | 285.64                               |                       |  |
| <b>20d</b> | $R_3Sn^1-Sn^2R'_2-Sn^3R'_2-Sn^3R'_2-Sn^2R'_2-Sn^1R_3$ | MMF                             | 322.61                               | $363^{[29]}$          | 328  |
|            |   | PM3                             | 318.05                               |                       |  |

R= Ph, R'= *t*Bu

The increase in the experimental values of  $\lambda_{\max}$  (Table 3.6) indicates the corresponding decrease in HOMO-LUMO energy difference with increasing oligostannane chain length (band gap). UV-visible spectral features were calculated in two ways: 1) using the Spartan routine (DF single-point energy calculation for the ground state, time-dependent DF energy calculations for excited states), 2) using the HOMO-LUMO energy difference for the ground state molecule. The calculated values for compounds **46**, **20a** and **20b** using the first method are in good agreement with the experimental ones; those for the two higher oligomers are not. The  $\lambda_{\max}$  calculated from HOMO-LUMO energy difference are  $\approx$  20-30 nm lower than the calculated by DFT for all oligomers. The likely reason for this difference is that the DFT calculations for  $\lambda_{\max}$

involved the excited states and  $\lambda_{\max}$  calculated from HOMO-LUMO energy difference is based on the ground state energy. It shows a pattern in the increase of  $\lambda_{\max}$  values with the increasing length of the chain or the number of tin atoms in the chain, and provides a basis for extrapolation to higher oligomers.

**Table 3.7** Calculated values  $\lambda_{\max}$  of alkyne inserted distannanes and oligostannanes.

| No.        | Compound  | Method of geometry optimization | $\lambda_{\max}$ Calcu. B3LYP/LACVP* |
|------------|---|---------------------------------|--------------------------------------|
| <b>30</b>  | $\text{Me}_3\text{SnCH=CHSnMe}_3$ (cis)           | MMF                             | 203.0                                |
|            |   | PM3                             | 200.2                                |
|            |   | DF                              | 203.0                                |
| <b>51</b>  | $\text{Me}_3\text{SnCH=CHSnMe}_3$ (trans)         | MMF                             | 202.6                                |
|            |   | PM3                             | 195.7                                |
|            |   | DF                              | 202.5                                |
| <b>50</b>  | $\text{Bu}_3\text{SnCH=CHSnBu}_3$ (trans)         | MMF                             | 228.3                                |
|            |   | PM3                             | 228.8                                |
|            |   | DF                              | 219.6                                |
| <b>50a</b> | $\text{Bu}_3\text{SnCH=CHSnBu}_3$ (cis)           | MMF                             | 221.2                                |
|            |   | PM3                             | 221.2                                |
|            |   | DF                              | 220.2                                |
| <b>32</b>  | $\text{Me}_3\text{SnCH=CPhSnMe}_3$ (cis)          | MMF                             | 249.6                                |
|            |   | PM3                             | 249.6                                |
|            |   | DF                              | 249.6                                |
| <b>54</b>  | $\text{Me}_3\text{SnCH=CPhSnMe}_3$ (trans)        | MMF                             | 230.0                                |
|            |   | PM3                             | 236.1                                |
|            |   | DF                              | 220.2                                |
| <b>55</b>  | $\text{Me}_3\text{SnCH=CPh-CH=CPhSnMe}_3$ (trans) | MMF                             | 297.5                                |
|            |   | PM3                             | 297.5                                |
|            |   | DF                              | 297.5                                |

**Table 3.8** Calculated values  $\lambda_{\max}$  of distannanes and oligostannanes

| No.       | Compound                     | Method of geometry optimization | $\lambda_{\max}$ Calcu. B3LYP/LACVP* |
|-----------|------------------------------|---------------------------------|--------------------------------------|
| <b>29</b> | $\text{Me}_3\text{SnSnMe}_3$ | MMF                             | 208.46                               |
|           |                              | PM3                             | 208.47                               |
|           |                              | DF                              | 208.46                               |
| <b>45</b> | $\text{Bu}_3\text{SnSnBu}_3$ | MMF                             | 220.82                               |
|           |                              | PM3                             | 226.43                               |
|           |                              | DF                              | 220.82                               |
| <b>46</b> | $\text{Ph}_3\text{SnSnPh}_3$ | MMF                             | 246.93                               |
|           |                              | PM3                             | 268.3                                |
|           |                              | DF                              | 252.5                                |

The energies for geometrically optimized molecular models for compounds prepared in our lab(both previously known and novel) were also calculated by using DF method 1, described above. Experimental values are not currently available for comparison. However, the energy and spectral calculations are helpful in predicting changes in electronic properties that can be verified, rationalized chemically, and used in designing useful polymers. For example, the results obtained for compound **54** and **55** in Table 3.7 suggests that HOMO-LUMO energy difference is decreasing, due to increased conjugation between the tin centers. The calculated values of  $\lambda_{\max}$  for the distannanes listed in Table 3.8 reveal the influence of the substituents. The  $\sigma$ - $\sigma^*$  transition is effect by the increase in electronic density moving from Me to Bu and Ph and additional the increased mixing of the  $\sigma$ - $\pi$  orbitals of Sn and the aromatic ring.

## 4.0 Conclusion:

Compound **13** was synthesized in good yield and polymerized to **5** by catalytic dehydrocoupling route using Wilkinson's catalyst. Acetylene was successfully inserted in compound **29** and **45** in dioxane using **27** as a catalyst to produce the model compound **30** and **50** respectively. Both compounds **30** and **50** were affected by the air/moisture and converted to compounds **52** and **42** respectively. The insertion of acetylene into polymer **5** to produce **53** was successfully achieved using a similar synthetic method and characterized by  $^{119}\text{Sn}$  NMR spectroscopy.

The insertion of phenylacetylene into compound **29** was achieved via neat reaction conditions and compound **32** (cis) and **54** (trans) isomers were produced. The sample in  $\text{C}_6\text{D}_6$  in NMR tube crystallized and the crystal structure and revealed head to head insertion of two phenylacetylene units into compound **29** to produce the novel carbodistannane **55**.

Compound **45** was successfully synthesized in high yield from the thermally driven dehydrocoupling of the tertiary stannane **43** under a variety of catalyst and solvent-free conditions. Compound **46** was also obtained in a similar way with lower conversion from the tertiary stannane **44**. A mixed distannane **48** was also prepared from the equimolar reaction of **43** and **44** under similar conditions. Evidence for the redistribution product **47** was found when aryl stannane **44** was used. Solvent and catalyst-free dehydrogenative coupling of the secondary distannane **13** at  $160^\circ\text{C}$  resulted in the formation of a modest molecular weight polystannane **5** and other linear and cyclic stannanes but favours only redistribution products at  $200^\circ\text{C}$ . This work has demonstrated

that dehydrocoupling of stannanes in the absence of catalyst under a variety of conditions may provide a viable route to valuable organic radical sources.

Dräger's series of oligostannanes **20(a-d)** were optimized using different computational methods and the  $\lambda_{\text{max}}$  calculated by density functional method. These calculations revealed that DFT method holds well compared to the other methods but only up to four Sn atoms. Bond angles calculated by MMF are relatively comparable with values obtained from crystal structures of these compounds. This calculation study revealed that for the molecules with higher number of tin atoms, MMF gave better and comparable results than given by other methods.

## 5.0 Future work:

For alkyne insertion into Sn-Sn backbone work is required to examine the insertion reactions of other polydialkylstannanes and complete the characterization of the inserted polymers under different conditions. The reaction between **29** and **26** with different ratios will be performed to study the changes in the mode of insertion of phenylacetylene units between Sn atoms and to investigate the stability of these compounds under different conditions.

Future efforts will be directed to the coupling of tertiary and secondary stannanes using other metal free routes including the use of light and microwave mediated coupling processes.

## 6.0 References:

1. (a) Sanderson, R.T. *Chemical bonds and bond energy*, 2<sup>nd</sup> ed., Academic Press, New York, 1976. (b) Cotrell, T. L. *The strengths of chemical bonds*, 2<sup>nd</sup> ed., Butterworths, London, 1958.
2. Falbe, J.; Regitz, M. *Römpf Lexikon Chemie*. 10 ed.; Thieme, Stuttgart, Vol. 6, 1999.
3. Abd-El-Aziz, A.S.; Carraher, C.; Charles, U.; Pitman, J.; Zeldin, M. eds., *Macromolecules containing metal and metal like elements, vol.4; Group IVA Polymers*, John Wiley & Sons Inc., 2005, chap. 10.
4. Henry, M.; Davidson, W. in *Organotin Compounds*, Vol. 3, A. K. Sawyer, ed., Dekker, New York, 1972.
5. Evans, C. J.; Karpel, S. *Organotin Compounds in Modern Technology*, Elsevier, Amsterdam, 1985.
6. Archer, R. *Inorganic and Organometallic Polymers*, Wiley, New York, 2001.
7. Abd-El-Aziz, A.S.; Carraher, C.; Pitman, C.; Sheats, J.; Zeldin, M. eds., *Macromolecules containing metal and metal like elements, vol.1; A half century of metal and metalloid containing polymers*, Wiley, Hoboken, NJ. 2003, chap. 6.
8. Carraher Jr, C. E. *Polymer Chemistry*, 6<sup>th</sup> ed., Dekker, New York, 2003.
9. Van Dyke, M. *Synthesis and properties of Silicones and Silicones modified materials*, American Chemical Society, Washington, D.C., 2003.
10. Clarson, S. J. *Silicones and Silicones modified materials*, Oxford university Press, New York, 2000.
11. Jurkschat, K.; Mehring, M. in *Organometallic polymers of Germanium, Tin and Lead*, Vol. 2, Z. Rappoport, ed., Wiley, New York, 2002, Ch. 22.

12. Wei, R. Ya, L.; Jinguo, W.; Qifeng, X. in *Polymer materials Encyclopedia*, J. Solomane, ed., CRC Press, Boca Raton, FL., p. 4826, 1996.
13. Sita, L. R. *Organometallics*, **1992**, *11*, 1442.
14. Frankland, E. *J. Chem. Soc.*, **1849**, 2, 263.
15. Löwig, C. *Liebigs, Ann. Chem.*, **1852**, *84*, 308.
16. Cahours, A. *Ann. Chem. Pharm. (Liebig's Ann.)*, **1860**, *114*, 227.
17. Cahours, A. *Ann. Chim. Phys., Sér. 3*, **1860**, *58*, 5.
18. Strecker, A. *Ann. Chem. Pharm. (Liebig's Ann.)* **1858**, *105*, 306.
19. Grüttner, G. *Ber. Deutsch. Chem. Gesell.* **1917**, *50*, 1808.
20. Ladenburg, A. *Ber. Deutsch. Chem. Gesell.* **1870**, *3*, 353.
21. Pope, W. J.; Peachy, S. J. *Proc. Chem. Soc.* **1903**, *19*, 290.
22. Krause, E.; Von Grosse, A. *Die Chemie der Metal-organization verbindungen*, Borntraeger, Berlin, **1937**.
23. Jensen, K. A.; Clauson-Kaas, N. *Z. anorg. allg. Chem.* **1943**, *250*, 277.
24. Sita, L. R.; Terry, K. W.; Shibata, K. *J. Am. Chem. Soc.* **1995**, *117*, 8049.
25. Neumann, W. P. *Angew. Chem.* **1962**, *74*, 122.
26. Neumann, W. P.; Pedain, J. *Ann. Chem. (Liebig's Ann.)* **1964**, *672*, 34.
27. Zou, W. K.; Yang, N.-L. *Polym. Prepr. (Am. Chem. Soc. Div. Polym.Chem.)* **1992**, *33*, 188.
28. Devylder, N.; Hill, M.; Molloy, K. C.; Price, G. J. *Chem. Commun.* **1996**, 711.
29. Adams, S.; Dräger, M. *Angew. Chem. Int. Ed. Engl.* **1987**, *26*, 1255.
30. Mochida, K.; Hayakawa, M.; Tsuchikawa, T.; Yokoyama, Y.; Wakasa, M.; Hayashi, H. *Chem. Lett.* **1998**, 91.

31. Imori, T.; Lu, V.; Cai, H.; Tilley, T.D. *J. Am. Chem. Soc.* **1995**, *117*, 9931.
32. Lu, V., Tilley, T. D., *Macromolecules* **2000**, *33*, 2403.
33. Choffat, F.; Kaser, S.; Wolfer, P.; Schmid, D.; Mezzenga, R.; Smith, P.; Caseri, W. *J. Mater. Chem.* **2007**, *40*, 7878.
34. Okano, M.; Matsumoto, N.; Arakawa, M.; Tsuruta, T.; Hamano, H. *Chem. Commun.* **1998**, 1799.
35. Choffat, F.; Smith, P.; Caseri, W. *J. Mater. Chem.* **2005**, *15*, 1789.
36. Choffat, F.; Buchmuller, Y.; Mensing, C.; Smith, P.; Caseri, W. *J. Inorg. Organomet. Polym.* **2009**, *19*, 715.
37. Braunstein, P.; Morise, X. *Chem. Rev.* **2000**, *100*, 3541.
38. De Haas, M. P.; Choffat, F.; Caseri, W.; Smith, P.; Warman, J. M. *Adv. Mater.* **2006**, *18*, 44.
39. Van der Kerk, G. J. M.; Noltes, G. J.; Luijtin, J. G. A. *J. Appl. Chem.* **1957**, *7*, 356.
40. Van der Kerk, G. J. M.; Noltes, G. J.; Luijtin, J. G. A. *J. Appl. Chem.* **1957**, *7*, 366.
41. Noltes, G. J.; van der Kerk, G. J. M. *Rec. Trav. Chim. Pays-Bas* **1961**, *80*, 623.
42. Noltes, G. J.; van der Kerk, G. J. M. *Rec. Trav. Chim. Pays-Bas* **1962**, *81*, 41.
43. Labadie, J. W.; MacDonald, S. A.; Willson, C. G. *Polymer Bulletin* **1986**, *16*, 427.
44. Finckh, W.; Tang, B.-Z.; Lough, A.; Manners, I. *Organometallics* **1992**, *11*, 2904.
45. Mitchell, T. N.; Amamria, A.; Killing, H.; Rutschow, D. *J. Organomet. Chem.* **1986**, *304*, 257.
46. Yamashita, Y.; Catellani, M.; Tanaka, M. *Chem. Lett.* **1991**, 241.
47. Herberhold, M.; Steffi, u.; Wrackmeyer, B. *J. Organomet. Chem.* **1999**, *577*, 76-81.

48. (a) Chabaud, L.; Landais, Y.; Renaud, P. *Org. Lett.* **2002**, *4*, 4257. (b) Harendza, M.; Lessman, K.; Neumann, W. P. *Synlett*, **1993**, *4*, 283. (c) Verlhac, J. B.; Chanson, E.; Jousseau, B.; Quintard, J. P. *Tetrahedron Lett.* **1985**, *26*, 6075.
49. (a) McIntee, J. W.; Sundararajan, C. *J. Org. Chem.* **2008**, *73*, 8236. (b) Ha, Y.-H.; Kang, S. K. *Org. Lett.* **2002**, *4*, 1143.
50. Crowe, A. J.; Hill, R.; Smith, P. J.; Cox, T. R. G. *Int. J. Wood. Preserv.* **1979**, *1*, 119.
51. Windus, T. L.; Gordon, M. S. *J. Am. Chem. Soc.* **1992**, *114*, 9559.
52. Jacobsen, H.; Ziegler, T. *J. Am. Chem. Soc.* **1994**, *116*, 3667.
53. See, for example: Podlech, J. Compounds of Group 14 (Ge, Sn, Pb). In *Science of Synthesis: Houben-Weyl Methods of Molecular Transformation - Category 1: Organometallics*, Vol. 5.; Moloney, M. G.; Thieme, G. Eds.; Verlag: Stuttgart, 2003, pp 273 – 283.
54. Davies, A. G.; Smith, P. J. In *Comprehensive Organometallic Chemistry*; Wilkinson, G.; Stone, F. G. A.; Abel, E. W. Eds.; Pergamon Press: Oxford, 1982, Vol. 2, chapter 11, pg 591.
55. Bumagin, N. A.; Gulevich, Y. V.; Beletskaya, I. P. *Bull. Acad. Sci. USSR Div. Chem. Sci. (Engl. Transl.)* **1984**, *33*, 1044.
56. Maddock, S. M.; Finn, M. G. *Angew. Chem. Int. Ed.* **2009**, *40*, 2138.
57. Nokami, J.; Nose, H.; Okawara, R. *J. Organomet. Chem.* **1981**, *212*, 325.
58. Savall, A.; Lacoste, G.; Mazerolles, P. *J. Appl. Elect.* **1981**, *11*, 61.
59. Gyldenfeldt, F.; Marton, D.; Tagliavini, G. *Organometallics* **1994**, *13*, 906.
60. Makosza, M.; Grela, K. *Synth. Commun.* **1998**, *28*, 2697.
61. Sawyer, A. K. *J. Am. Chem. Soc.* **1965**, *87*, 537.

62. Jousseau, B.; Chanson, E.; Bevilacqua, M.; Saux, A.; Pereyre, M.; Barbe, B.; Petraud, M. *J. Organomet. Chem.* **1985**, 294, C41.
63. Jousseau, B.; Chanson, E.; Pereyre, M. *Organometallics* **1986**, 5, 127.
64. McAlonan, H.; Stevenson, P. J. *Organometallics* **1995**, 14, 4021.
65. Handa, Y.; Inanaga, J.; Yamaguchi, M. *J. Chem. Soc., Chem. Commun.* **1989**, 298.
66. Darwish, A.; Chong J. M. *Synth. Commun.* **2004**, 34, 1985.
67. Sita, L. R.; Terry, K. W.; Shibata, K. *J. Am. Chem. Soc.*, **1995**, 117, 8049.
68. (a). Allen, F. H.; Bellard, S.; Brice, M. D.; Hummelink, T. W. A.; Hummelink-Peters, B. G.; Kennard, O.; Motherwell, W. S. D.; Rogers, J. R.; Watson, D. G. *Acta Cryst.* **1979**, B35, 2331; (b) Allen, F. H. *Acta Cryst.* **2002**, B58, 380.
69. (a) Bergerhoff, G.; Hundt, R.; Sievers, R.; Brown, I. D. *J. Chem. Inf. Comput. Sci.* **1983**, 23, 66; (b) Belsky, A.; Hellenbrandt, M.; Karen, V. L.; Luksch, P. *Acta Cryst.* **2002**, B58, 364.
70. Imori, T.; Tilley, T. D. *J. Chem. Soc., Chem. Commun.* **1993**, 1607.
71. Kasai, N.; Yasuda, K.; Okawara, R. *J. Organometal. Chem.* **1965**, 3, 172.
72. Lee, A. S.-Y.; Zhang, S.-L.; Pan, O.-G. *J. Chin. Chem. Soc.* **1997**, 44, 625.
73. King, B.; Eckert, H.; Denney, D. Z.; Herber, R. H. *Inorg. Chim. Acta*, **1986**, 122, 45.
74. Wharf, I.; Simard, M. G. *J. Organomet. Chem.* **1997**, 532, 1.
75. Sharma, H. K.; Arias-Ugarte, R.; Metta-Magana, A. J.; Pannell, K. H. *Angew. Chem. Int. Ed.* **2009**, 48, 6309.
76. Sharma, H. K.; Pannell, K. H. In *Tin Chemistry: Fundamentals, Frontiers and Applications* Davies, A. G.; Gielen, M.; Pannell, K. H.; Tickink, E. R. T. Eds.; Wiley: New York, 2008, pp. 371-387 and references therein.

77. Woo, H-G.; Song, S-J.; Kim, B-K. *Bull. Korean. Chem. Soc.* **1998**, *19*, 1161.
78. Adams, S.; Dräger, M. Unpublished results.
79. Preut, H.; Haupt, H. J.; Huber, F. *Z. Anorg. Allg. Chem.* **1973**, *81*, 396.
80. Hague, D. N.; Prince, R. H. *J. Chem. Soc.* **1965**, 4690.
- 81.(a) Drenth, W. ; Janssen, M. J. ; van der Kerk, G. J. M.; Vliegthart, J. A. J. *Organomet. Chem.* **1964**, *2*, 265. (b) Drenth, W. ; Willemsens, L. C. ; van der Kerk, G. J. M.; Vliegthart, J. A. J. *Organomet. Chem.* **1964**, *2*, 279.

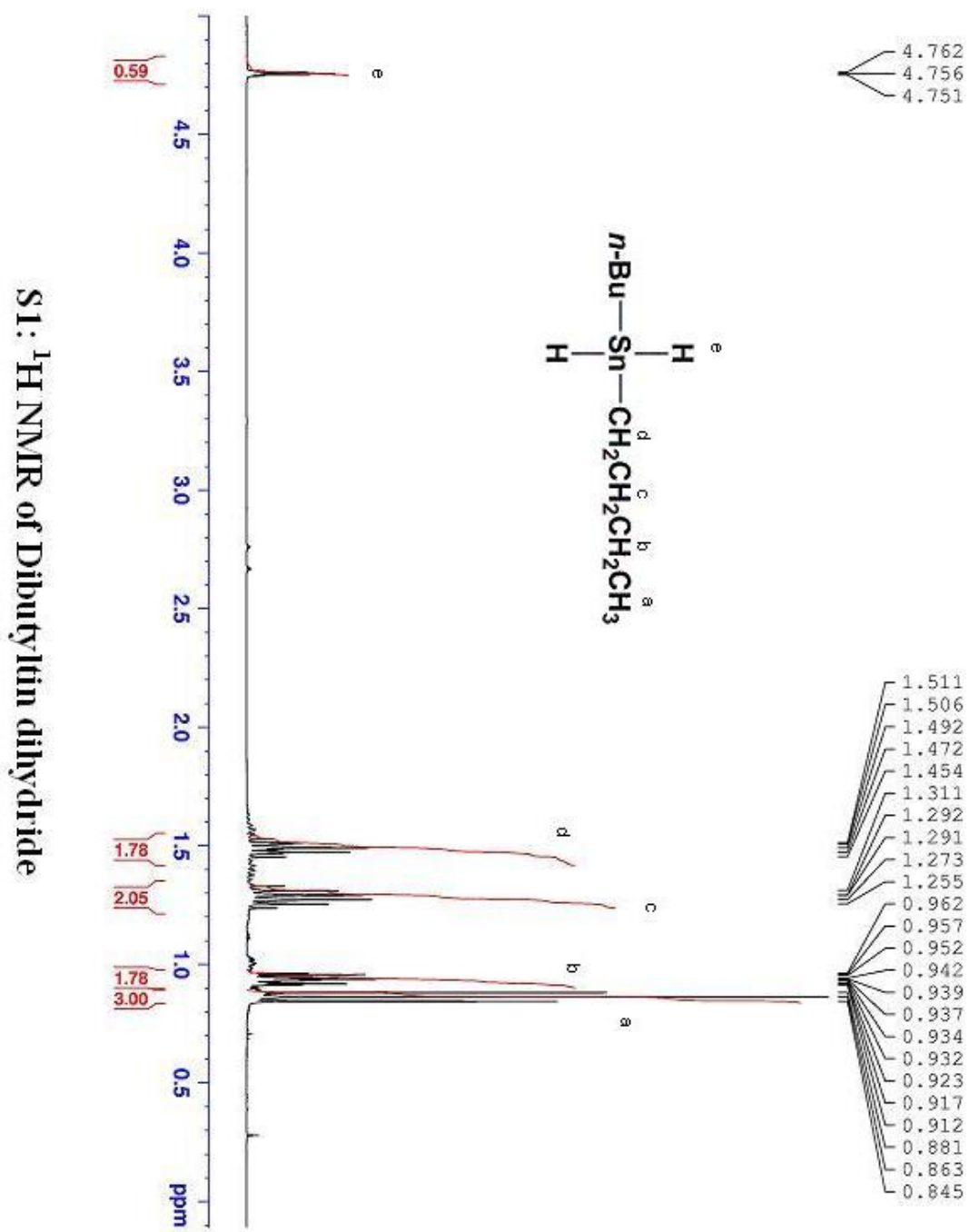
## **Appendices**

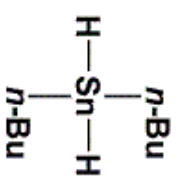
# Appendix I

## List of NMR spectra of the compounds

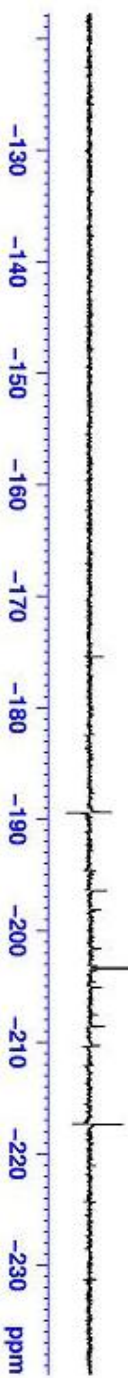
|      |  |       |
|------|--|-------|
| S1   | $^1\text{H}$ NMR of dibutyltin dihydride $n\text{-Bu}_2\text{SnH}_2$ <b>13</b>   | iv    |
| S2   | $^{119}\text{Sn}$ NMR of dibutyltin dihydride $n\text{-Bu}_2\text{SnH}_2$ <b>13</b>  | v     |
| S3   | $^{13}\text{C}$ NMR of dibutyltin dihydride $n\text{-Bu}_2\text{SnH}_2$ <b>13</b>  | vi    |
| S4   | $^1\text{H}$ NMR of polydibutylstannane $(n\text{Bu}_3\text{Sn})_n$ <b>5</b>   | vii   |
| S5   | $^{119}\text{Sn}$ NMR of polydibutylstannane $(n\text{Bu}_3\text{Sn})_n$ <b>5</b>  | viii  |
| S6   | $^1\text{H}$ NMR of hexabutyl-distannyl ethylene $(n\text{Bu})_3\text{SnCH=CHSn}(n\text{Bu})_3$ <b>50</b>                                    | ix    |
| S7   | $^1\text{H}$ NMR Pd(PPh <sub>3</sub> ) <sub>4</sub> catalyzed reaction of $n$ -dibutyltin dihydride<br>$n\text{-Bu}_2\text{SnH}_2$ <b>13</b> | x     |
| S8   | $^1\text{H}$ NMR of ethylene inserted $(n\text{-Bu}_2\text{Sn})_6$ <b>7</b>  | xi    |
| S9   | $^{119}\text{Sn}$ NMR of ethylene inserted $(\text{Bu}_2\text{Sn})_6$ <b>7</b>   | xii   |
| S10  | $^1\text{H}$ NMR of Hexamethyl-distannyl ethylene $\text{Me}_3\text{SnCH=CHSnMe}_3$ <b>30</b>  | xii   |
| S11  | $^{119}\text{Sn}$ NMR of Hexamethyl-distannyl ethylene $\text{Me}_3\text{SnCH=CHSnMe}_3$ <b>30</b>   | xiv   |
| S12  | $^1\text{H}$ NMR of Hexamethyl-1-phenyl-distannyl ethylene<br>$\text{Me}_3\text{SnCH=CPhSnMe}_3$ <b>32</b>                                   | xv    |
| S13  | $^{119}\text{Sn}$ NMR of Hexamethyl-1-phenyl-distannyl ethylene<br>$\text{Me}_3\text{SnCH=CPhSnMe}_3$ <b>32</b>                              | xvi   |
| S14  | $^{119}\text{Sn}$ NMR of reaction of Hexamethyl-distannane & phenylacetylene<br>without catalyst   | xvii  |
| S15: | $^{119}\text{Sn}$ NMR of Hexamethyl-1,4-diphenyl-distannyl-1,3- butadiene<br>$\text{Me}_3\text{SnCPh=CH-CH=CPhSnMe}_3$ <b>55</b>             | xviii |
| S16: | $^1\text{H}$ NMR of Hexabutyl-distannane <b>45</b>   | xix   |

|  |       |
|--|-------|
| S17: $^{119}\text{Sn}$ NMR of Hexabutyldistannane <b>45</b>                                    | xx    |
| S18: $^{13}\text{C}$ NMR of Hexabutyldistannane <b>45</b>                                      | xxi   |
| S19: $^{119}\text{Sn}$ NMR of Hexaphenyldistannane   | xxii  |
| S20: $^{13}\text{C}$ NMR of Hexaphenyldistannane   | xxiii |
| S21: $^{119}\text{Sn}$ NMR of Tetraphenyltin   | xxiv  |
| S22: $^{13}\text{C}$ NMR of Tetraphenyltin   | xxv   |
| S23: $^{119}\text{Sn}$ NMR spectrum of the products from the heating of 13 at 160°C<br>for 6 h | xxvi  |



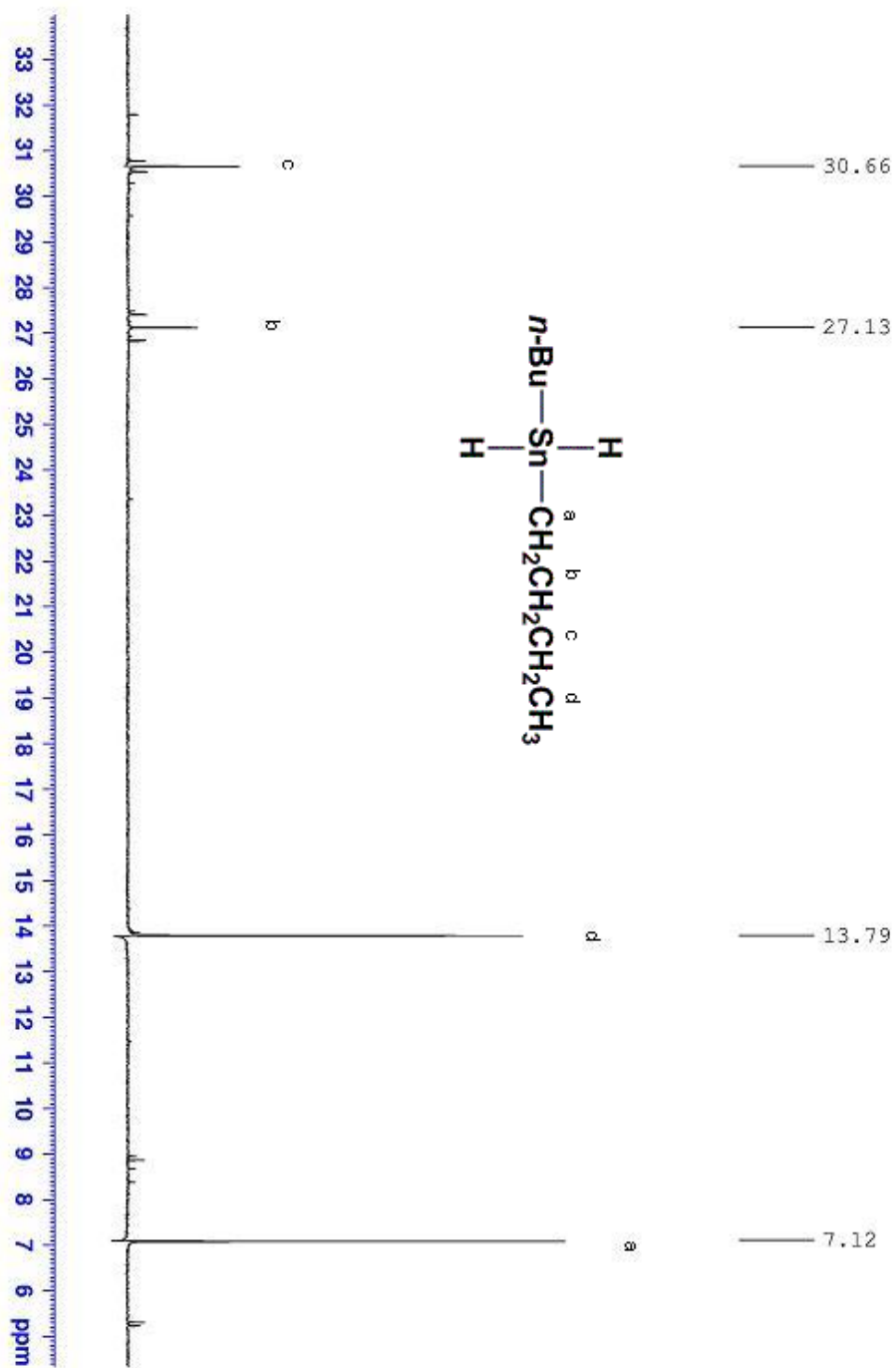


— -203.36

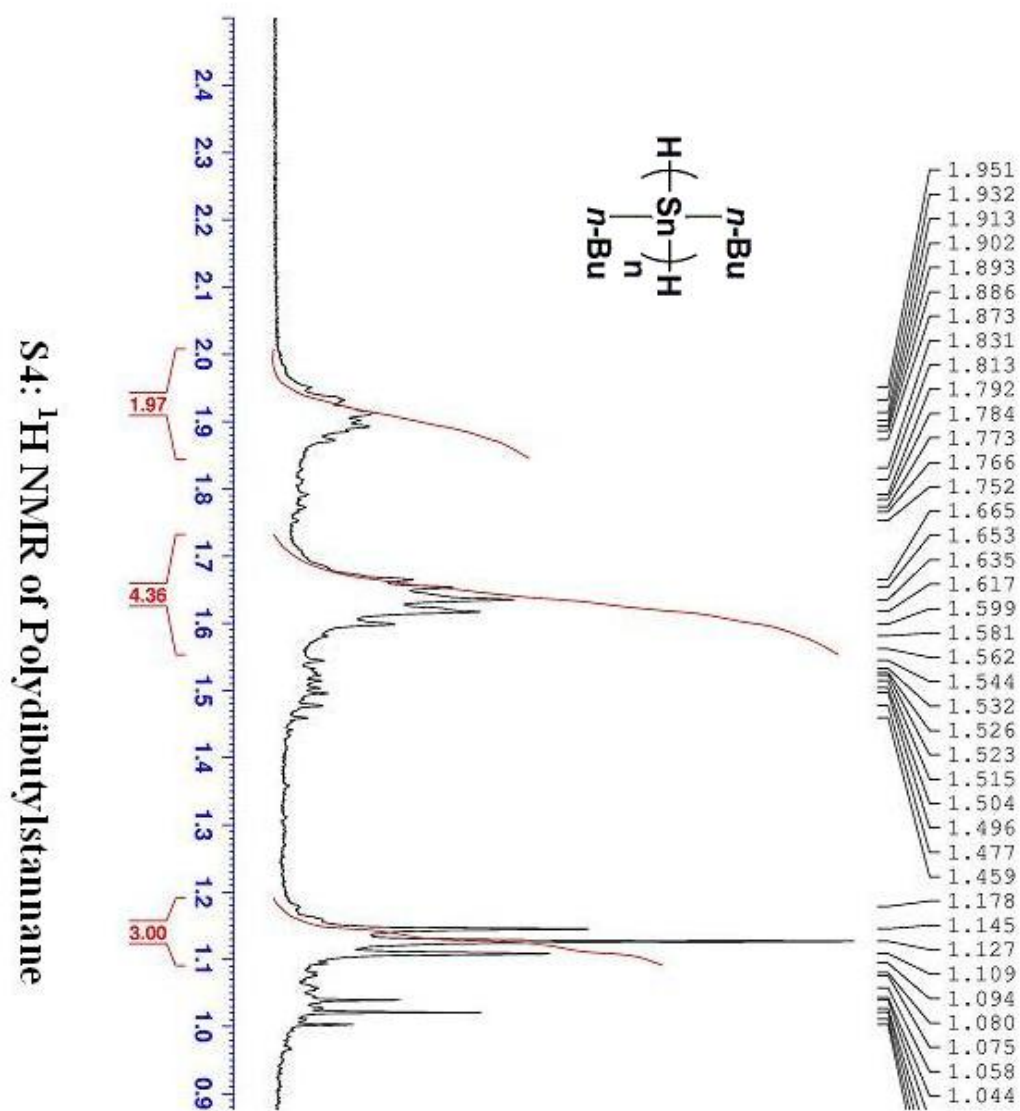


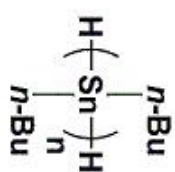
S2:  $^{119}\text{Sn}$  NMR of Dibutyltin dihydride

<sup>13</sup>C NMR of Dibutyltin dihydride



S3: <sup>13</sup>C NMR of Dibutyltin dihydride

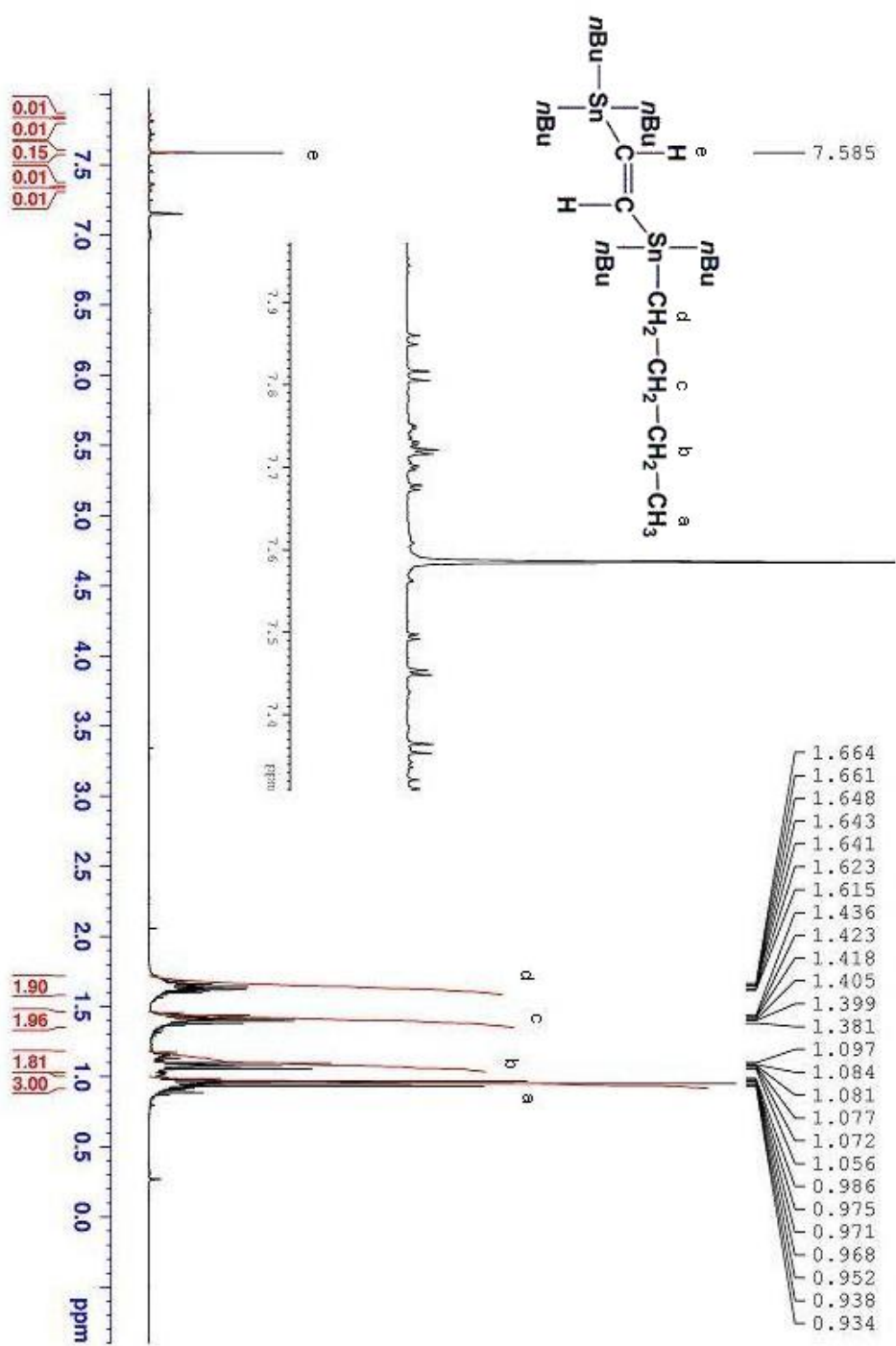




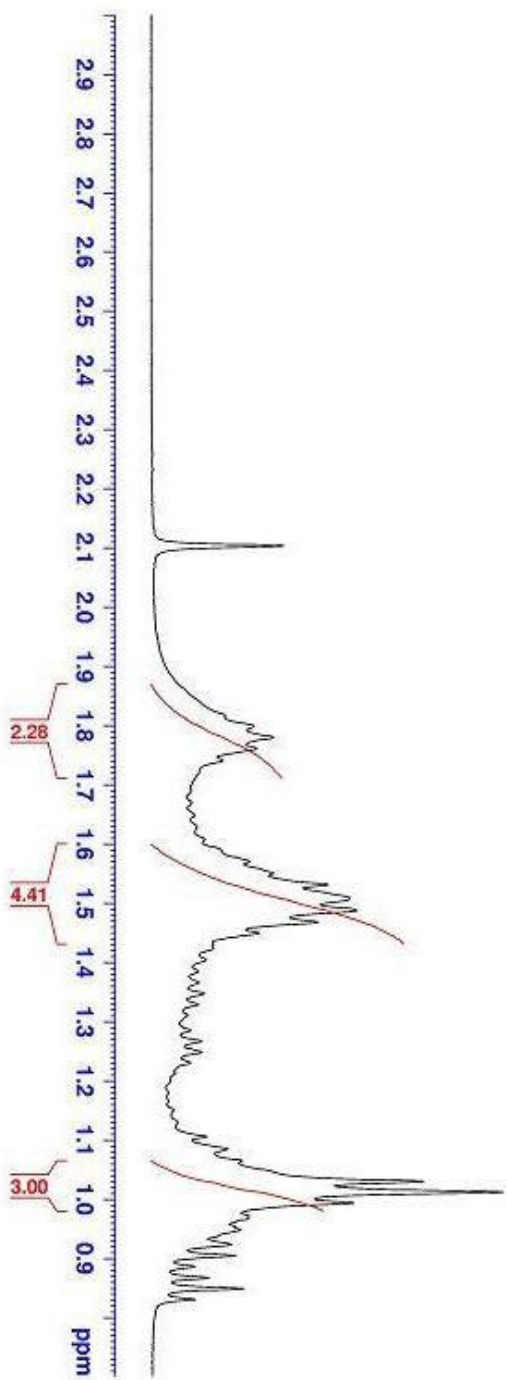
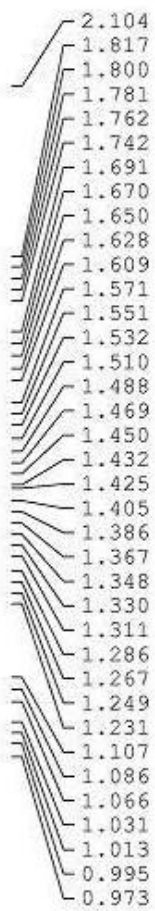
$\delta = -190.06$



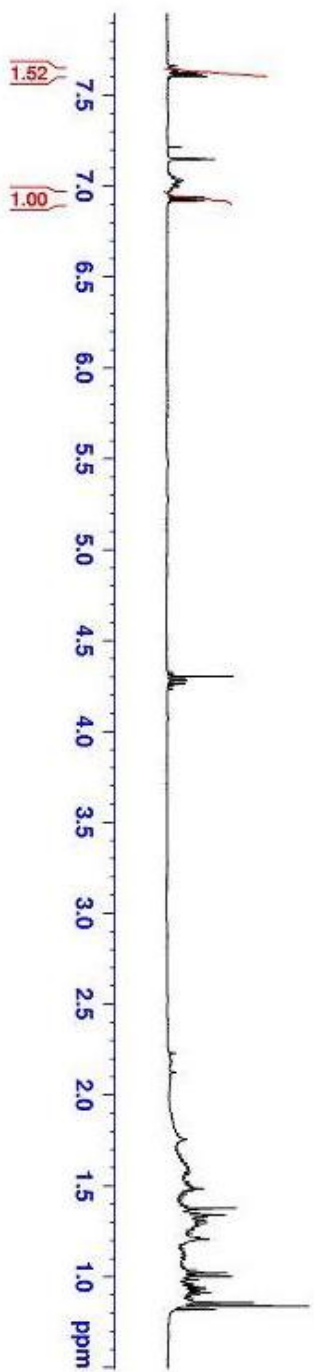
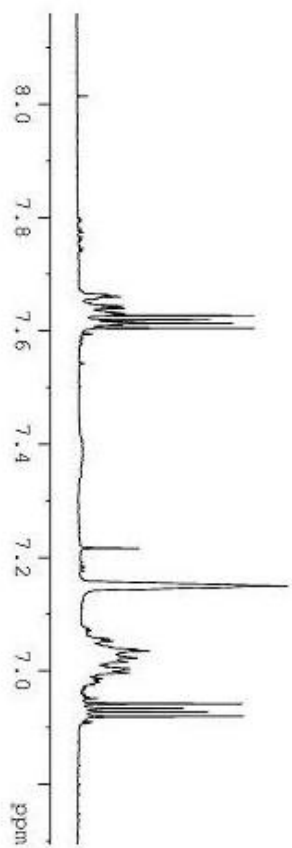
S5:  $^{119}\text{Sn}$  NMR of Polydiethylstannane



S6: <sup>1</sup>H NMR of Hexabutyldistannyl ethylene



**S7:  $^1\text{H}$  NMR  $\text{Pd}(\text{PPh}_3)_4$  catalyzed reaction of *n*-dibutyltin dihydride**

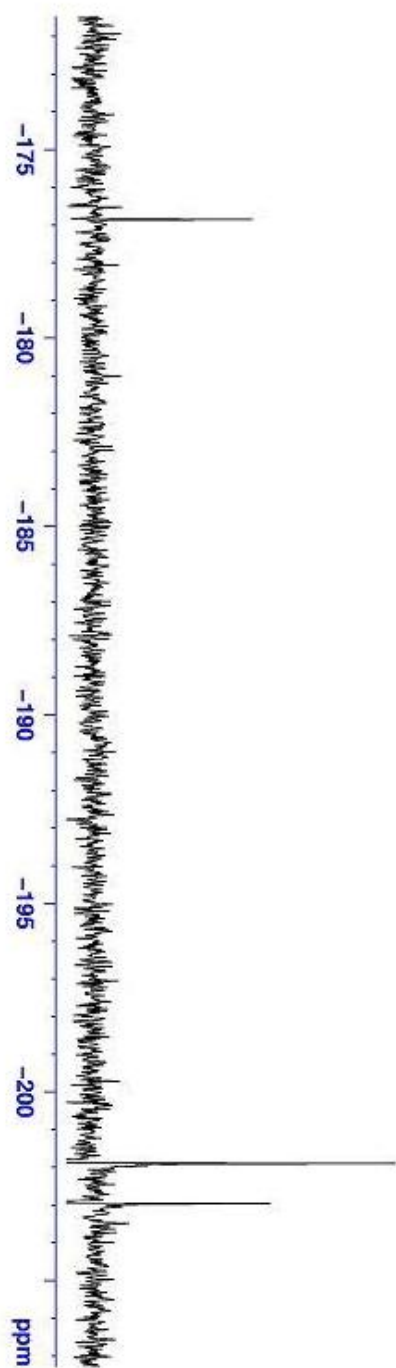


**S8: <sup>1</sup>H NMR of ethylene inserted (Bu<sub>2</sub>Sn)<sub>6</sub>**

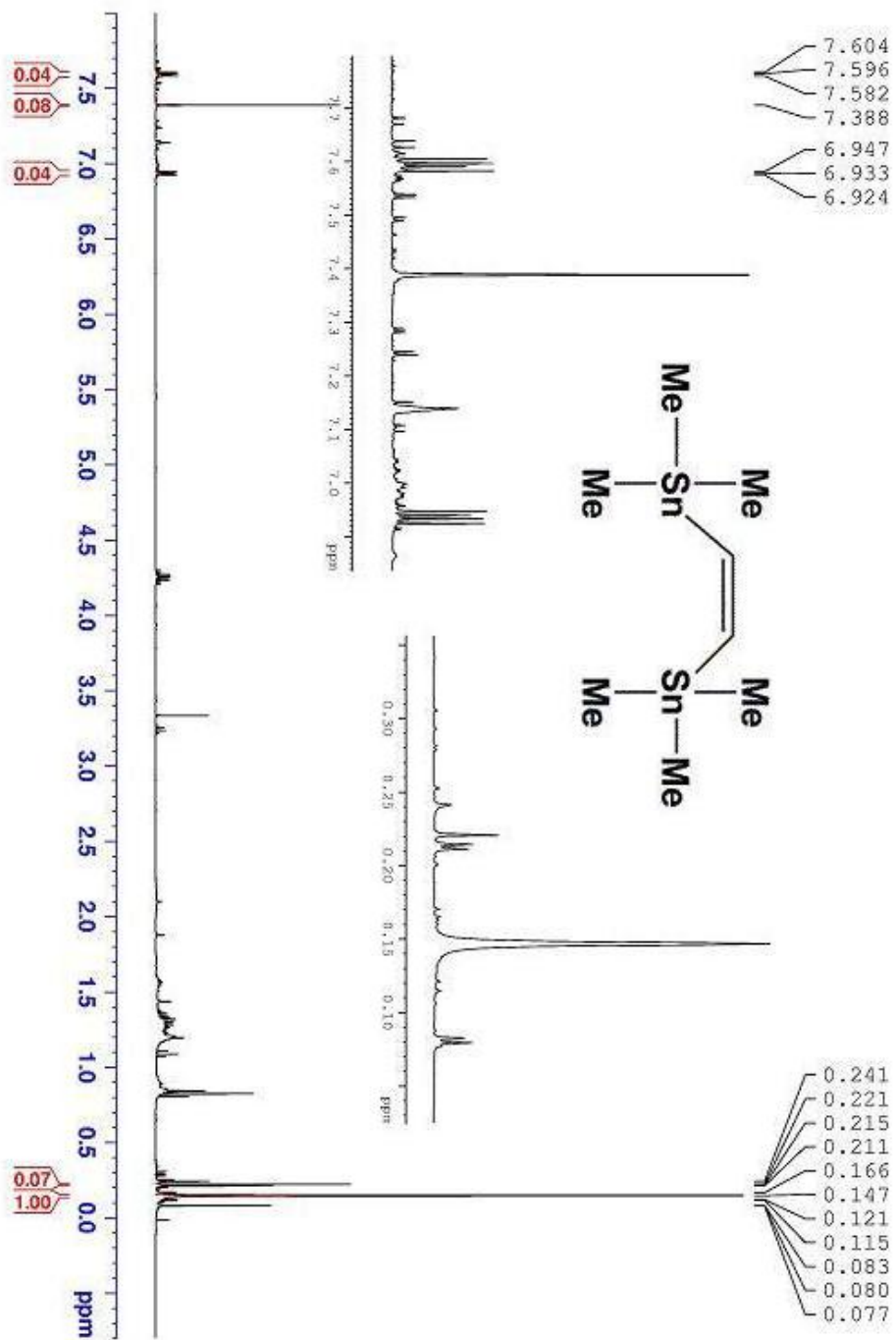
— -176.85

— -201.89

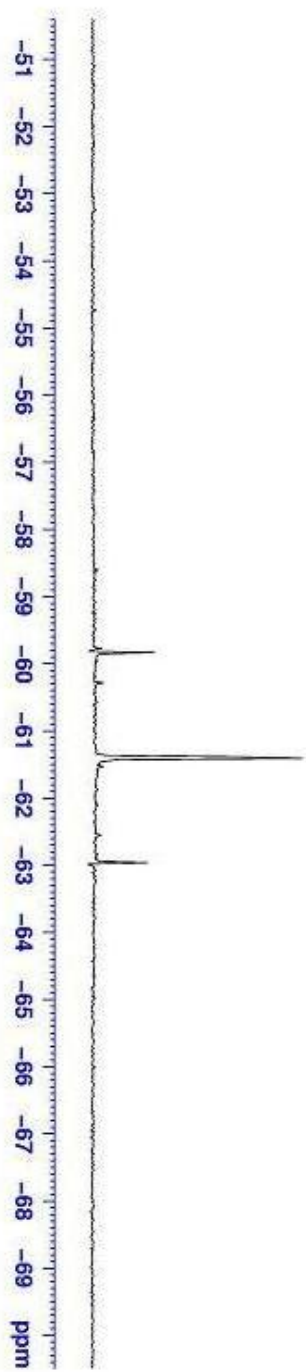
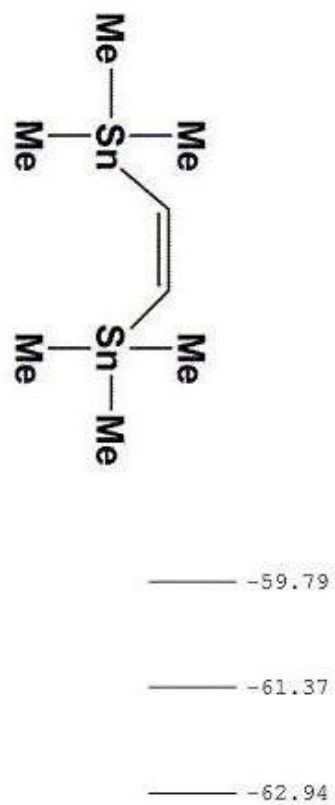
— -202.95



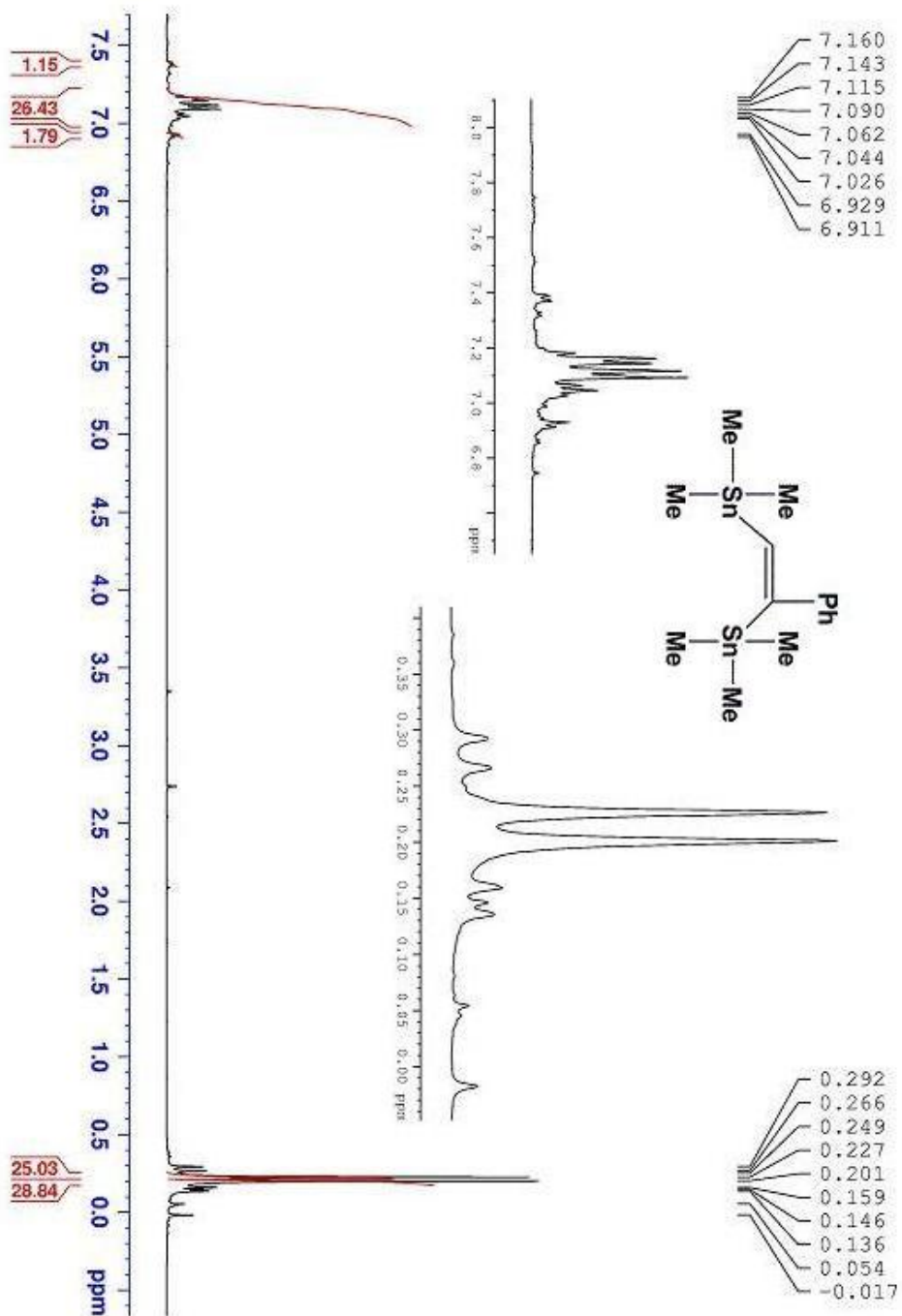
**S9:  $^{119}\text{Sn}$  NMR of ethylene inserted  $(\text{Bu}_2\text{Sn})_6$**



**S10: <sup>1</sup>H NMR of Hexamethyldistannyl ethylene**

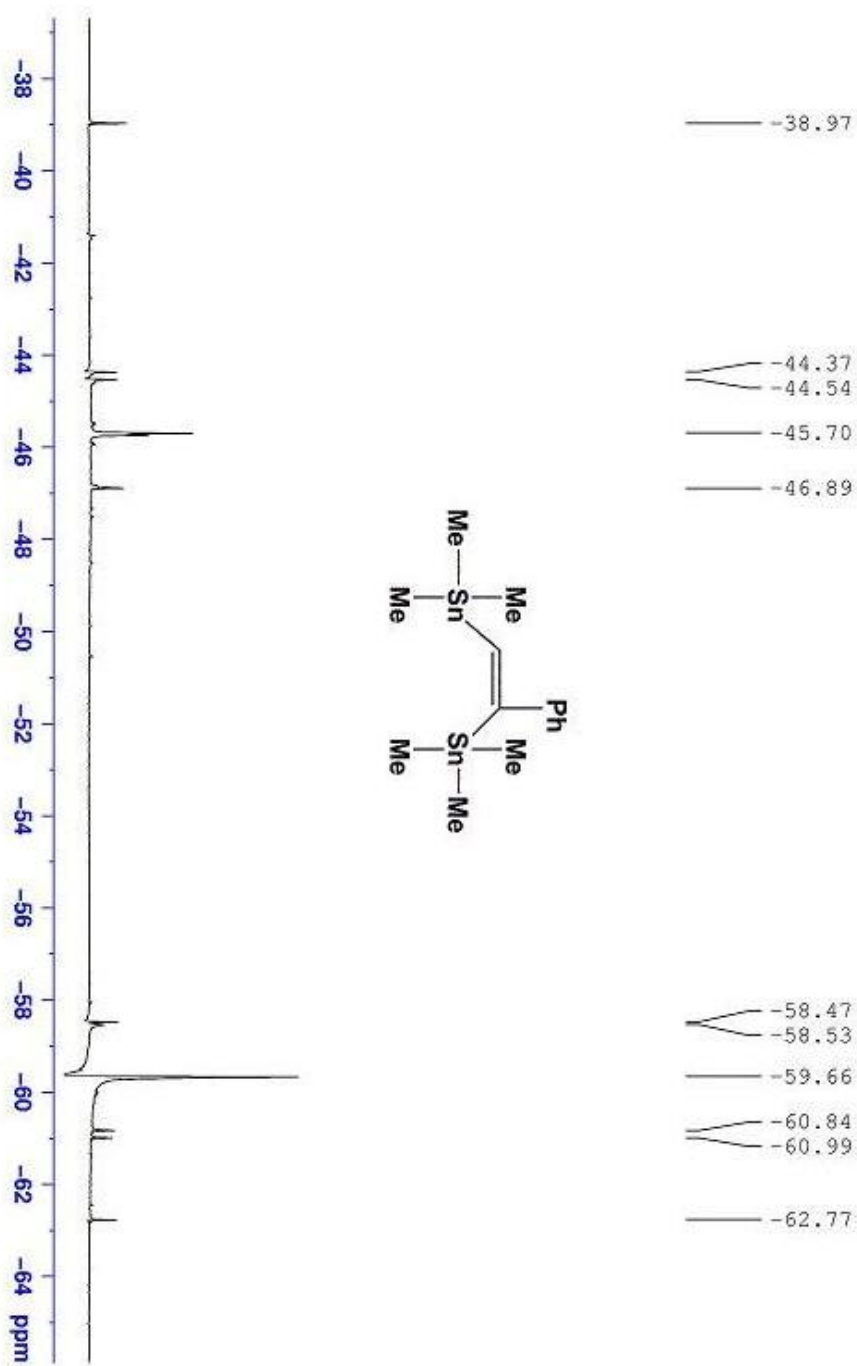


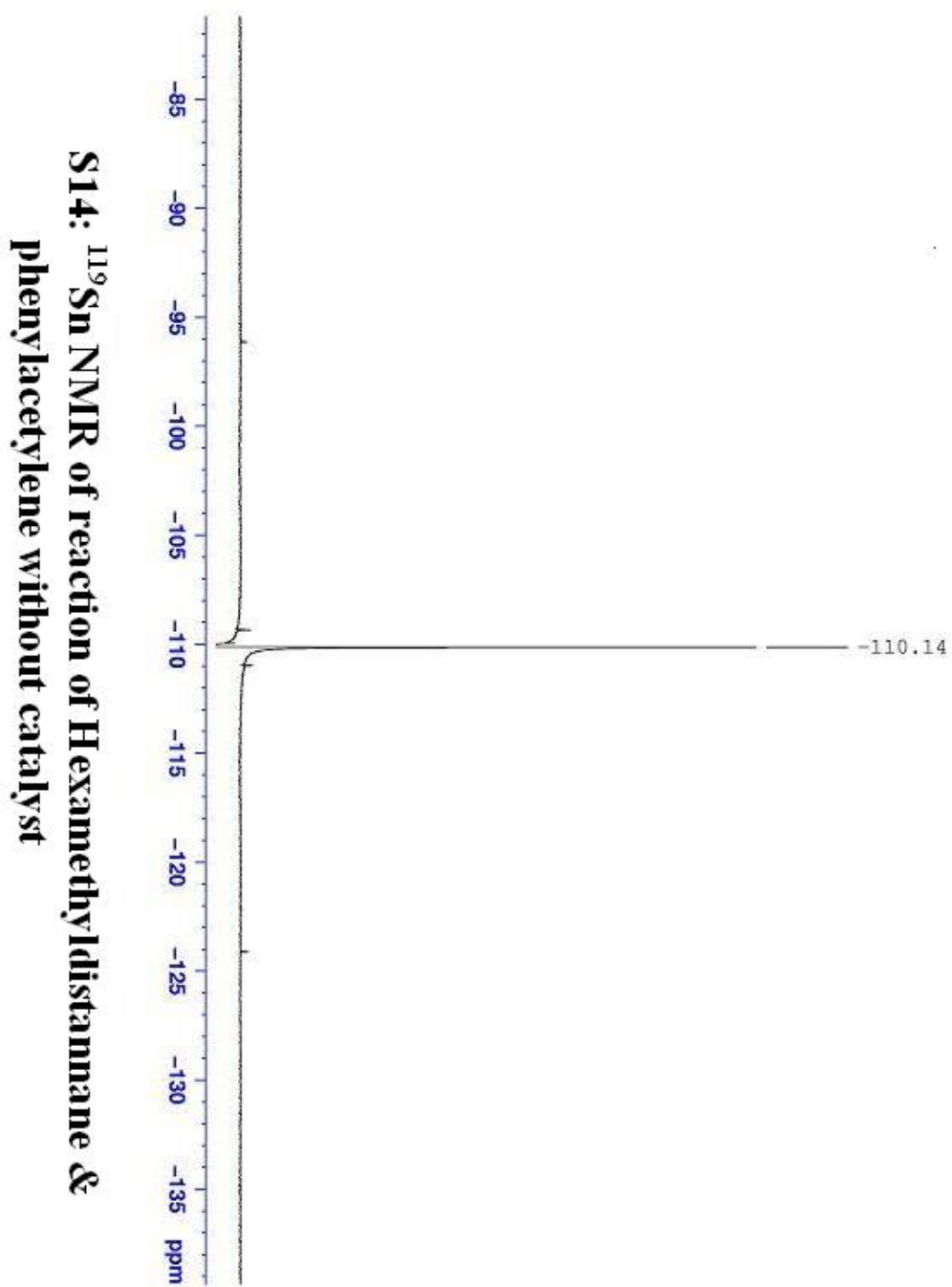
**S11:  $^{119}\text{Sn}$  NMR of Hexamethyldistannyl ethylene**

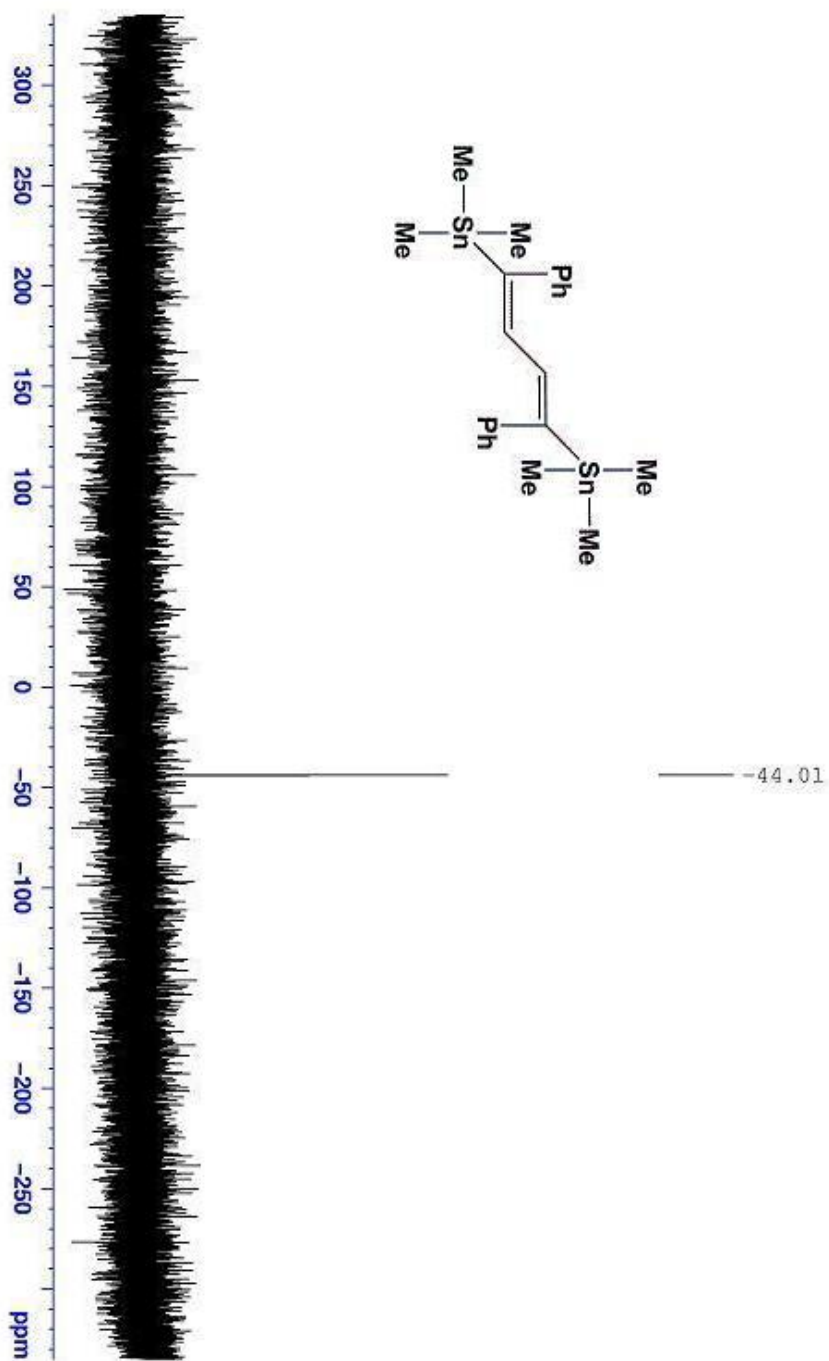
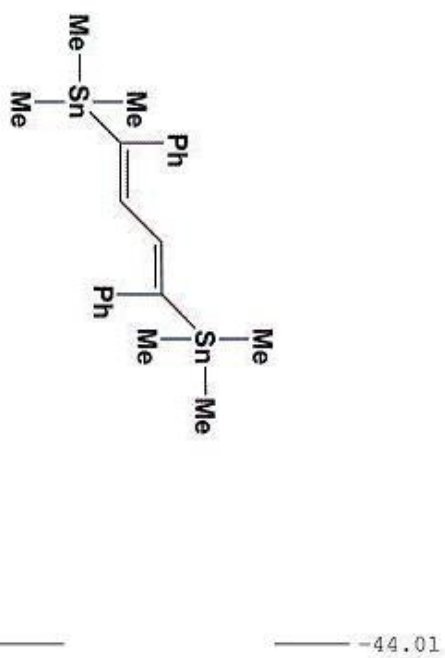


**S12: <sup>1</sup>H NMR of Hexamethyl-1-phenyldistannyl ethylene**

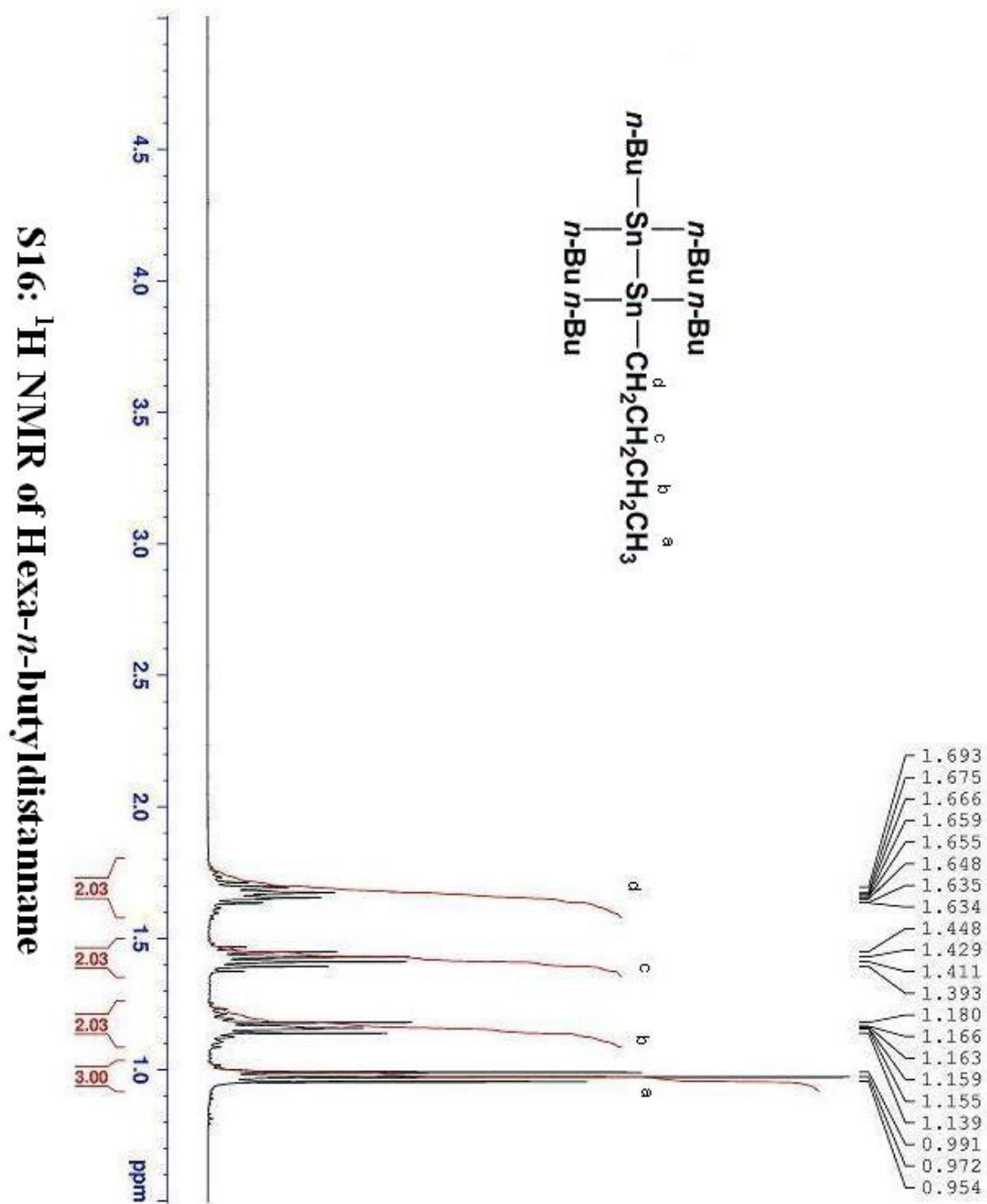
**S13:  $^{119}\text{Sn}$  NMR of Hexamethyl-1-phenyldistannyl ethylene**

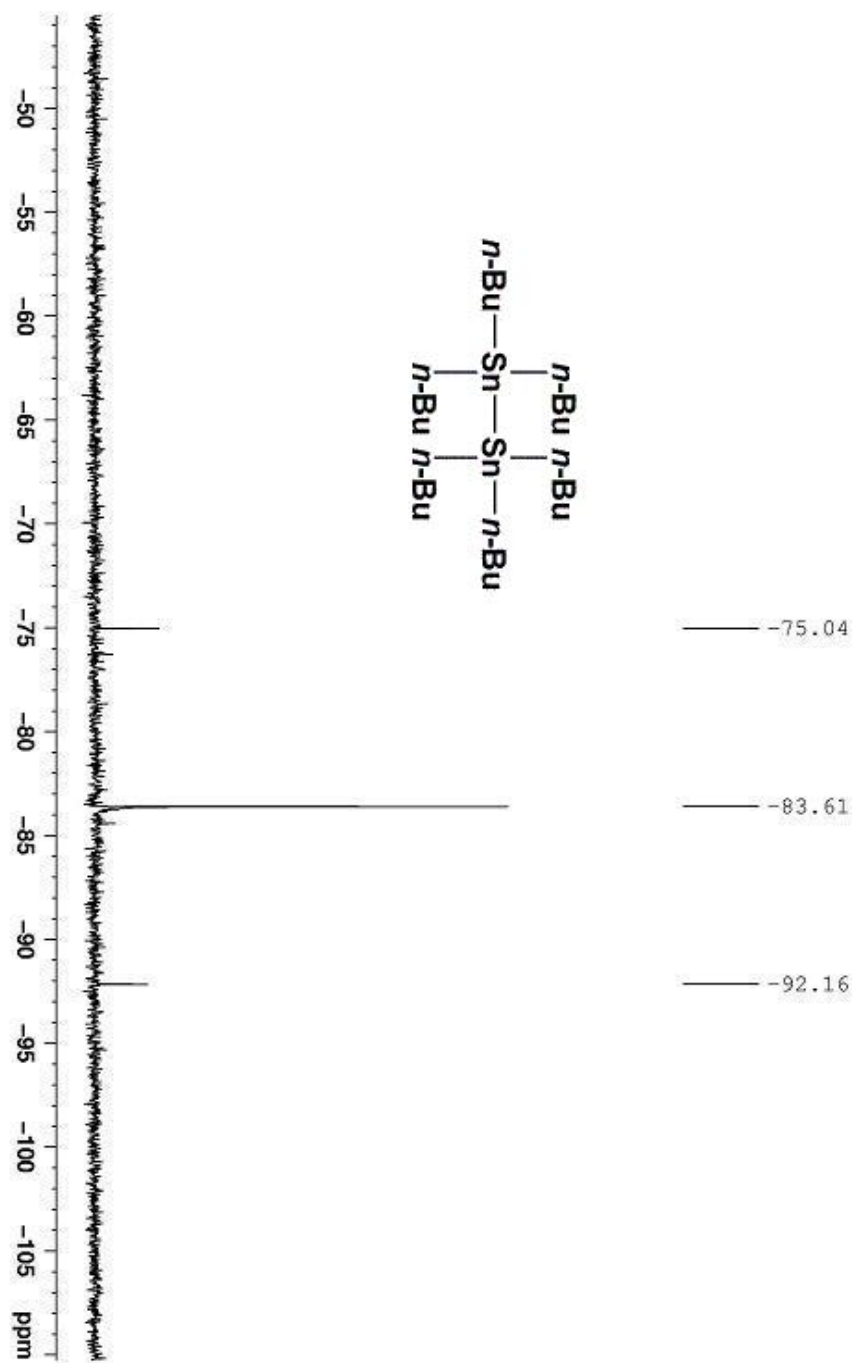






**S15:  $^{119}\text{Sn}$  NMR of Hexamethyl-1,4-diphenyldistannyl-1,3-butadiene**

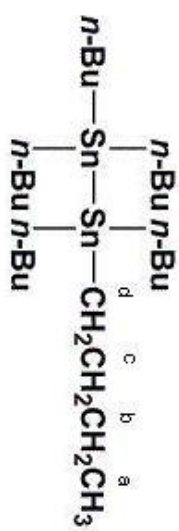




**S17: <sup>119</sup>Sn NMR of Hexa-*n*-butylstannane**

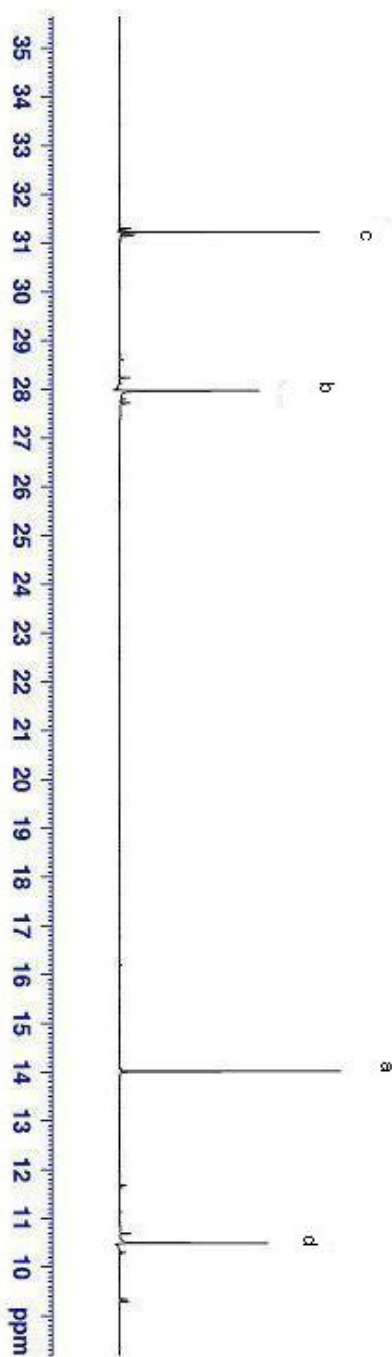
— 31.23

— 27.98

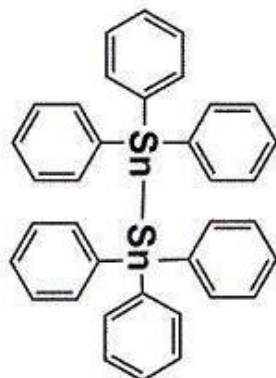


— 14.02

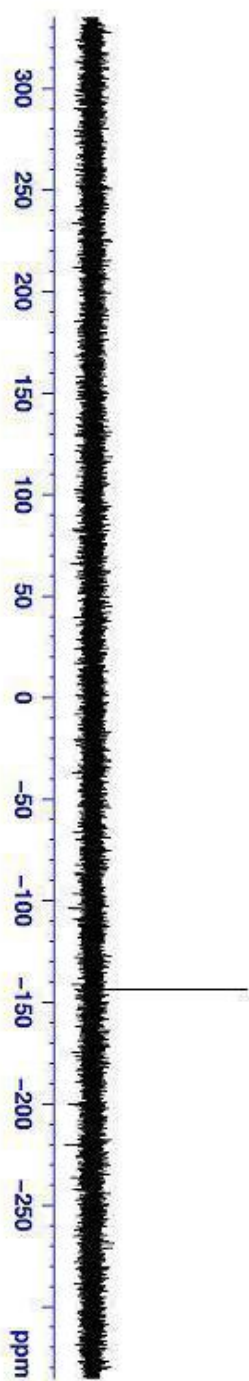
— 10.49



**S18: <sup>13</sup>C NMR of Hexa-*n*-butylstannane**

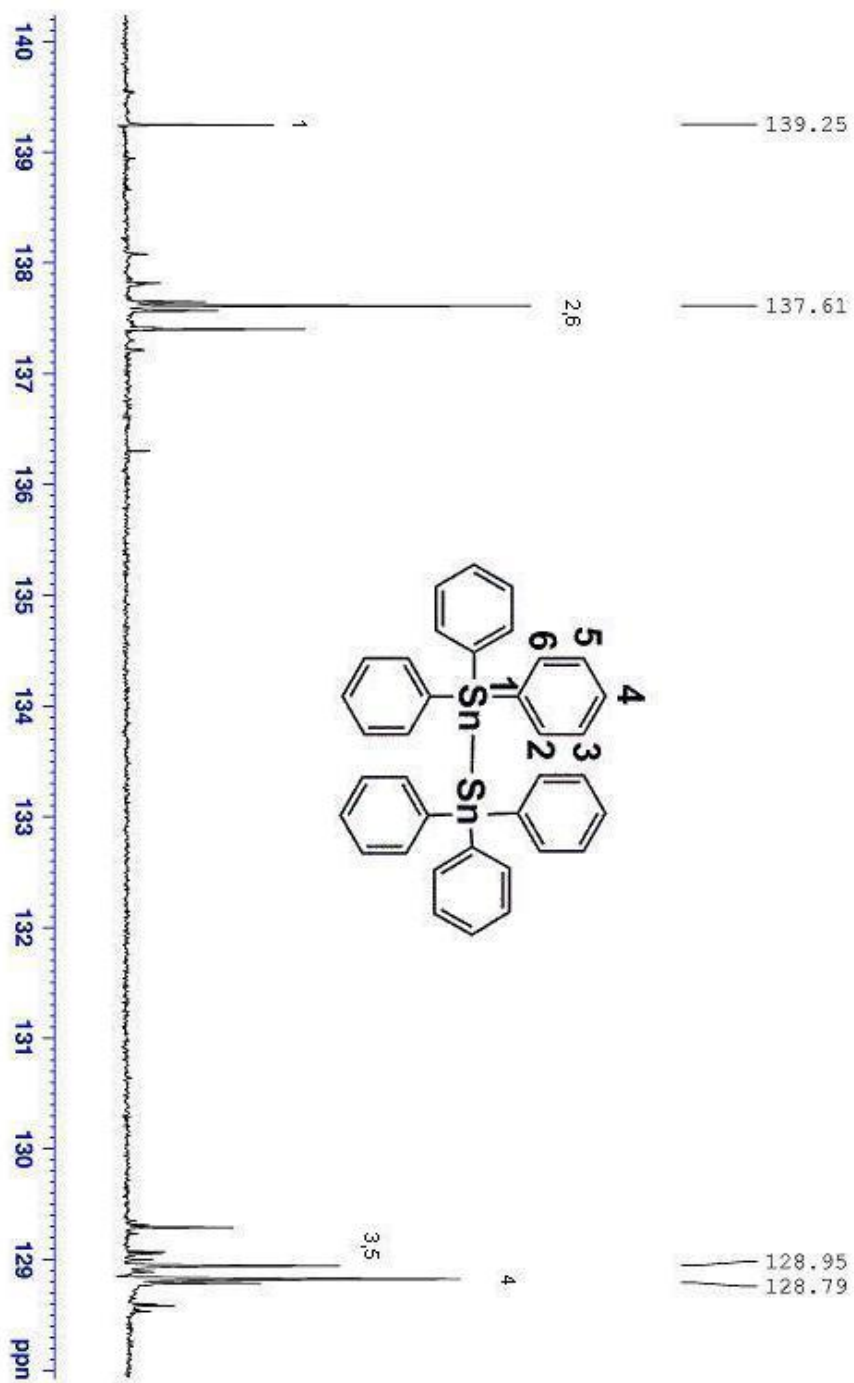


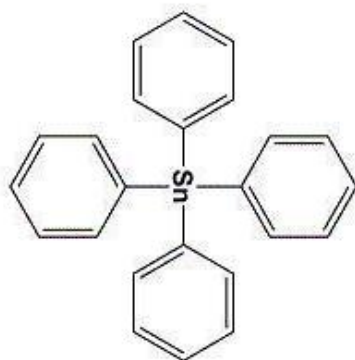
-143.78



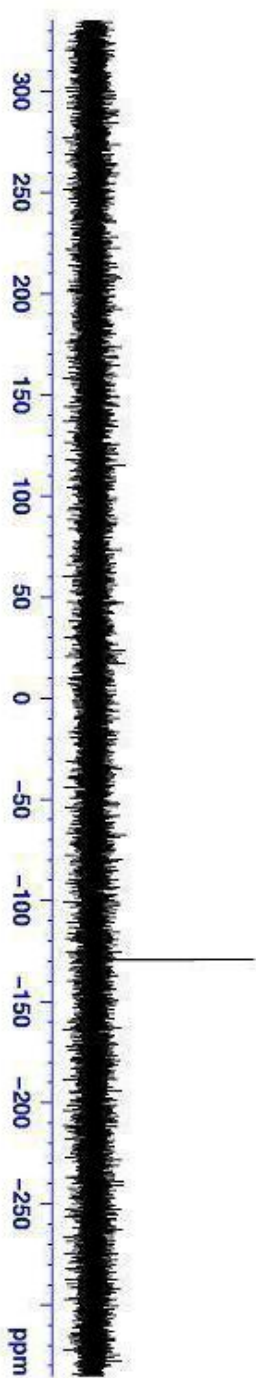
**S19:  $^{119}\text{Sn}$  NMR of Hexaphenyldistannane**

# **S20: $^{13}\text{C}$ NMR of Hexaphenyldistannane**



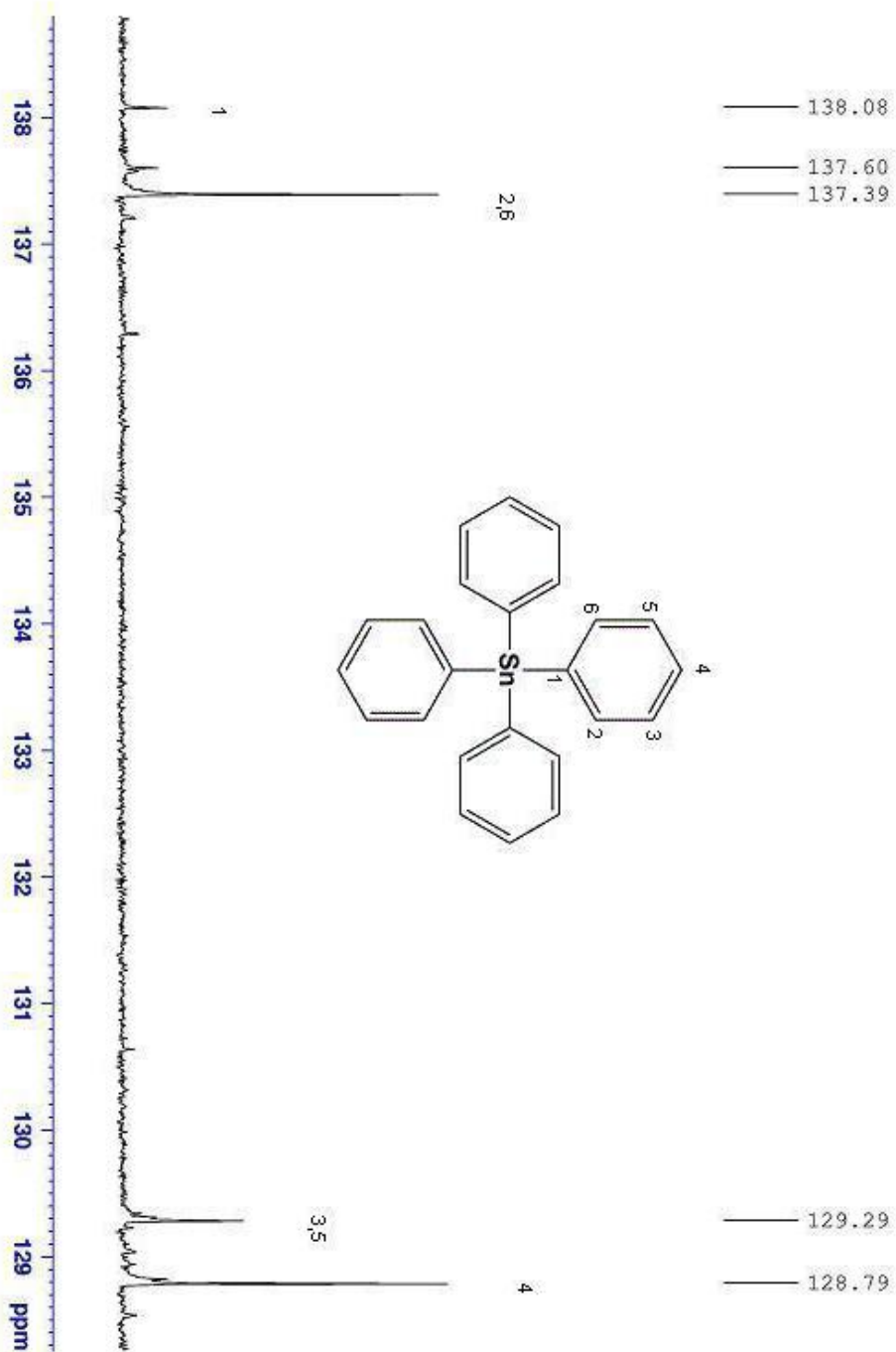


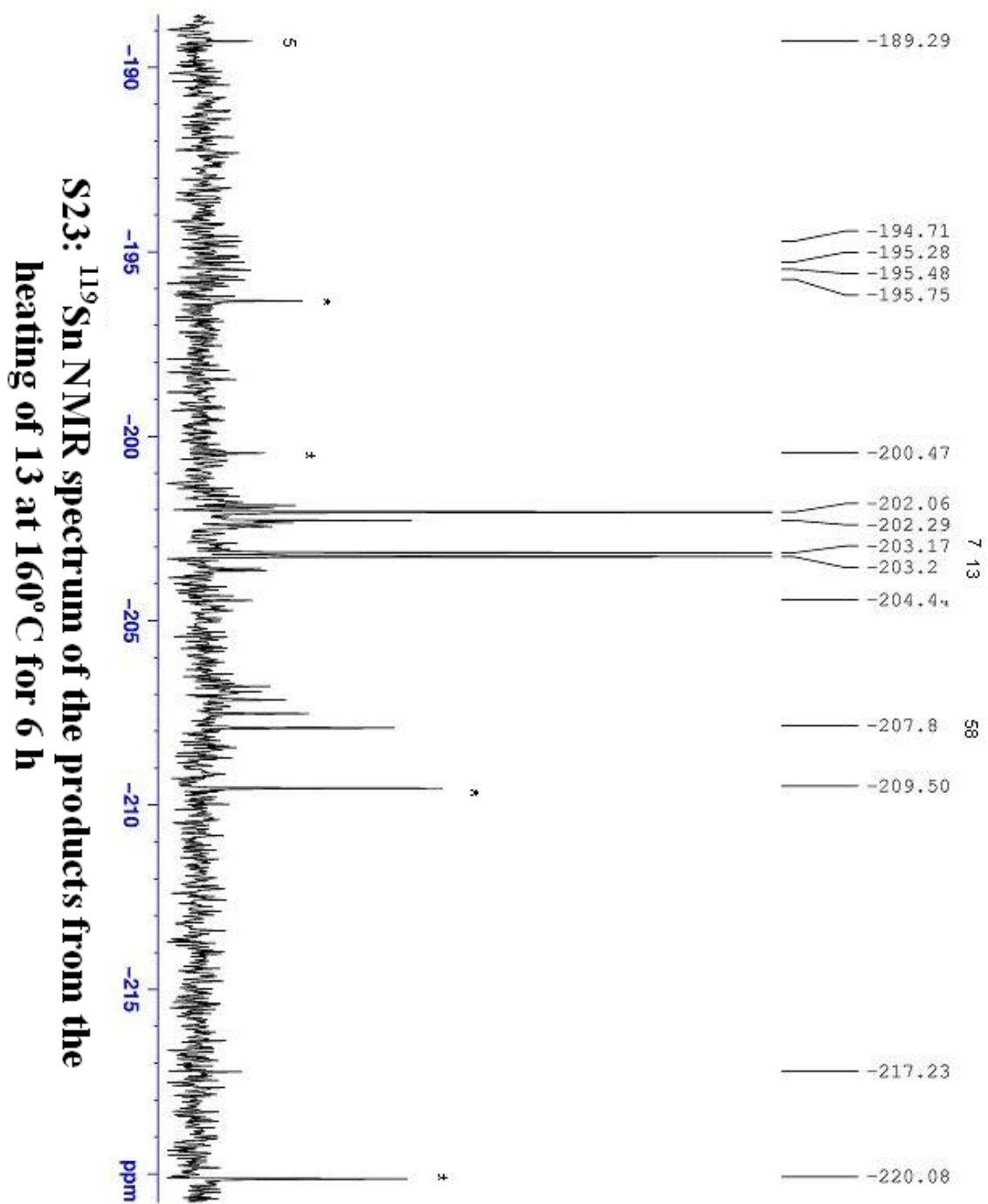
— -129.32



**S21:  $^{119}\text{Sn}$  NMR of Tetraphenyltin**

# **S22: $^{13}\text{C}$ NMR of Tetraphenyltin**





## Appendix II

Crystal data and structure refinement **57**

Atomic coordinates ( $\times 10^4$ ) and equivalent isotropic displacement parameters

Atomic coordinates ( $\times 10^4$ ) and equivalent isotropic displacement parameters

Bond lengths [ $\text{\AA}$ ] and angles

Anisotropic displacement parameters, The anisotropic displacement factor

Hydrogen coordinates (  $\times 10^4$ ) and isotropic displacement parameters

Table 1 Crystal data and structure refinement for k1059a.

|                                   |   |                       |
|-----------------------------------|---|-----------------------|
| Identification code               | k1059a  |                       |
| Empirical formula                 | C <sub>22</sub> H <sub>30</sub> Sn <sub>2</sub> |                       |
| Formula weight                    | 531.84  |                       |
| Temperature                       | 150(1) K  |                       |
| Wavelength                        | 0.71073 Å                                       |                       |
| Crystal system                    | Orthorhombic                                    |                       |
| Space group                       | P c a 21  |                       |
| Unit cell dimensions              | a = 16.1862(3) Å                                | $\alpha = 90^\circ$ . |
|                                   | b = 6.2126(6) Å                                 | $\beta = 90^\circ$ .  |
|                                   | c = 22.2214(11) Å                               | $\gamma = 90^\circ$ . |
| Volume                            | 2234.5(2) Å <sup>3</sup>                        |                       |
| Z                                 | 4   |                       |
| Density (calculated)              | 1.581 Mg/m <sup>3</sup>                         |                       |
| Absorption coefficient            | 2.236 mm <sup>-1</sup>                          |                       |
| F(000)                            | 1048  |                       |
| Crystal size                      | 0.16 x 0.10 x 0.10 mm <sup>3</sup>              |                       |
| Theta range for data collection   | 2.68 to 27.46°.                                 |                       |
| Index ranges                      | -20 ≤ h ≤ 21, -8 ≤ k ≤ 8, -22 ≤ l ≤ 28          |                       |
| Reflections collected             | 13220   |                       |
| Independent reflections           | 4024 [R(int) = 0.0906]                          |                       |
| Completeness to theta = 27.46°    | 99.3 %  |                       |
| Absorption correction             | Semi-empirical from equivalents                 |                       |
| Max. and min. transmission        | 0.767 and 0.658                                 |                       |
| Refinement method                 | Full-matrix least-squares on F <sup>2</sup>     |                       |
| Data / restraints / parameters    | 4024 / 1 / 222                                  |                       |
| Goodness-of-fit on F <sup>2</sup> | 1.036   |                       |
| Final R indices [I > 2σ(I)]       | R1 = 0.0590, wR2 = 0.1328                       |                       |
| R indices (all data)              | R1 = 0.1033, wR2 = 0.1620                       |                       |
| Absolute structure parameter      | 0.58(9)   |                       |
| Largest diff. peak and hole       | 2.028 and -1.675 e.Å <sup>-3</sup>              |                       |

Table 2. Atomic coordinates ( $\times 10^4$ ) and equivalent isotropic displacement parameters ( $\text{\AA}^2 \times 10^3$ ) for k1059a.  $U(\text{eq})$  is defined as one third of the trace of the orthogonalized  $U_{ij}$  tensor.

|       | x        | y         | z        | $U(\text{eq})$ |
|-------|----------|-----------|----------|----------------|
| Sn(1) | 5647(1)  | 8269(1)   | 2090(1)  | 36(1)          |
| Sn(2) | 3243(1)  | 7029(1)   | 4328(1)  | 36(1)          |
| C(1)  | 4436(8)  | 6250(20)  | 3967(7)  | 31(3)          |
| C(2)  | 4697(8)  | 6970(20)  | 3417(6)  | 34(3)          |
| C(3)  | 4244(8)  | 8440(20)  | 3034(6)  | 36(3)          |
| C(4)  | 4468(8)  | 9210(20)  | 2494(6)  | 35(3)          |
| C(5)  | 4979(8)  | 4780(20)  | 4311(8)  | 38(3)          |
| C(6)  | 5209(8)  | 2800(20)  | 4123(8)  | 44(4)          |
| C(7)  | 5696(7)  | 1350(20)  | 4400(8)  | 41(4)          |
| C(8)  | 5952(9)  | 1890(30)  | 4972(7)  | 46(4)          |
| C(9)  | 5727(10) | 3910(30)  | 5218(8)  | 48(4)          |
| C(10) | 5245(9)  | 5330(30)  | 4892(7)  | 49(4)          |
| C(11) | 3921(7)  | 10756(18) | 2160(7)  | 30(3)          |
| C(12) | 3660(9)  | 10380(30) | 1577(7)  | 49(4)          |
| C(13) | 3151(9)  | 11810(30) | 1282(7)  | 47(4)          |
| C(14) | 2928(9)  | 13690(30) | 1572(8)  | 51(4)          |
| C(15) | 3194(7)  | 14180(20) | 2142(8)  | 41(3)          |
| C(16) | 3690(7)  | 12640(20) | 2445(6)  | 32(3)          |
| C(17) | 5756(9)  | 9590(30)  | 1216(9)  | 51(5)          |
| C(18) | 6587(9)  | 9530(30)  | 2665(8)  | 52(4)          |
| C(19) | 5716(7)  | 4910(20)  | 2047(9)  | 45(4)          |
| C(20) | 3077(10) | 10399(19) | 4405(12) | 64(6)          |
| C(21) | 2347(9)  | 5620(30)  | 3740(7)  | 48(4)          |
| C(22) | 3135(10) | 5700(30)  | 5223(7)  | 51(4)          |

Table 3. Bond lengths [Å] and angles [°] for k1059a.

|                   |           |
|-------------------|-----------|
| Sn(1)-C(19)       | 2.090(14) |
| Sn(1)-C(17)       | 2.115(19) |
| Sn(1)-C(18)       | 2.135(16) |
| Sn(1)-C(4)        | 2.189(13) |
| Sn(2)-C(20)       | 2.117(12) |
| Sn(2)-C(21)       | 2.140(15) |
| Sn(2)-C(1)        | 2.148(14) |
| Sn(2)-C(22)       | 2.160(15) |
| C(1)-C(2)         | 1.37(2)   |
| C(1)-C(5)         | 1.481(19) |
| C(2)-C(3)         | 1.445(18) |
| C(3)-C(4)         | 1.343(19) |
| C(4)-C(11)        | 1.501(18) |
| C(5)-C(6)         | 1.354(18) |
| C(5)-C(10)        | 1.40(2)   |
| C(6)-C(7)         | 1.342(19) |
| C(7)-C(8)         | 1.38(2)   |
| C(8)-C(9)         | 1.41(2)   |
| C(9)-C(10)        | 1.38(2)   |
| C(11)-C(12)       | 1.38(2)   |
| C(11)-C(16)       | 1.385(18) |
| C(12)-C(13)       | 1.38(2)   |
| C(13)-C(14)       | 1.38(2)   |
| C(14)-C(15)       | 1.37(2)   |
| C(15)-C(16)       | 1.416(19) |
| C(19)-Sn(1)-C(17) | 109.8(7)  |
| C(19)-Sn(1)-C(18) | 110.9(7)  |
| C(17)-Sn(1)-C(18) | 110.4(6)  |
| C(19)-Sn(1)-C(4)  | 109.4(5)  |
| C(17)-Sn(1)-C(4)  | 110.2(5)  |
| C(18)-Sn(1)-C(4)  | 106.1(6)  |
| C(20)-Sn(2)-C(21) | 111.6(8)  |
| C(20)-Sn(2)-C(1)  | 111.5(6)  |

|                   |           |
|-------------------|-----------|
| C(21)-Sn(2)-C(1)  | 106.8(6)  |
| C(20)-Sn(2)-C(22) | 107.2(9)  |
| C(21)-Sn(2)-C(22) | 110.5(6)  |
| C(1)-Sn(2)-C(22)  | 109.3(6)  |
| C(2)-C(1)-C(5)    | 118.8(13) |
| C(2)-C(1)-Sn(2)   | 122.5(10) |
| C(5)-C(1)-Sn(2)   | 118.7(10) |
| C(1)-C(2)-C(3)    | 125.2(12) |
| C(4)-C(3)-C(2)    | 128.0(12) |
| C(3)-C(4)-C(11)   | 120.8(12) |
| C(3)-C(4)-Sn(1)   | 120.4(10) |
| C(11)-C(4)-Sn(1)  | 118.8(9)  |
| C(6)-C(5)-C(10)   | 114.9(13) |
| C(6)-C(5)-C(1)    | 124.3(15) |
| C(10)-C(5)-C(1)   | 120.6(13) |
| C(7)-C(6)-C(5)    | 128.9(16) |
| C(6)-C(7)-C(8)    | 116.0(14) |
| C(7)-C(8)-C(9)    | 119.5(13) |
| C(10)-C(9)-C(8)   | 120.6(16) |
| C(9)-C(10)-C(5)   | 120.0(15) |
| C(12)-C(11)-C(16) | 119.2(12) |
| C(12)-C(11)-C(4)  | 122.4(13) |
| C(16)-C(11)-C(4)  | 118.4(13) |
| C(13)-C(12)-C(11) | 121.5(15) |
| C(12)-C(13)-C(14) | 118.6(15) |
| C(15)-C(14)-C(13) | 122.3(14) |
| C(14)-C(15)-C(16) | 118.0(13) |
| C(11)-C(16)-C(15) | 120.3(13) |

---

Symmetry transformations used to generate equivalent atoms:

Table 4. Anisotropic displacement parameters ( $\text{\AA}^2 \times 10^3$ ) for k1059a. The anisotropic displacement factor exponent takes the form:  $-2\pi^2 [h^2 a^{*2} U^{11} + \dots + 2 h k a^* b^* U^{12}]$

|       | U <sup>11</sup> | U <sup>22</sup> | U <sup>33</sup> | U <sup>23</sup> | U <sup>13</sup> | U <sup>12</sup> |
|-------|-----------------|-----------------|-----------------|-----------------|-----------------|-----------------|
| Sn(1) | 35(1)           | 35(1)           | 38(1)           | -1(1)           | 4(1)            | 1(1)            |
| Sn(2) | 36(1)           | 37(1)           | 36(1)           | 1(1)            | 3(1)            | 2(1)            |
| C(1)  | 32(8)           | 36(7)           | 27(8)           | 3(6)            | 2(6)            | -5(6)           |
| C(2)  | 26(7)           | 45(8)           | 30(7)           | -6(6)           | 1(6)            | 5(6)            |
| C(3)  | 37(7)           | 34(7)           | 38(8)           | 3(6)            | 15(7)           | 1(6)            |
| C(4)  | 29(7)           | 44(8)           | 31(8)           | -3(7)           | 14(6)           | 5(6)            |
| C(5)  | 41(7)           | 35(7)           | 39(8)           | 12(9)           | -4(9)           | 4(5)            |
| C(6)  | 38(7)           | 17(6)           | 75(13)          | 4(7)            | 5(7)            | -6(6)           |
| C(7)  | 26(7)           | 38(7)           | 58(11)          | 3(8)            | -2(8)           | 8(5)            |
| C(8)  | 42(8)           | 58(10)          | 37(9)           | 29(8)           | -10(7)          | -7(7)           |
| C(9)  | 56(11)          | 51(10)          | 36(10)          | 2(8)            | -17(8)          | 2(8)            |
| C(10) | 63(10)          | 55(10)          | 28(9)           | -3(8)           | -2(8)           | -5(8)           |
| C(11) | 24(6)           | 24(6)           | 41(8)           | 16(7)           | -7(7)           | -4(5)           |
| C(12) | 43(8)           | 61(11)          | 44(10)          | -3(9)           | 7(8)            | 9(8)            |
| C(13) | 55(10)          | 69(11)          | 18(7)           | -9(7)           | -6(7)           | 28(9)           |
| C(14) | 39(8)           | 66(11)          | 47(10)          | 13(9)           | -5(8)           | 12(7)           |
| C(15) | 48(8)           | 27(6)           | 47(9)           | 1(7)            | 15(9)           | 3(5)            |
| C(16) | 23(6)           | 54(9)           | 21(7)           | 7(6)            | 0(5)            | 7(6)            |
| C(17) | 40(9)           | 43(9)           | 69(13)          | -5(8)           | 11(8)           | -4(7)           |
| C(18) | 41(9)           | 69(12)          | 48(10)          | -1(9)           | 3(8)            | 8(8)            |
| C(19) | 35(7)           | 67(10)          | 33(9)           | 6(10)           | 9(8)            | -16(7)          |
| C(20) | 78(11)          | 14(6)           | 100(16)         | 7(10)           | 28(13)          | 7(6)            |
| C(21) | 44(9)           | 58(10)          | 41(9)           | 4(8)            | 5(8)            | -14(7)          |
| C(22) | 70(12)          | 64(11)          | 18(8)           | 13(7)           | -12(8)          | 4(9)            |

Table 5. Hydrogen coordinates (  $\times 10^4$ ) and isotropic displacement parameters ( $\text{\AA}^2 \times 10^3$ ) for k1059a.

|        | x    | y     | z    | U(eq) |
|--------|------|-------|------|-------|
| H(2A)  | 5218 | 6478  | 3277 | 41    |
| H(3A)  | 3724 | 8906  | 3182 | 44    |
| H(6A)  | 4997 | 2366  | 3743 | 52    |
| H(7A)  | 5854 | 42    | 4212 | 49    |
| H(8A)  | 6278 | 913   | 5200 | 55    |
| H(9A)  | 5908 | 4289  | 5610 | 57    |
| H(10A) | 5094 | 6677  | 5061 | 58    |
| H(12A) | 3837 | 9117  | 1375 | 59    |
| H(13A) | 2957 | 11509 | 888  | 57    |
| H(14A) | 2579 | 14680 | 1369 | 61    |
| H(15A) | 3049 | 15501 | 2328 | 49    |
| H(16A) | 3866 | 12913 | 2846 | 39    |
| H(17A) | 6330 | 10016 | 1144 | 76    |
| H(17B) | 5396 | 10847 | 1180 | 76    |
| H(17C) | 5593 | 8504  | 918  | 76    |
| H(18A) | 6357 | 9779  | 3067 | 79    |
| H(18B) | 6790 | 10895 | 2500 | 79    |
| H(18C) | 7043 | 8501  | 2692 | 79    |
| H(19A) | 5913 | 4349  | 2432 | 67    |
| H(19B) | 6100 | 4492  | 1726 | 67    |
| H(19C) | 5167 | 4324  | 1960 | 67    |
| H(20A) | 3094 | 11052 | 4003 | 96    |
| H(20B) | 3520 | 11006 | 4653 | 96    |
| H(20C) | 2542 | 10697 | 4592 | 96    |
| H(21A) | 2193 | 6662  | 3428 | 72    |
| H(21B) | 1855 | 5219  | 3972 | 72    |
| H(21C) | 2581 | 4334  | 3550 | 72    |
| H(22A) | 3461 | 6564  | 5504 | 76    |
| H(22B) | 3342 | 4214  | 5223 | 76    |
| H(22C) | 2554 | 5705  | 5346 | 76    |